Cellular interactions during gastrulation in the amphipod crustacean, *Parhyale hawaiensis*

by

Ro Crystal Chaw

A dissertation submitted in partial satisfaction of the

requirements for the degree of

Doctor of Philosophy

in

Integrative Biology

in the

Graduate Division

of the

University of California, Berkeley

Committee in charge:

Professor Nipam H. Patel, chair
Professor David Bilder
Professor John Gerhart
Professor Leslea Hlusko

Fall 2011

Cellular interactions during gastrulation in the amphipod crustacean, *Parhyale hawaiensis*

by

Ro Crystal Chaw

Abstract

Cellular interactions during gastrulation in the amphipod crustacean, *Parhyale hawaiensis*

by
Ro Crystal Chaw

Doctor of Philosophy in Integrative Biology

University of California, Berkeley

Professor Nipam H. Patel, Chair

How animals develop the complex structures and morphologies that result in diversification and speciation is a fundamental question in evolutionary biology that can be addressed through studies of embryogenesis. Gastrulation is an early morphogenetic event that establishes the embryonic tissue layers that will give rise to the various organs and characteristics of the adult. Cells and their interactions are the basis of this process. Outside of *Drosophila melanogaster,* little is known about the behavior of cells during gastrulation in arthropods.

This dissertation focuses on cell behavior during gastrulation in the amphipod crustacean *Parhyale hawaiensis*. Using a variety of techniques, we make novel observations about cell shape change, the autonomy of cell behavior, and investigate possible molecular regulators of the entire process. I found cell shape change in the rosette that confirms previous hypotheses suggesting that gastrulation in *Parhyale* proceeds through ingression or invagination. I also found that the rosette and epithelial sheet act autonomously, and that the descendants of different lineages within the rosette are able to internalize independently. Using drug inhibition, I identified *rho-kinase* as important to epithelial integrity during gastrulation, and discovered a phenotype that may be associated with abnormal cell division. Finally, I investigated several candidate genes in an effort to discover a molecular marker for early mesoderm and ectoderm fate. This study provides valuable information about the process of cell internalization, cell autonomy during gastrulation, and suggests potential highly conserved mechanisms for cell behavior during *Parhyale* gastrulation.

This thesis is lovingly dedicated to my Dad, Shaw Yung Chaw (1947-2003). A constant companion on fishing expeditions, in cooking elaborate meals, and on long walks through neighborhoods and on mountains, my father was my partner in crime and my biggest cheerleader. I miss him every day. This dissertation is as much his as it is mine.

Table of Contents

Table of Figures

Acknowledgements

First, thanks go to Nipam Patel for giving me endless opportunities, and for teaching me to always think twice. Thanks for everything.

Enormous thanks to my qualifying exam and dissertation committee members- David Bilder, John Gerhart, Leslea Hlusko, Mimi Koehl, and David Lindberg. It has been an honor and a pleasure. Some of my most memorable scientific moments and discussions have been with you, and I appreciate it whole-heartedly.

Patel lab members from 2006-2011, I simply wouldn't have survived without you. Special thanks to Melinda Modrell, Meredith Protas, Cristina Grande, E. Jay Rehm, Kira O'Day Heller (class of '05), Danielle Liubicich, Paul Liu, Ron Parchem, Julia Serano, and Evie Huang.

Thank you to the funding agencies and departmental entities without which graduate school would have been a practical impossibility for me. The NSF-GRFP and the HHMI, and the Integrative Biology and Molecular and Cellular Biology support staffs.

Members of the Bilder, Harland, Hlusko, King, Levine, Rohksar, and Weisblatt labs, thank you for your smiles, support, and resources. Working among you was remarkable. Special thanks to Isabelle Phillip, Jen-Yi Lee, Saori Haigo, and Theresa Greico. Thanks too, to my virtual and anonymous colleagues on Phinished.org, an internet forum for finishing graduate students. Without their round-the-clock support, writing my dissertation would have been much lonelier indeed.

Deep thanks to friends and family who supported me even as I focused time and energy away from them. My Physics posse, Reed transplants, high school friends, Berkeley tour group #1, and Apple geniuses, you kept me from losing my mind completely. Steve and Kay, I wouldn't be here without you. Mom, Walter, Carolyn, Mia, and Cole; I'll be home for Christmas this year.

Thank you, perhaps most of all, to my husband Tony Williams. I couldn't have dreamed a better match or better support, even as things were the most difficult.

Chapter I: Introduction

How the unique attributes of a given species arise is a central question of evolutionary biology that can be addressed through studying embryogenesis. Evolution acts through natural selection on heritable traits. This process often manifests through changes in morphology that result in diversification and speciation. In 1866, Ernst Haeckel synthesized Charles Darwin's theory of natural selection (Darwin, 1855) with work from embryologists like Johann Meckel (1781-1833) and Karl-Ernst von Baer (1792-1876). Haeckel came to the infamous conclusion that "ontogeny recapitulates phylogeny" (Haeckel, 1866; Sander, 2002). This idea had several lasting implications. Most importantly, it introduced the idea that morphological similarities between the embryos of different species are due to common ancestry, indicating that ontogeny is a powerful way to investigate morphological change and ultimately phylogenesis (Sander, 2002; Gerson, 2007).

Since Haeckel's time, the field of evolutionary developmental biology has expanded to include studies of conserved genes, gene pathways, and gene networks. In addition, the field is now defined by pursuit of data from new and varied organisms and by its interest in how development and its mechanisms themselves evolved. In all cases, how morphogenesis occurs remains a central question.

In this dissertation, I focus on gastrulation, the main morphogenetic event of early development in animals with multiple tissue layers. Gastrulation is the process that defines and organizes the embryo into "germ" layers that will give rise to the vital systems of the adult organism. The number of layers established during gastrulation divides animals into diploblasts, those with two layers (endoderm and ectoderm), and triploblasts, those with three layers (endoderm, ectoderm, and mesoderm). These germ layers give rise to specific systems of the adult animal: Ectoderm will include the skin and nervous system. Endoderm becomes the gut and associated organs. Mesoderm, when present, gives rise to muscle and supporting structures in the body.

How animals gastrulate has been the subject of study for over 100 years because of its importance to the evolutionary history of animals and because it is one of the earliest manifestations of an animal's unique morphology. Gastrulation is evidence of the evolutionary transition from an animal with one embryonic tissue layer to one with multiple tissue layers. These layers permitted the formation of a variety of internal and external structures, facilitating the diversification that enabled the invasion of a greater number of ecological niches (Knoll and Carroll, 1999; King, 2004). How that first animal, the ancestor to animals with two tissue layers like the diploblastic Cnidarians and Ctenophores and those with three tissue layers like the triploblastic Bilateria, might have organized itself into something other than a hollow ball of cells remains a fundamental question in studies of evolution and development. For example, gastrulation modes among the triploblastic Bilateria organize them into whether the anus or the mouth forms first. These categories (mouth first = protostome, anus first = deuterostome), remain important concepts to the study of the evolution of different body plans (Grobben, 1908; Arendt et al., 2001; Hejnol and Martindale, 2008). Studying this transition directly through the fossil record is nearly impossible due to a

lack of well-preserved embryos. However, through comparison of gastrulation strategies in different organisms, inferences can be made toward understanding how this transition may have occurred.

Studies of gastrulation also pertain to the formation of an animal's unique characteristics. Prior to gastrulation, the embryos of most animals form a "blastula," a stage with a single layer of cells, the blastoderm, surrounding a space, a blastocoel, that can be empty or partially comprised of yolk or fluid. Gastrulation transforms the cellular monolayer of the blastoderm into a three-dimensional precursor to the adult, complete with directional axes and cells in the appropriate position to give rise to various structures. Observing the dynamics and investigating the mechanisms of gastrulation allows tracing the vital systems of an organism to their cellular origin, revealing the significance of each region of the embryo. It is the first manifestation of what the animal will ultimately become.

Several challenges exist in making evolutionary comparisons of gastrulation. One is its inherent complexity and, subsequently, the wide variety of existing approaches in the literature. To discern homology, it is necessary to compare, as it were, apples to apples in different species. Because gastrulation is a multi-step process that occurs with the added dimension of time, comparison of the entire process between species is often too broad and is not necessarily appropriate. As a result, studies of gastrulation regularly focus on a single aspect such as a conserved molecular pathway or a single event like the initiation of gastrulation or the elongation of a specific tissue. This specificity improves the potential for useful comparison, but has an added difficulty in that each model system is more amenable to certain techniques versus others. For example, embryos of the frog *Xenopus laevis* are large in size and robustly survive microsurgery, but *Xenopus'* large genome and chromosome number make it less attractive for genetic and genomic assays. On the other hand, the fruit fly *Drosophila melanogaster* is well suited for genetic assays, but its fast developmental time, small size, and certain developmental characteristics (such as an early syncytium) make some stages unsuitable for microsurgery. The strengths and weaknesses of different systems can make choosing a narrow focus difficult for comparative work.

Another challenge is a lack of data from non-model systems. Current model systems for gastrulation include *Xenopus, Drosophila,* the roundworm *Caenorhabditis elegans,* mice (*Mus musculus)*, chicks (*Gallus gallus)*, and zebrafish *(Danio rerio)*. This is a broad sampling from several phyla, but in some cases only a single species is used as a representative of an phylum. More and more studies are being done in non-model organisms to remedy this issue. However, to ensure accurate interpretations of ancestral evolutionary nodes, having as complete a sample as possible from different species is ideal (Bolker, 1995; Jenner and Wills, 2007).

To address these challenges, this dissertation focuses on cellular behavior during gastrulation in the emerging model system *Parhyale hawaiensis*. Because tissues and the cells that comprise them are the basic components of gastrulation, orienting gastrulation work on cellular behavior is an appropriate beginning (Hardin, 1996). The movements and changes in cells in response to molecular signals and the level of cellular interconnectedness and independence constitute and establish the germ layers. An understanding of cells and their behavior can thus provide a framework for

studies at the micro-scale of molecular pathways and at the macro-scale of embryo-wide tissue remodeling. An understanding of the cellular foundation of gastrulation in *Parhayle* is the first step toward making useful comparisons with other species.

Parhyale is an amphipod crustacean. Crustaceans are incredibly diverse morphologically and may be a polyphyletic clade with Insecta. Their diversity and relatively close relationship with insects make them a possible point of comparison for the well-studied model organism *Drosophila* (Regier et al., 2010). Little is understood about the cellular interactions and the motors driving those interactions during crustacean gastrulation. However, *Parhyale* embryos are amenable to a number of embryological techniques (Rehm et al., 2009a-d). Previous work implies complex cellular dynamics during *Parhyale* gastrulation, but direct experimental manipulation of cell populations during gastrulation has not yet been done (Browne, 2005; Price and Patel, 2008; Alwes et al. 2011). *Parhyale's* phylogenetic position and the relative ease of cellular manipulations make it an attractive candidate for an analysis of gastrulation.

For the next section of this introduction, I will discuss examples of gastrulation and cell migration during morphogenesis from a few model systems. The purpose of these limited overviews is to provide a sense of the complexity of gastrulation and the various approaches to studying it while highlighting specific cellular behaviors that are useful when thinking about *Parhyale* gastrulation.

CELL BEHAVIOR AND GASTRULATION IN MODEL SYSTEMS

Historically, five terms describe specific cellular gastrulation movements that are conserved across taxa: invagination (the formation of multiple tissue layers through the bending of an epithelium), epiboly (one adjacent layer enveloping a neighboring layer), involution (the collective rolling of a sheet of cells around a point to the interior), delamination (oriented cell division which results in the internalization of one daughter), and ingression (the inward migration of a single cell or small group of cells) (Willmer, 1990). Depending on the organism, gastrulation comprises one, some, or all of these five basic actions in combination with more recently described movements such as convergent extension, cell intercalation, and epithelial to mesenchymal transitions (EMT) (for review see Keller, 2005; Stern, 2004; Theiry, 2009).

I review what is known about early gastrulation events that require a process called apical constriction. The active narrowing of the apical surface of cells, apical constriction appears during a variety of morphological processes across taxa, and is most often associated with ingression, invagination, involution, and EMT. The importance of apical constriction varies between processes, in some cases it drives embryo-wide morphogenesis and in others it functions to move only a specific group of cells (reviewed in Sawyer 2010). The processes in the frog, urchin, worm, and fruit fly described here all served as models for my work with *Parhyale*. A schematic of the evolutionary relationships between these organisms and *Parhyale* is shown in Figure 1.1.

Bottle cells during Xenopus laevis *gastrulation*

Gastrulation in the African clawed frog *Xenopus laevis* begins when there are approximately 1000 cells and involves the semi-autonomous behavior of several

different regions. Visible signs of gastrulation begin with the formation of a unique group of cells that are bottle or flask shaped–narrow at the apex and broad at the base. Since their initial discovery in the late 1800s, *Xenopus* bottle cells have gone from status as the force-generating mechanism of gastrulation (reviewed in Hardin and Keller, 1988) to cells of questionable importance (Keller, 1981; Hardin and Keller, 1988; Keller, 1996). Their unique shape and position as the first group of cells to exhibit morphological change during gastrulation continues to spark scientific interest (Kurth and Hausen, 2000; Lee and Harland, 2007; 2010).

Bottle cell formation occurs through apical constriction and causes a localized bending of the adjacent epithelium. This initial "dent" in the embryo marks the dorsal-most lip of the blastopore, the circular gastrulation center through which mesendoderm internalizes. Bottle cells continue to form laterally and finally ventrally around the circumference of the blastopore. Early experiments showing that cultured bottle cell explants migrate in a high pH environment by extending protrusions from their basal ends (Holtfreter, 1943), suggested that bottle cells drag the mesoderm with them as they crawl to the interior. However, if the bottle cells are removed, animals are able to complete gastrulation after only a slight delay. Moreover, the only observed defects are a truncation of developing gut, which is the structure to which bottle cells contribute (Hardin and Keller, 1988). Apical constriction of these cells may therefore be a way for the bottle cells themselves to internalize because removal of the bottle cells does not prevent the internalization of other cells.

Recent work provides some insight into the cytoskeletal and molecular components regulating shape change in *Xenopus* bottle cells. Specifically, work with cytoskeletal inhibitors indicates that normal apical constriction in bottle cells relies on both actin and myosin, suggesting acto-myosin contractility (Lee and Harland, 2007). Existing microtubules appear to be important to bottle cell elongation, a process that occurs as the cells form and migrate (Lee and Harland, 2007). Finally, endocytosis is essential to efficient apical constriction of bottle cells, perturbation of endocytosis results in disrupted contraction (Lee and Harland, 2010).

Interestingly, bottle cell formation may be linked to mesoderm specification, if not migration. The molecular signals for mesoderm patterning in the marginal zone of the *Xenopus* embryo are well known (Kimelman and Kirschner, 1987; Sasai et al., 1994; De Robertis and Kuroda, 2004). Briefly, TGF-β signaling from the vegetal half of the embryo in combination with FGF signaling from the animal cap elicits mesoderm specification in the marginal zone (Stein et al., 1993; Dale and Jones, 1999). Normal bottle cells occur in a region of overlap between high TGF-β signaling and FGF-signaling. By injecting mRNA encoding TGF-β signaling molecules into the FGF expressing region of the embryo, it is possible to induce ectopic bottle cells that, in turn, result in changes that mimic the molecular environment of normal bottle cells (Kurth and Hausen, 2000). This suggests that the method of specification for mesoderm and the induction of bottle cell behavior is linked (Kurth and Hausen, 2000). The bottle cell phenotype is a direct result of interacting molecular signals from different regions of the embryo, relies on elements of the cytoskeleton, and also exerts local influence on neighboring cells.

*Ingression during Sea urchin gastrulation (*Strongylocentrotus spp., Lytechinus spp., Heliocidaris spp.)

Studies of gastrulation in sea urchins focus on species that have planktotrophic larvae. In these animals, cell fates begin their establishment by the 16-cell stage. Of particular interest are the vegetal micromeres, which act as an organizing center and are necessary and sufficient for the formation of the vegetal plate at the blastula stage (Hörstadius, 1973; Ransick and Davidson, 1993). Gastrulation proceeds through the ingression of the primary mesenchyme cells (PMC; give rise to skeletogenic mesenchyme), and the invagination of the secondary mesenchyme cells (SMC; give rise to non-skeletogenic mesenchyme) and the endoderm. Both the mesoderm and endoderm derive from the vegetal plate (Hardin, 1996).

The cellular behavior of the PMCs and the SMCs and endoderm serve as models of ingression and invagination, respectively. PMC ingression is a clear example of an epithelial to mesenchymal transition (EMT) (Wu et al., 2007). The urchin homolog of the *Drosophila* transcriptional repressor *Snail* down regulates e-cadherin in PMCs to facilitate the loss of apical junctions. The cells then crawl to the interior using short, actin-based protrusions called filopodia (Hardin, 1996; Wu et al., 2007). Following the ingression of the PMC, the archenteron (the gut primorida) forms through two phases: a primary and secondary invagination. During primary invagination, a ring of apically constricting cells surrounds a central ring of flattened cells at the vegetal pole. Laser ablation studies in the urchin *L. pictus* show that formation of bottle cells is necessary for initiating primary invagination (Kimberly and Hardin, 1998). During secondary invagination, the archenteron elongates from the vegetal plate, through the interior blastocoel, to the animal pole (Hardin, 1996).

The molecular and cytoskeletal components of the apically constricting cells remain elusive. However, several signaling pathways including Wnt, calcium, and FGF signaling have all been implicated (Sawyer et al., 2010). Furthermore, primary invagination in the urchin *L. variegatus* relies on RhoA, a member of the Rho family of small GTPases that are central to regulating acto-myosin contractility during morphogenesis (Beane et al., 2006). Although the data from Beane et al. (2006) suggest that primary invagination relies on a pathway resulting in acto-myosin contractility, treatment with Cytochalasin D, a potent inhibitor of actin polymerization, does not fully disrupt the process (Lane et al., 1993). This suggests that other forces may be contributing to the initial formation of the archenteron. In urchins, contrary to the case in *Xenopus,* apically constricting cells during gastrulation are crucial to the process of tissue internalization.

Ingression of the endoderm in Caenorhabditis elegans

The roundworm *C. elegans* provides an example of mostly autonomous cell behavior during gastrulation. At the 26-cell stage, the *C. elegans* embryo is an epithelium with a small blastocoel. Gastrulation occurs when two endoderm precursors ingress into the blastocoel and the six surrounding cells close the gap left on the surface of the embryo (Nance et al., 2005). Extensive analyses of cell polarity, the behavior of blastomeres when grown in isolation, and candidate signaling pathways all provide some clues to the mechanisms of ingression and migration.

Evidence from a number of studies shows that apical constriction through acto-myosin contractility is the mechanism for internalization of the endoderm. *C. elegans* blastulae have an apico-basal polarity based on cell contacts. Non-muscle myosin II localizes at cell apices in response to the asymmetrical enrichment of members of the PAR protein family (Nance and Priess, 2002; Nance et al., 2003). Perturbation of specific PAR proteins significantly slows endoderm ingression as compared to controls (Nance et al., 2003). In addition, phosphorylation of myosin, and therefore contraction of the apical membrane, relies on Wnt/Frizzled signaling. In the absence of Wnt signaling, apical constriction does not occur and internalization of the endoderm is arrested (Lee et al., 2006).

Migration of the remaining six cells is less well understood. In vitro experiments revealed that gastrulation movements occur without the vitelline membrane and do not rely on chemotactic cell-cell signals. Rearranging the positions of the endoderm precursors randomizes the axes of movement among the remaining cells, suggesting that their migration is passive (Lee and Goldstein, 2003; Nance et al., 2005). Finally, microspheres placed on the surface of a cell neighboring the endoderm roll toward the site of ingression. This could indicate that differential adhesion on the surface of neighboring cells facilitates a "rolling" mechanism for their migration after internalization of the endoderm (Lee and Goldstein, 2003; Nance et al., 2005).

What is clear is that the endoderm and the six remaining cells do not require specific neighbors to execute movement. Cells grown in isolation and with varying combinations of other cells all engage in migration movements on par with controls (Lee and Goldstein, 2003). The apical constriction behavior in *C. elegans* appears to be largely autonomous.

Invagination of the mesoderm in Drosophila melanogaster

Mechanically and molecularly, apical constriction during *Drosophila* gastrulation is an important source of information for understanding how cell shape change can influence embryo-wide tissue remodeling. In particular, *Drosophila* gastrulation is an example where the molecular pathway from the genes that determine cell fate to those that regulate cell behavior is well characterized. Internalization of the mesoderm through invagination is the first step. The shape change in these cells is thought to be the motor that drives the internalization of adjacent mesoderm and the movement of ectoderm to the ventral midline (Leptin, 2005).

Drosophila mesoderm begins as a band that runs along the ventral side of the blastula stage embryo. The band is approximately twenty-cells wide. These cells include two populations that are behaviorally distinct. The central population, which is 10 cells wide, is the group that apically constricts. Changes in the central cells are first obvious as a flattening of the apical surface. The central cells then constrict their apices and undergo apico-basal shortening, causing a furrow in the ventral epithelium. The adjacent mesoderm does not constrict, but, suggesting passive movement, their apical sides stretch as they are drawn toward and into the furrow (Leptin and Grunewald, 1990; Sweeton et al., 1991). Finally, the presumptive ectoderm, which flanks the mesoderm band, is drawn to the midline where it zips closed.

Several observations indicate that the force for ventral furrow formation and mesoderm invagination comes from the central population of cells. First, ectopic expression of ventralizing genes can cause a furrow to form anywhere on the embryo (Anderson et al., 1985; Leptin and Roth, 1994). Second, disruption of the genes that confer lateral and dorsal fate does not prevent ventral furrow formation (Leptin and Grunewald, 1990; Leptin, 1995). If the lateral and dorsal cells were active during ventral furrow formation, disruption of their fate would prevent furrow development. Thus, furrow formation is specific to ventral fate and lateral, dorsal cells are passive during ventral furrow formation and mesoderm invagination.

There are multiple components to the molecular control of apical constriction in the central cells. Mesoderm is determined through maternally provided morphogens. At the time of gastrulation, a gradient of the transcription factor *Dorsal* has been established, with the highest concentrations in ventral-most nuclei. The high concentration of *Dorsal* up regulates the zygotic transcription factor *twist,* which acts as a co-factor for activating the transcriptional repressor *snail*. Both *twist* and *snail* play direct roles in mesoderm formation and invagination. Mutants with defunct *twist* and *snail* genes fail to form a ventral furrow and lack mesoderm (Ip et al., 1992; 1994).Expansion or reduction of *snail* expression correlates with increased or decreased mesoderm and furrow formation, and *snail* restricts the activity of neuroectodermal genes to the lateral and dorsal sides of the embryo by repressing their activity ventrally (Ip et al., 1994). *Twist* mutants have a much narrower stripe of apically constricting cells (Leptin and Grunewald, 1990).

This process also relies on the proteins Concertina and Folded Gastrulation (Fog). *Fog* is a direct target of *twist,* and is directly upstream of *concertina*. In embryos without *fog* and *concertina,* the initial flattening and constriction of mesoderm cells is disorganized and disrupted (Parks and Wieschaus, 1991; Costa et al., 1994). Furthermore, a heat-shock activated form of *fog* results in the apical flattening of cells outside the normal mesoderm (Morize et al., 1998). How all of this is tied to the cytoskeletal changes that occur during apical constriction involves a connection between *concertina* and the Rho guanosine 5' triphosphate-exchange factor RhoGEF2.

The *Rho* family of small GTPases are able to directly phosphorylate myosin (Jaffe and Hall, 2005). Phosphorylated myosin slides actin filaments over each other to shorten their overall length and to cause contraction during apical constriction (Sawyer et al., 2010). In *Drosophila,* RhoGEF2 works with the heteromeric g-protein Concertina to activate the downstream target *rho-kinase (rock),* which then phosphorylates myosin in the apical domain of cells (Nikolaidou and Barrett, 2004; Dawes-Hoang et al., 2005; Kölsch et al., 2007). Thus, the molecular pathway from mesoderm determination all the way to cell shape change is at least partially understood in *Drosophila* gastrulation. In *Drosophila*, invagination of the mesoderm directly influences the movement of adjacent cells, and molecular cues at the level of fate determination and cytoskeletal regulation are known.

GASTRULATION IN CRUSTACEANS AND *PARHYALE*

From the almost complete autonomy of *C. elegans* embryos to the interdependence of cellular populations during *Drosophila* gastrulation, apical constriction as a mechanism for internalization has a range of influence from small groups of cells to embryo-wide change. Outside of *Drosophila,* little is known about cellular interaction, whether apical constriction occurs, and how it is used during gastrulation in arthropods.

My study contributes novel insight into the cellular interactions and shape changes that occur during the first part of gastrulation in *Parhyale*. Although the phylogeny of crustaceans is not well-resolved, it is fairly certain that malacostrocan crustaceans are monophyletic (Giribet et al., 2001; Gerberding and Patel, 2004; Regier et al., 2010). This is supported by limited data from several taxa indicating shared early developmental and gastrulation characteristics (Gerberding and Patel, 2004). Descriptive studies of malacostrocans with superficial cleavage such as isopods (*Porcellio saber,* pill or sow bugs) and crayfish (Marmokrebs, marbled crayfish) show that they gastrulate through ingression at a blastopore located at what will become the posterior end of the germ band (Alwes and Scholtz, 2006; Wolff, 2009). Previous work argues that this strategy appears to be the ancestral state for malacostraca, which makes the total cleavage and ingression, invagination, and epibolic strategies of examined amphipods (*Parhyale hawaiensis, Orchestia cavimana,* beach hoppers) and some decapods (paneoid shrimp, prawns and tiger shrimp) derived states (Gerberding et al., 2002; Wolff and Scholtz, 2002; Gerberding and Patel, 2004; Price and Patel, 2008; Alwes et al., 2011).

Little is known about the mechanics of how malacostrocan crustaceans accomplish gastrulation movements. In paneoid shrimp like *Sicyonia ingentis*, stereotyped cleavage is a hallmark of early development. Gastrulation involves the ingression of mesendoderm followed by invagination of the "crown cells," which give rise to the mesoderm of the head (Pawlak et al., 2010). In some species, oriented cell division accompanies gastrulation and is thought to provide some of the force required to push cells to the interior (Hertzler and Clark, 1992). The injection of fluorescent lineage tracers into embryos of the terrestrial amphipod *Orchestia cavimana* revealed that establishment of cell fate begins at the 8-cell stage. Gastrulation begins with the formation of a sickle-shaped group of ectoderm cells around the precursors to the mesoderm of the head and germline. The germline precursors initiate gastrulation by "sinking into" the yolk, and then the ectoderm "overgrows" the mesendoderm (Wolff and Scholtz, 2002). For reference, a cladogram of the arthropod species discussed in this dissertation is shown in Figure 1.2.

Parhyale gastrulation resembles that of *Orchestia* with a few exceptions. Notably, *Parhyale* gastrulation is multiphasic. The first phase of gastrulation involves two populations of cells that are called the rosette and the epithelial sheet. They are easily distinguished with brightfield microscopy and/or lineage tracing (Gerberding et al., 2002; Browne et al., 2005; Price and Patel, 2008; Alwes et al., 2011). Initially distinct, the rosette and epithelial sheet come together to form a multilayered "germ cap" with the epithelial sheet on top of the rosette (Price and Patel, 2008; Alwes et al., 2011; Fig. 1.3). This is the first time the embryo exhibits multiple tissue layers, and the

germ cap marks the anterior region of the developing embryo (Browne et al., 2005; Alwes et al., 2011). We refer to this phase as "rosette internalization."

Because of an 8-cell fate map and extensive lineage tracing, the origin of the rosette and epithelial sheet are well understood (Gerberding et al., 2002; Alwes et al. 2011, Fig. 1.3). The rosette is a cluster of roughly 12-16 cells comprising descendants from the sister blastomeres **Mav** and **g**. The fates of these cells are anterior and visceral mesoderm (Mav) and germline (g). The epithelial sheet is a cluster of roughly 50 cells made of descendants from the blastomeres **El, Er,** and **Ep**. These cells will give rise to the left (El), right (Er) and posterior (Ep) portions of the ectoderm (See Fig. 1.3). Later phases of gastrulation involve the inward migration of the somatic mesoderm (from the blastomeres **ml** and **mr)** and endoderm (**en)** (Gerberding et al., 2002; Alwes et al. 2011, Fig 1.3).

For this study, we focus on rosette internalization. There are conflicting hypotheses about how the rosette and epithelial sheet interact. One hypothesis is that the rosette is passive during rosette internalization. This suggests that epibolic movements carry the epithelial sheet over stationary rosette cells (Price and Patel 2008). Another possibility is that the rosette actively internalizes. In this scenario, the rosette acts autonomously and may influence neighboring epithelial sheet cells while internalizing via ingression or invagination (Gerberding et al., 2002; Alwes et al., 2011). A third possibility is that the movement of each population of cells is autonomous. When half of the embryo at the 2-, 4-, and 8-cell stage is removed, the remaining half of the embryo produces a reduced but normal-looking germ cap. These results suggest that that the remaining cells of the rosette and epithelial sheet might undergo gastrulation movements regardless of the presence or absence of the opposing aggregation (Extavour, 2005).

Using microinjection of lineage tracers, cell ablation, immunohistochemistry, pharmacological inhibition, and *in situ* hybridization, I set out to investigate one main question: how is the rosette internalizing? I broke this into two sub-questions: Are the rosette and epithelial sheet autonomous? What molecular mechanisms are at work during rosette internalization? In Chapter II, I describe the process of rosette internalization with an emphasis on cell shape changes in the rosette. In Chapter III, I test the interdependence of the rosette and epithelial sheet using manual and photoablation. Chapter IV investigates the effect of cytoskeletal inhibitors on rosette internalization, and Chapter V is a summary of our attempts to find early patterning genes responsible for establishment of the mesoderm and ectoderm. Chapter VI discusses our results and suggests directions for future research.

Figure 1.1. Schematic of phylogenetic relationships between model systems discussed in this dissertation and *Parhyale*.
Simplified, schematic metazoan phylogeny showing the model organisms discussed in this dissertation and their relationship to each other and *Parhyale*. Estimated divergence time of select nodes is shown (mya= millions of years ago). Relationships and divergence times are based on several sources (Giribet et al., 2001; King, 2004; Ponting, 2008). Different colors indicate that the species belongs to a different phylum. Containing deuterostome/protostome group is shown at the top. The anemone *Nematostella vectensis* is used as an outgroup and is not discussed.

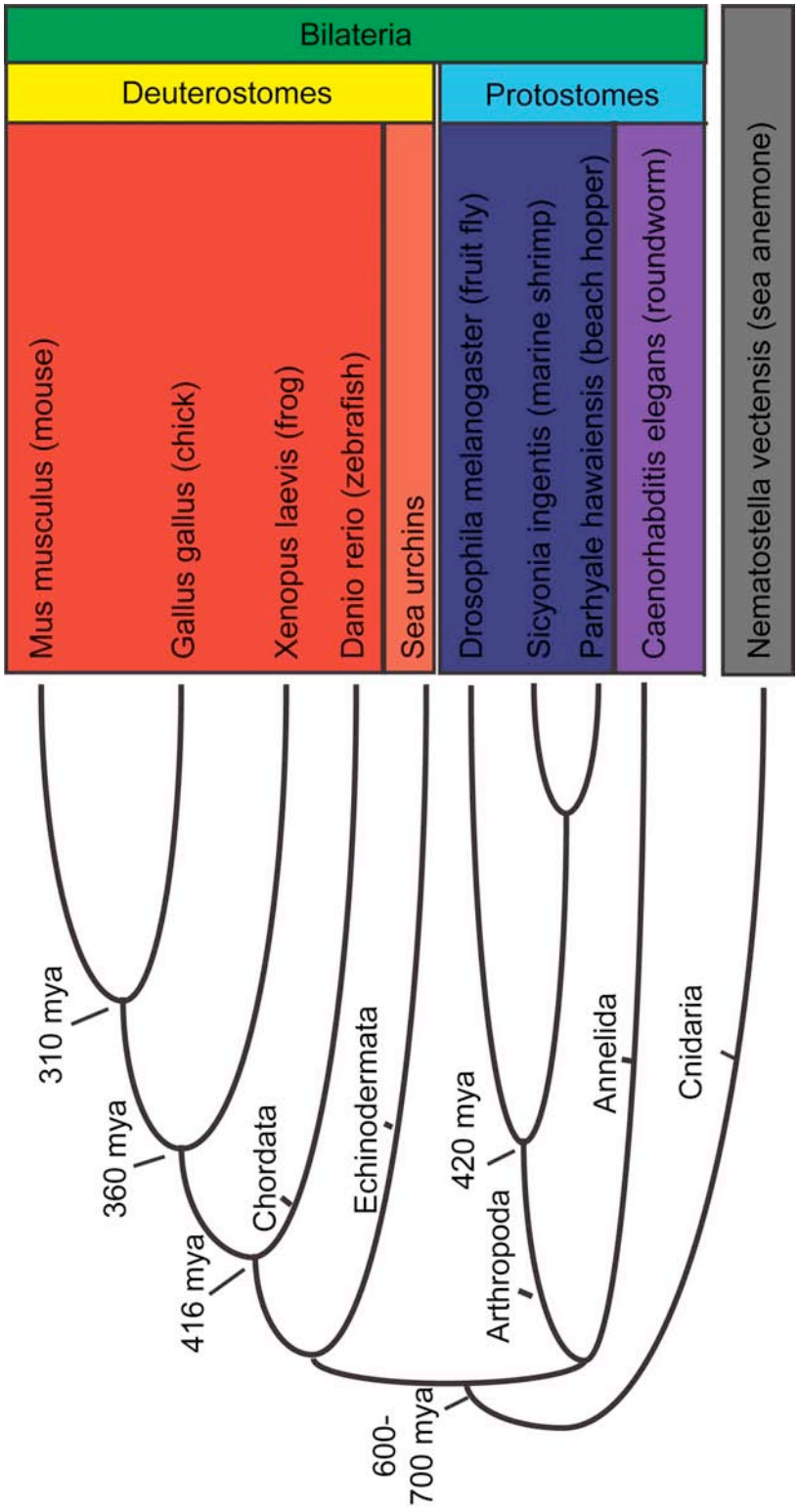
Bilateria
Deuterostomes
Protostomes
Mus musculus (mouse)
Gallus gallus (chick)
Xenopus laevis (frog)
Danio rerio (zebrafish)
Sea urchins
Drosophila melanogaster (fruit fly)
Sicyonia ingentis (marine shrimp)
Parhyale hawaiensis (beach hopper)
Caenorhabditis elegans (roundworm)
Nematostella vectensis (sea anemone)
310 mya
360 mya
416 mya
600-
700 mya
420 mya
Chordata
Echinodermata
Arthropoda
Annelida
Cnidaria

Figure 1.2. Cladogram of arthropod species discussed in this dissertation. Simplified cladogram of arthropod species discussed in this dissertation and their relationship to *Parhyale*. Approximate divergence times for some nodes are shown (mya = millions of years). Relationships are based on three sources and information from the tree of life web project (tolweb.org) (Giribet et al., 2001; Ponting, 2008; Regier et al., 2010). Colors indicate different super- and sub-orders.

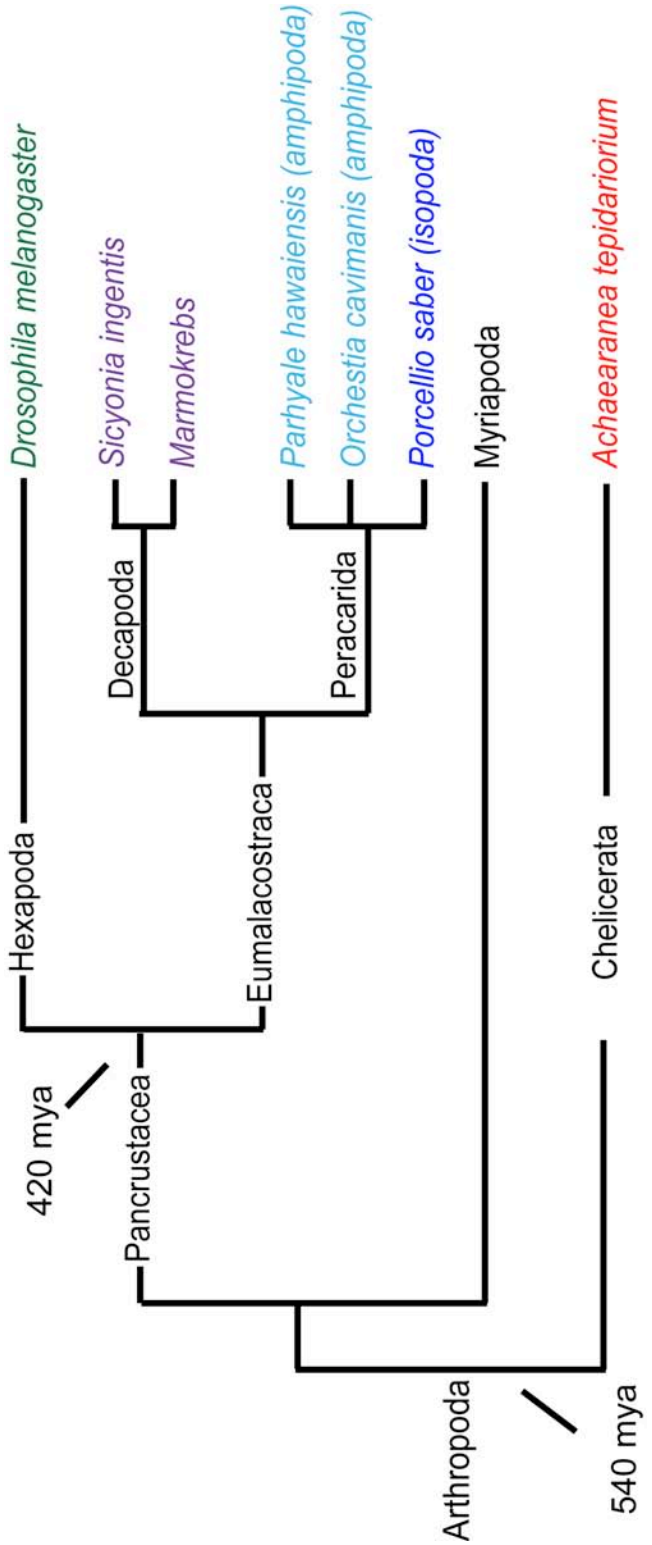
Drosophila melanogaster
Sicyonia ingentis
Marmokrebs
Parhyale hawaiensis (amphipoda)
Orchestia cavimanis (amphipoda)
Porcellio saber (isopoda)
Myriapoda
Achaearanea tepidariorium
Hexapoda
Decapoda
Peracarida
Eumalacostraca
420 mya
Pancrustacea
Chelicerata
Arthropoda
540 mya

Figure 1.3. Schematic of fate map and gastrulation in *Parhyale*.
(A) Fate map at the 8-cell stage, vegetal view. Each blastomere gives rise to a different portion of each germ layer. (B) Schematic of germ band stage, ventral view, anterior is up. (C-G) Schematic of gastrulation stages. The epithelial sheet is shown in blue, the rosette is comprised of orange and yellow Mav and g descendants. Axes indicate rough dorsal/ventral and anterior/posterior orientation of each view. By the end of rosette internalization (C-E), the rosette is underneath the epithelial sheet. Later, the somatic mesoderm internalizes (F-G). Asterisk indicates epithelial sheet in C, arrowhead indicates rosette. Scale bar in A and G are 100 microns, meant to give the reader a sense for how large the embryos are. The different systems of the embryo (germ band formation, cellular populations) are not drawn to scale. Figure modified from Price and Patel (2008).

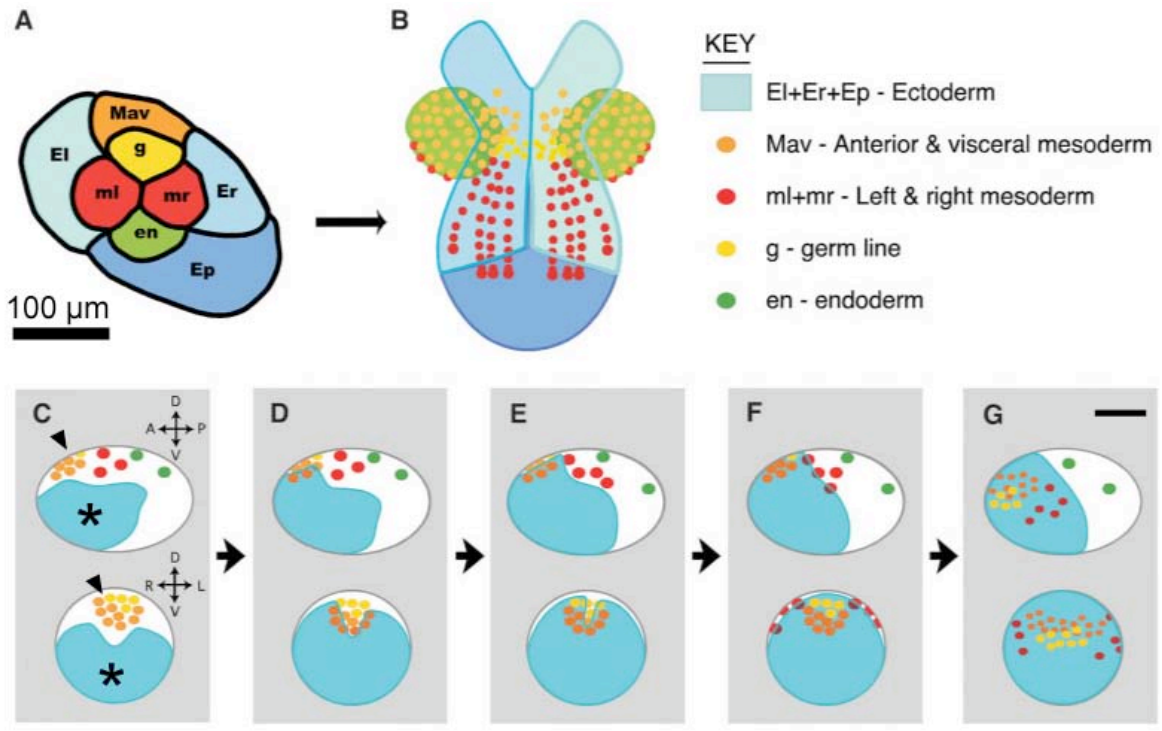

rosette internalization

Chapter II: Cell shape change in the rosette during internalization

SUMMARY

Changes in cell shape are the result of specific molecular programs and can drive morphogenetic events. This investigation is the first to study cell shape change during *Parhyale* development. In this chapter, we provide an hourly staging table of rosette internalization and we observe cell shape changes in the rosette using immunohistochemistry, microscopy, and thick sectioning. During internalization, some Mav descendants assume bottle cell morphology, suggesting apical constriction. The germline was never observed to apically constrict at the rosette stage, but germline descendants do exhibit long, tubulin rich protrusions. Finally, contrary to a recent study, we observe that g descendants internalize after Mav descendants.

INTRODUCTION

Cell shape change is a key part of morphogenesis and is an informative characteristic of actively migrating cells. During morphogenesis, the active narrowing of cellular apices (apical constriction) results in a "bottle cell," a cell with a narrow apex and broad basal domain (Holtfreter, 1943; Hardin and Keller, 1988). The bottle cell phenotype is an indicator of active cell migration during morphogenesis across metazoa because of its correlation with apically constricting cells (Sawyer et al. 2010). Any one of several cell behaviors including invagination (the internalization of cells through epithelial folding), ingression (the movement of individual or small groups of cells to the interior), and epithelial to mesenchymal transitions (EMT; the transition of a cell from stationary to motile) can involve apical constriction as a result of distinct molecular and mechanical cues (reviewed in Keller et al., 2003; see also Sawyer et al., 2010).

The extent of apical constriction's effect on the morphology of an embryo depends on the interdependence of cells during gastrulation. *Drosophila* gastrulation provides an example of how apically constricting cells cooperate with neighboring cells to initiate invagination. Gastrulation begins when mesoderm cells along and near the ventral midline of the embryo apically constrict due to *rho/rho-kinase* dependent phosphorylation of myosin (Leptin and Grunewald, 1990; Dawes-Hoang et al., 2003). This is followed by cell shape changes including apico-basal lengthening and shortening. The cellular changes in these cells provide the force that buckles the ventral epithelium, resulting in the invagination of mesoderm and the movement of ectoderm to the ventral midline (Leptin and Grunewald, 1990; reviewed in Sawyer et al., 2010).

In contrast, cells during gastrulation in the roundworm *C. elegans* act autonomously. Two endoderm cells apically constrict as they ingress during gastrulation. The six cells surrounding the endoderm move to close the gap once the cells ingress. As in *Drosophila,* the shape change in these cells relies on acto-myosin contractility. However, through extensive cell isolation experiments, it is clear that each cell type is able to undergo gastrulation movements regardless of cell-cell contacts (Lee and Goldstein, 2003; Nance et al., 2005). Apically constricting cells can influence embryo-wide changes, as in *Drosophila,* or apical constriction can affect only

the internalization of a subpopulation of cells without influencing the behavior of neighboring populations.

Outside of *Drosophila,* little is known about general cellular interactions, whether apical constriction occurs, and how apical constriction is used during arthropod gastrulation. Among crustaceans, descriptive lineage tracing experiments in the amphipod *Parhyale hawaiensis* suggest dynamic cellular interactions. In *Parhyale,* gastrulation proceeds through multiple phases. We focus on the first phase, which involves two cellular aggregations. These populations are called the rosette and the epithelial sheet, and are easily distinguished with brightfield microscopy and/or lineage tracing (Gerberding et al., 2002; Browne et al., 2005; Price and Patel, 2008; Alwes et al., 2011). At the end of the first phase, a multilayered germ cap forms with the rosette underneath the epithelial sheet. Several hypotheses about this interaction suggest that the rosette moves underneath the epithelial sheet using ingression or invagination (Gerberding et al., 2002; Browne et al., 2005; Price and Patel, 2008; Alwes et al., 2011). However, cell shape change in the rosette had not been the subject of study prior to the present work.

In this chapter I ask whether rosette cells assume bottle cell morphology during their inward migration. I complete a staging table for rosette formation and internalization. I find that there are bottle cells in Mav descendants and that actin has an apico-lateral concentration. I also observe that g descendants have long, tubulin-rich extensions that trail behind the cells. Finally, in contrast to Alwes et al. (2011), I find that g descendants ingress after Mav descendants.

MATERIALS AND METHODS

Husbandry, dissection, and fixation

Husbandry of adults and embryos and embryo collection, fixation, and dissection was done according to published protocols (Rehm et al. 2009b) with the following minor modifications. Briefly, pre-germ band embryos were first incubated in a high salt fix (8 parts ASW, 1 part 10x PBS, 1 part 37% formaldehyde) for 1-2 minutes. This allows for easier dissection because the tissue shrinks slightly from the chorion. Embryos were then transferred to seawater fix (9 parts ASW, 1 part 37% formaldehyde) and dissected and fixed as in Rehm et al. (2009b). Prior to fixation, drug-treated embryos were washed 3 times over 15 minutes in 100% ASW. All fixed embryos were rinsed (3 quick washes) in ASW and then either stored in ASW at 4ºC or washed in PT (0.1% Triton-X 100 in PBS) 3 X10 minutes. Embryos were then processed for sectioning or antibody staining.

Staging table and cell tracking in time-lapse video

To assemble a staging table of rosette formation and internalization, a single embryo was incubated at 26ºC and photographed hourly. Timing was verified by observation over several dozens of embryos and comparison to existing staging tables (Browne et al. 2005). For filming, embryos were left in ASW or embedded in 1.5% low melt agarose in ASW in glass bottom dishes (Mattek, P35G-1.0-14-C). The agarose was heated to boiling and then cooled to 37º C. After solidifying, dishes were

filled with 70% ASW to prevent a lethal increase in salinity over long filming times. Capture occurred at 10x in 5-minute intervals on an inverted scope (Zeiss Axiovert 200m using a Hammamatsu Orca-ER or Orca-R^2 camera, respectively) with PerkinElmer's Volocity Acquisition software (v. 5.5.1 or v. 5.4.1). Tracking was accomplished by coloring cells frame by frame using Adobe Photoshop.

Thick sectioning

Embryos were embedded in plastic molds with 2.5% low melt agarose (Promega V211) in PBS. The agarose mixture was heated to boiling and then cooled to 37º C. Embryos were oriented using forceps and a hypodermic needle. Each block was sectioned into a bath of PBS using a Pelco 101 vibratome (speed 5.5, amplitude 4.5). Sections were approximately 80μm thick.

Antibody and phalloidin staining of whole embryos and sections

Antibody staining was performed according to published protocols (Rehm et al., 2009a) with the following minor modifications. Phalloidin was added to application of the secondary antibody (1:40 of 6.6μM phalloidin stock solution). We used the following antibodies and phalloidin at these concentrations: Rat anti-Tubulin (Abcam; 1:500), Alexa fluor 488 and 546 (Molecular Probes; 1:1000), phalloidin 488 (Invitrogen, 1:40 of 6.6μM stock).

Microinjection

Microinjection for lineage tracing and ablation was done as previously described (Gerberding et al., 2002; Price et al., 2010). We injected FITC (Fluorescein isothiocyanate–dextran, Sigma FD250S) at a concentration of 2mg/ml (diluted in deionized water) or 5mg/ml; TRITC (Tetramethylrhodamine isothiocyanate–dextran, Sigma T1287) at a concentration of 2mg/ml; and/or an mRNA encoding a nuclear-localized dsRed protein (dsRed-NLS, Gerberding et al., 2002) at a concentration of 1μg/mL. Embryos were then kept at either 26º C or at 18º C. In all cases, the injected amount was approximately 14 picoliters for micromeres or 113 picoliters for macromeres.

RESULTS

Timing of and movements during rosette formation and internalization

Current staging tables describe stages prior to, during, and after gastrulation. Respectively, these are the soccerball stage (S6, ~12 hours post fertilization (hpf), the rosette stage (S7, ~18), and the germ cap stage (S8, ~25 hpf). To add to existing knowledge about the process of rosette internalization, I created an hourly staging table beginning at soccerball stage and progressing until the rosette is no longer discernible from the epithelial sheet in brightfield. I found that rosette formation begins at 14h, when condensation in the rosette makes those cells appear more compact than neighboring cells. As previously explained elsewhere, "condensation" at this stage in the *Parhyale* literature describes the movement of yolk from cells to the interior of the embryo. The yolk ranges from purple to amber in *Parhyale* embryos. Prior to

condensation, cells are large and yolky with the nuclei visible in brightfield as a clear area surrounded by white, refringent cytoplasm. During condensation, the nuclei and associated cytoplasm moves to the apical surface. The yolk then either leaves the cell or is pinched off from the cell, leaving behind the nucleus and associated cytoplasm. Condensation of the yolk to the interior occurs through an as yet unknown mechanism (Alwes et al., 2011; Fig. 2.2). By 16h, epithelial sheet cells are obvious as ectoderm precursors on the opposite side of the embryo also begin to condense. Rosette internalization is underway at approximately 17h of development, and it is important to note that the ectoderm precursors adjacent to the rosette have condensed at this point and are difficult to discern from rosette cells using only brightfield microscopy (Fig. 2.1, 2.5). By approximately 20 hours of development, the rosette is completely underneath the epithelial sheet (Fig. 2.1).

I also manually traced cells in the rosette and the epithelial sheet during gastrulation through 129 frames of timelapse video using Photoshop© (Fig. 2.1, supplemental movie 1). Tracing of a rosette cell and an epithelial cell (Fig. 2.1) illustrates the movement of the cells toward one side of the egg during rosette internalization. In addition, the apical domain of the traced Mav cell appears to shrink during internalization (purple cell, Fig. 2.1) while the cytoplasmic area surrounding the nucleus of the epithelial cell appears to remain roughly the same (red cell, Fig. 2.1). However, the membrane of the epithelial cell initially encompasses the white, refringent cytoplasm as well as the more blotchy and dark yolk. As rosette internalization progresses, the cell membrane shrinks to the cytoplasm surrounding the nucleus (dotted line, Fig. 2.1). This indicates yolk extrusion. Although cells in the rosette and epithelial sheet do divide during gastrulation (Gerberding et al., 2002; Browne et al., 2005; Price and Patel, 2008; Alwes et al., 2011), yolk extrusion accounts for the vast change in cell size in cells of the epithelial sheet before and after rosette internalization (Fig. 2.2).

My observations of rosette formation and internalization fell into three overlapping events: 1) yolk extrusion (condensation), 2) the rosette migrates inward and the epithelial sheet undergoes epibolic movements, and 3) both the rosette and epithelial sheet move toward one side of the egg (summarized Fig. 2.5). When viewed vegetally, the direction of migration is always away from the region occupied by precursors of the somatic mesoderm and endoderm.

Bottle cells in the rosette

If the rosette is actively internalizing, then rosette cells should have cell-shape changes that are characteristic of migrating cells. To look for the presence of bottle cells in the rosette, I lineage traced Mav with dsRed-NLS and stained embryos and thick sections of embryos at the rosette stage (S7) for actin and/or tubulin. We found that some Mav descendants exhibit bottle cell morphology with an apico-lateral concentration of actin (Fig. 2.3). Of 10 embryos analyzed through either thick sectioning or confocal microscopy during gastrulation, we observed 8 with bottle cells in Mav descendants (representative embryos in Fig. 2.3). It should be noted that the absence of bottle cells in some of the samples could be due to loss of the appropriate section and does not conclusively indicate a lack of bottle cells in those specimens. The

presence of bottle cells indicates that the rosette is a potential site of active cell migration. The apico-lateral concentration of actin may indicate an apical constriction mechanism that relies on acto-myosin contractility.

Germline descendants in the 10 embryos were never observed to apically constrict at the rosette stage. However, I find that at the time of rosette formation (14h) g descendants have long, tubulin-rich protrusions trailing from their rear edges (Fig. 2.4; Extavour, 2005). Tubulin is a main component of the cytoskeleton, and this unique configuration of tubulin may indicate a role for it in the mechanism of germline internalization.

The germline migrates inward after Mav

Some controversy exists regarding the order of internalization between Mav and g descendants. Before gastrulation, g descendants are visible as a cluster at the edge of the rosette (Fig. 2.4; Fig. 2.5; Alwes et al., 2011) During gastrulation, we observed that g progeny migrate over the internalizing Mav cells and then move inward either randomly or as a group (Fig. 2.4). Our observation that the germline migrates inward after Mav descendants directly conflicts with Alwes et al. (2011), but agrees with Price and Patel (2008). It is possible that the conflict is due to methods of lineage tracing; Price and this study injected lineage tracers, which may be an advantage over tracking cells in brightfield (Alwes et al., 2011) because the cells are easier to visualize. Alternatively, the injection of lineage tracers could cause the cells to behave differently during development, suggesting that the order of internalization of Mav and g progeny is flexible and does not affect later development.

DISCUSSION

My categorization of three overlapping processes provides guidelines for investigations into cell shape change and migration. Whether the three characteristics I observed (yolk extrusion, inward rosette migration, and the movement of the rosette and epithelial sheet to one side of the embryo) are intertwined remains unknown. It is possible, for example, that a delay in yolk extrusion from one cell to another is responsible for the movement of the rosette and epithelial sheet to one side of the egg. From our observations, the rosette cells are the first to condense, followed by the condensation of ectoderm precursors adjacent to and on the animal half of the embryo. Then, as the epithelial sheet migrates, condensation of the remaining ectoderm precursors in between the rosette and epithelial sheet occurs. The movement of yolk from cells to the interior of the egg involves shifting a large portion of each cell to a new location, and it is possible that this extrusion enables or constrains the migration of cells during rosette internalization. Future studies could focus on describing and understanding the process of yolk extrusion during *Parhyale* development through a fine time series of thick sections and cytoskeletal staining.

The discovery of bottle cells during rosette internalization is the first cytoskeletal evidence supporting ingression or invagination as a mechanism. Discerning between ingression and invagination will require further description. For example, a characteristic of ingressing cells is often that they only influence single or small populations of cells while invagination often implies the deformation of a larger

portion of an epithelial sheet. Future work might quantify the changes that I observed during cell tracking in time-lapse video by calculating the extent of change over time in specific Mav cells. This technique would also answer whether only a sub-population of Mav cells apically constricts and if those changes influence adjacent cells. Cell-cell junctions might also be informative. The theory that apical constriction in a subset of cells can provide enough mechanical force to cause an epithelium to buckle during invagination was first posited in 1980 (Odell et al., 1980; 1981). It relies on the observation that cells in an epithelium are joined through actin-based junctions in the apical domain of cells. Because of these connections, when a cell constricts at its apex, it pulls adjoining cells toward its center. This is the movement that occurs when the mesoderm of *Drosophila* begins to invaginate (Leptin and Grunewald, 1990; Sawyer et al., 2010). Work focusing on changes in cell-to-cell junctions during rosette internalization may be informative as to whether ingression or invagination is at work.

That some Mav descendants have bottle cell morphology indicates that apical constriction might be responsible for their internalization. To confirm whether the apices are actively constricting, further descriptive and functional studies are necessary. Future studies could examine changes in cell-cell junctions during internalization, as well as look to the cytoskeleton immediately beneath the apical cell membrane for a rippling or bending phenotype that indicates contracting actin filaments and endocytosis of apical membrane (Lee and Harland, 2007; 2010). Functional tests with pharmacological cytoskeletal inhibitors and knockdown constructs would inform whether conserved apical constriction regulation is at work.

Finally, my observation that g internalizes separately and does not apically constrict implies that the two lineages of the rosette act as individual groups. This kind of cell autonomy confirms previous reports of normal blastomere migration pre-gastrulation despite the ablation of different micromeres (Alwes et al. 2011). Thus it is important to treat the descendants of each blastomere in *Parhyale* as having unique and intrinsic signals, even at this early stage.

Because it directly conflicts with Alwes et al. (2011), but agrees with Price and Patel (2008), our observation that g migrates inward after Mav cells suggests that different modes of studying cell lineage can give different results. Furthermore, our observation that g cells migrate over internalizing Mav cells suggests that the internalizing cells converge on a gastrulation center as in the amphipod *Orchestia cavimana*. Previous reports indicate that *Parhyale* does not have a visible blastopore, but the movement of cells toward a single area for internalization during this phase combined with our observation that some cells are bottle cells suggests that a blastopore (as defined as a gastrulation center through which cells internalize) does exist. How the cells of the somatic mesoderm and endoderm internalize remains unknown, but they appear internalize through a temporally and spatially distinct mechanism from the cells of the rosette (Gerberding 2002; Browne et al., 2005; Price and Patel, 2008; Alwes et al., 2011). The significance of the presence of a blastopore is discussed in chapter six.

Figure 2.1. Rosette internalization formation and internalization.
(Left). Hourly staging table of vegetal and lateral view of rosette formation and internalization. Time is indicated in hours post fertilization at 26ºC. Blue asterisks indicate the approximate location of the rosette, red asterisks indicate the location of the epithelial sheet. (Right). Stills from a timelapse video with one cell of the rosette (purple) and of the epithelial sheet (red) outlined using Photoshop ©. Stills are before (top), during (middle) and after (bottom) rosette internalization. Traced area covers the nucleus and surrounding cytoplasm. Dashed white line indicates cell boundary of the epithelial sheet cell before (top) and after (bottom) condensation. White X marks the location of the epithelial cell at the onset of rosette formation during (middle) and after (bottom) rosette internalization. Total elapsed time from top to bottom still is 6 hours. Numbers in red at top right are from filming, showing total elapsed time since the beginning of the film in hours: minutes: seconds. Scale bars are approximately 100μm.

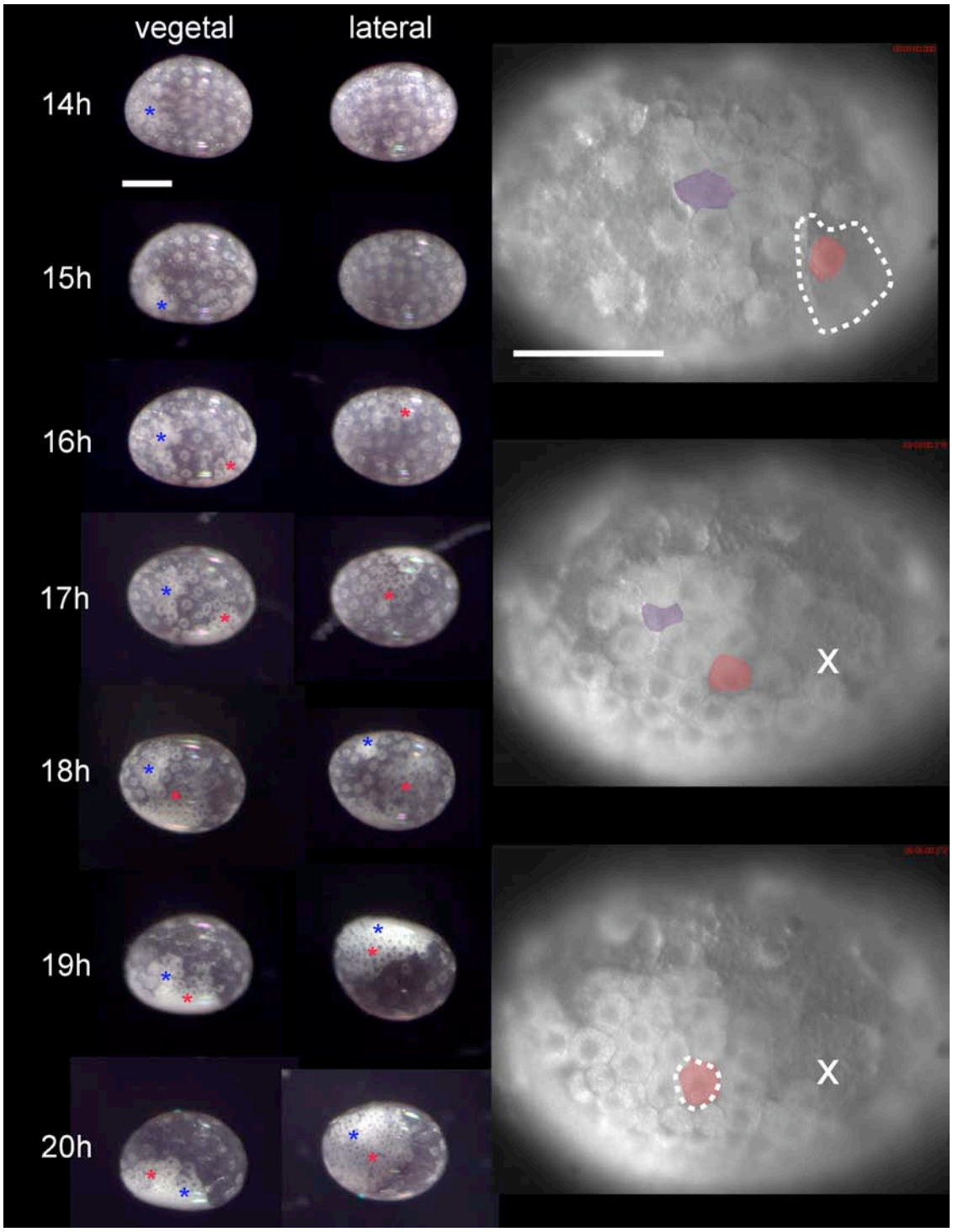
vegetal
lateral
14h
15h
16h
17h
18h
19h
20h
X
X

Figure 2.2. Condensation of the yolk.
Condensation of the yolk occurs during gastrulation. Confocal projections through an 80μm section of 12h (A) and 20h (B) *Parhyale* embryo. Embryos were microinjected at the 4- or 8-cell stage to label the lineages of the rosette (dsRed-NLS, red nuclei). Left, 10x view of the section. Area within the white box is pictured on the right (A', B'). Scale bars are 100μm.

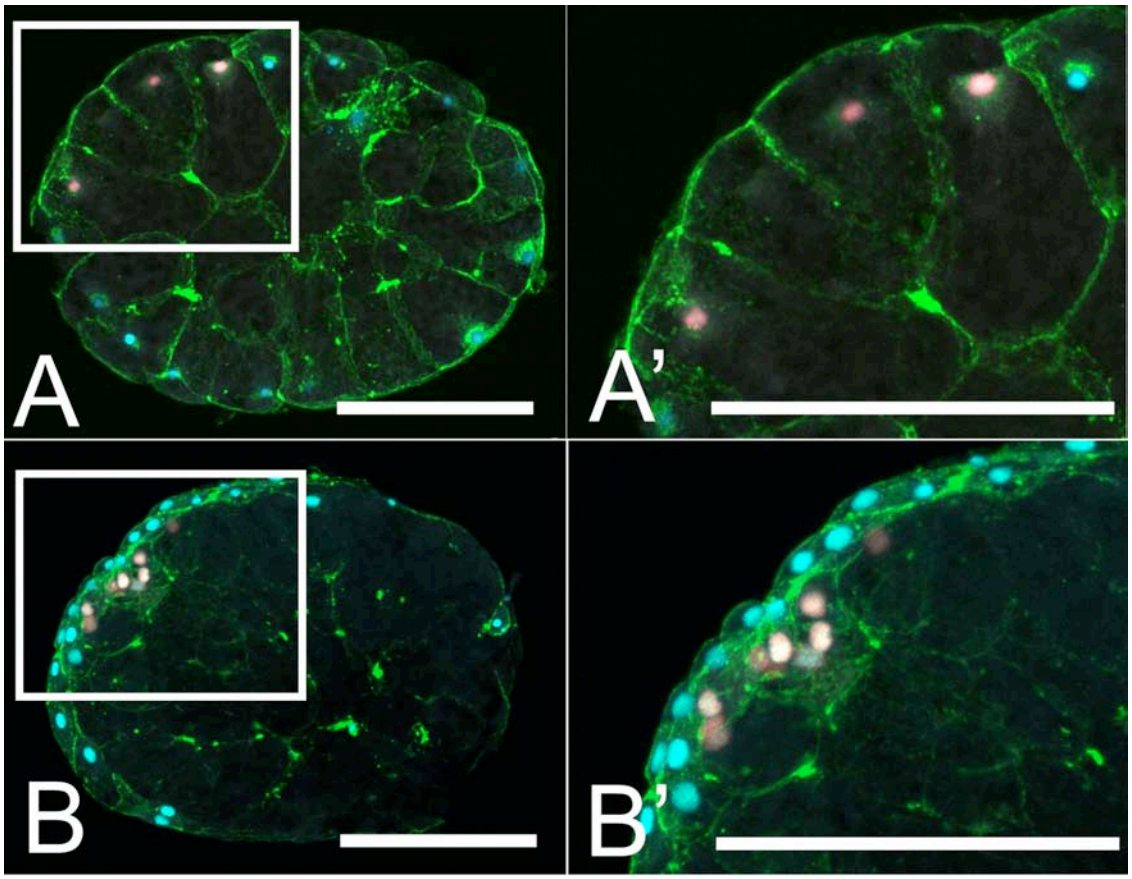
A
A'
B
B'

Figure 2.3. Mav daughters exhibit bottle cell morphology during rosette internalization.
(A-A'') Confocal projection showing the rosette of an 18h embryo stained with phalloidin (green). Red line = XZ plane shown in A', blue line is YZ plane shown in A''. Asterisks indicate bottle cell outlined in dashed white line in A-A''. (B) Confocal projection of an 80μm section through an 18h embryo. Mav was injected at the 8-cell stage with dsRed-NLS mRNA (red nuclei). Area indicated by bracket is shown in B'. (B') Fluorescent overlay of phalloidin stain (green) and dsRed-NLS (red). Arrows indicate bottle cells with an apico-lateral concentration of actin.

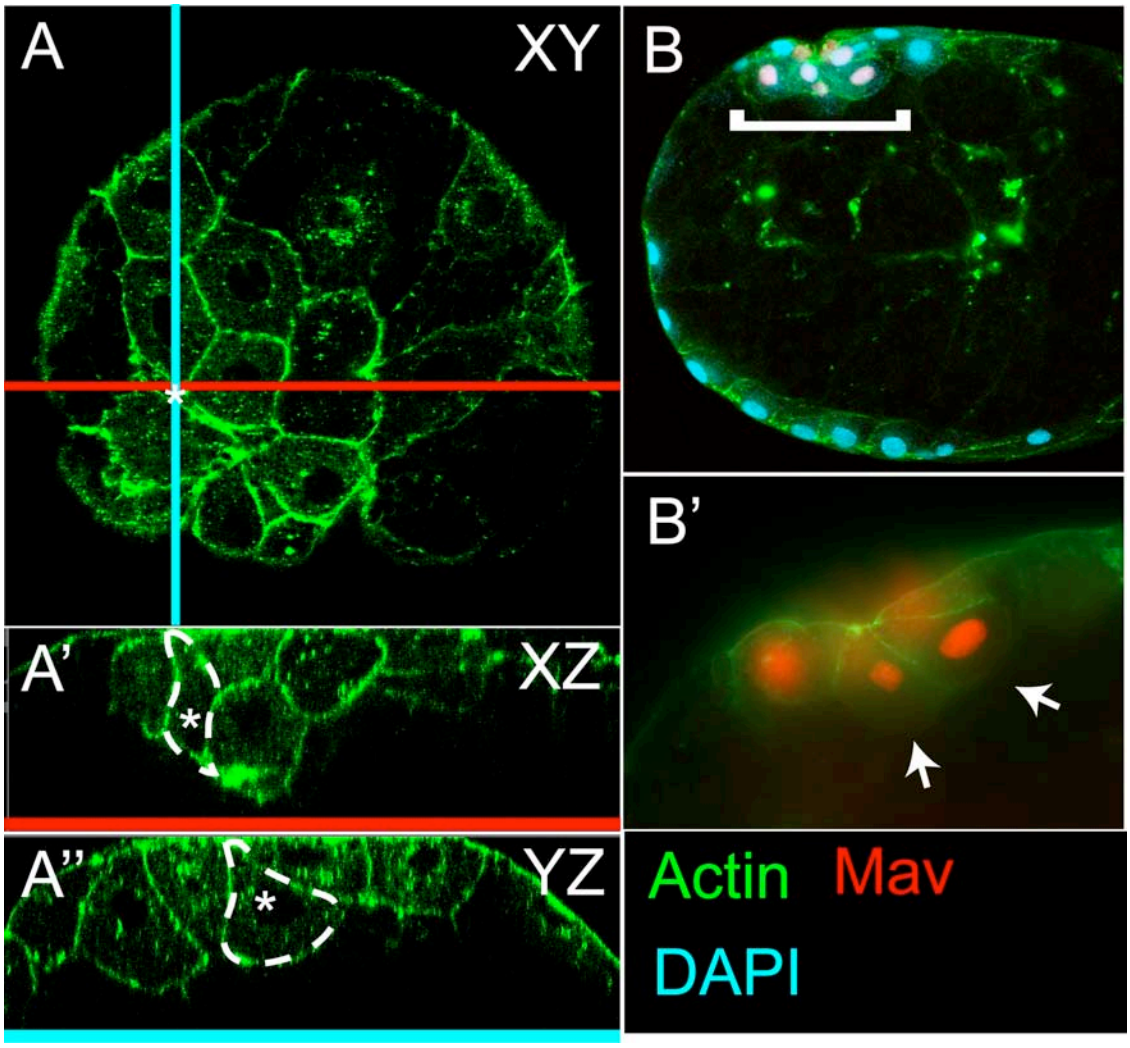
A
XY
A'
XZ
A''
YZ
B
B'
Actin
Mav
DAPI

Figure 2.4. The g cells ingress separately after ingression/invagination of Mav cells and have characteristic tubulin staining.
(A) Stills from a timelapse video of gastrulation showing separate internalization of Mav daughters (FITC, green) and g daughters (dsRed-NLS, red nuclei) under the epithelial sheet (El, Er, and Ep daughters, TRITC, red). 13h: Entire embryo at 13h of development. 13h'-21h: Area in white box in 13h is shown throughout rosette internalization. (B) Approximately 14h embryo with lineage tracer (dsRed-NLS, red) injected into Mav/g. Left, top: Overlay of tubulin (green) and dsRed-NLS. Left, bottom: dsRed-NLS expression. Area in white box is shown to the right. Right: The dotted line contains the g-lineage. Arrowheads indicate long tubulin fibers at one end of g-cells. Compare to the smooth border of a Mav cell (arrow).

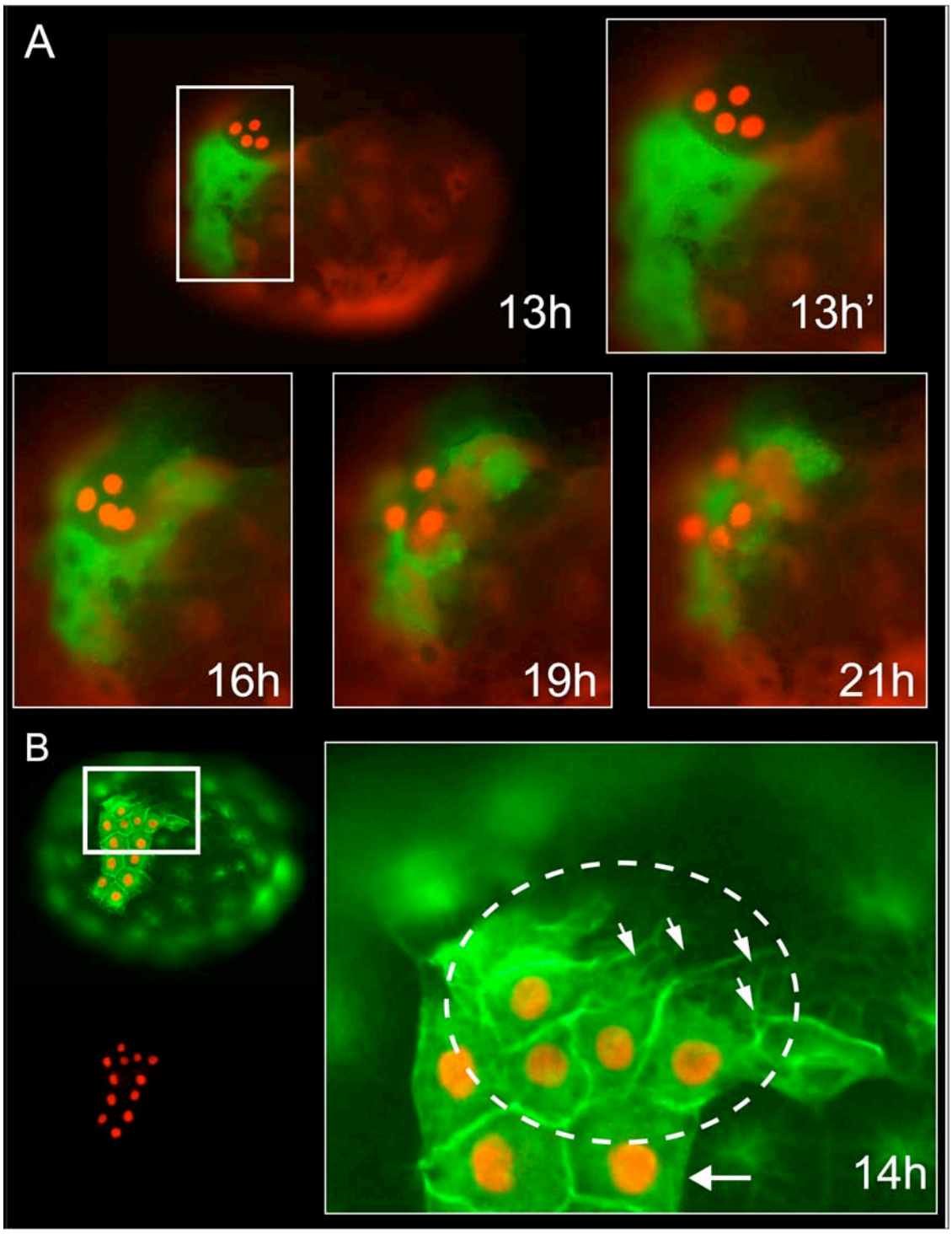
A
13h
13h'
16h
19h
21h
B
14h

Figure 2.5. Two embryos and a schematic show a vegetal view of the first phase of gastrulation.
(A) The *Parhyale* fate map at the 8-cell stage (top) and a schematic of the rosette and the epithelial sheet during rosette internalization (bottom). Lineages that give rise to the rosette are the anterior and visceral mesoderm (Mav, orange) and the germline (g, yellow). Lineages that give rise to the epithelial sheet are the left, right, and posterior ectoderm (El, Er, and Ep, respectively; blue). The left and right somatic mesoderm (ml and mr) and the endoderm (en) are not colored. Colors correspond to Price and Patel (2008). (B) Brightfield images of a single embryo at 14h, 17h, and 20h of development at 26ºC. Dashed lines estimate areas covered by the rosette (green) and the epithelial sheet (red). Arrow at 17h indicates condensing and migrating epithelial sheet cells, some of these cells originated on the animal half of the embryo. By 20h, the rosette is no longer visible because it lies underneath the condensed epithelial sheet cells. (C) The rosette and epithelial sheet move to one side of the embryo during internalization. Stills taken from a timelapse video of embryos at room temperature (~22 ºC). Images are cropped to focus on a single embryo. Embryos were microinjected at the 8-cell stage to label the lineages of the rosette (FITC, green) and the epithelial sheet (TRITC, red). Stills were chosen to match staging of brightfield images; total elapsed time from left to right image is 8 hours. X indicates the approximate center of the rosette before internalization.

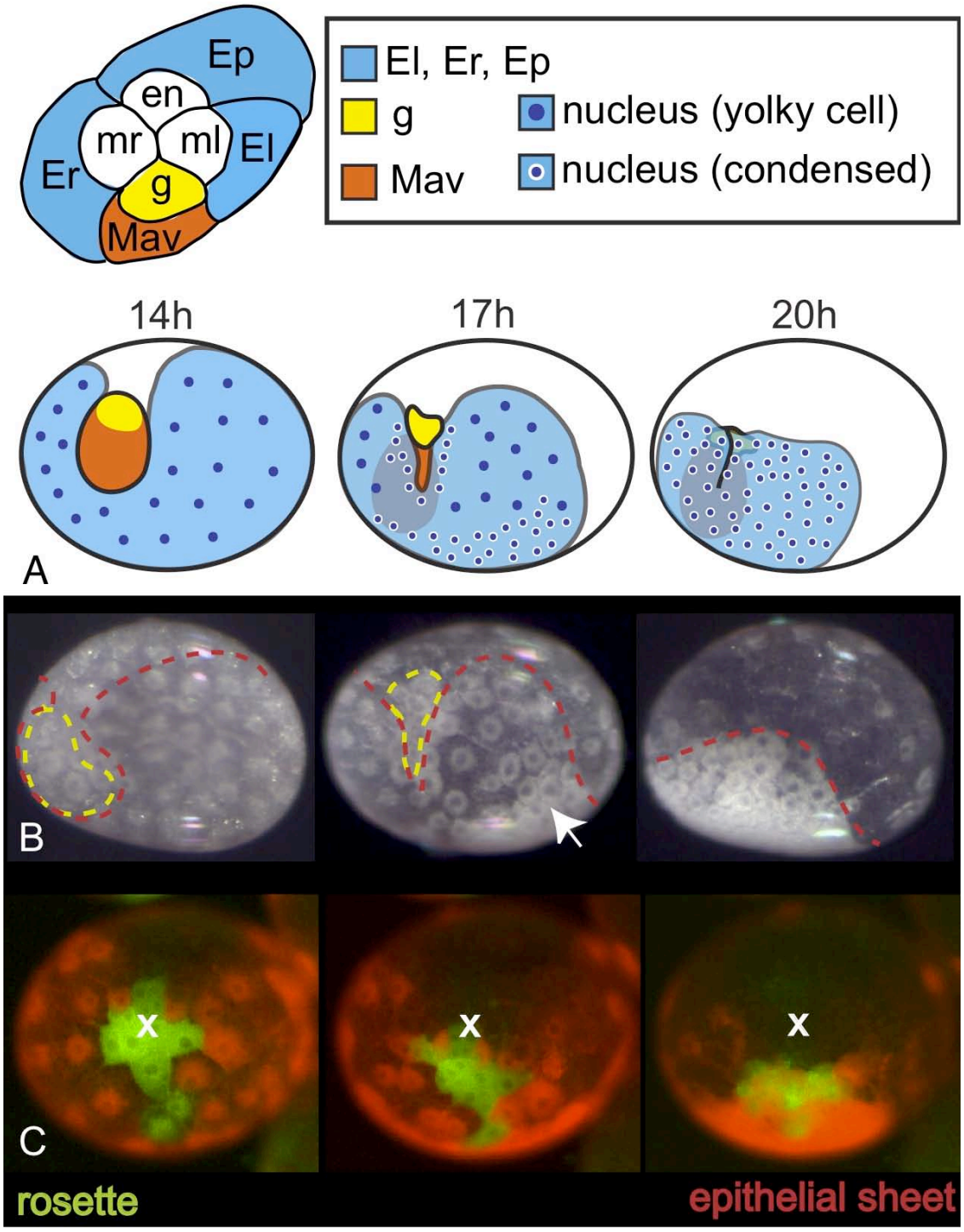
Ep
en
mr
ml
El
Er
g
Mav
El, Er, Ep
g
Mav
nucleus (yolky cell)
nucleus (condensed)
14h
17h
20h
A
B
C
x
x
x
rosette
epithelial sheet

Chapter III: Cellular interactions during rosette internalization.

SUMMARY

Whether populations of cells act autonomously or not during morphogenesis indicates the ability of groups of cells to induce, either molecular or mechanistically, cellular behaviors in neighboring cells. Although hypotheses exist for the extent of cellular interaction during *Parhyale* rosette internalization, this is the first study to directly manipulate cells in the rosette and epithelial sheet. In this chapter, we use photo and manual ablation to investigate whether the rosette or the epithelial sheet is necessary for the first phase of *Parhyale* gastrulation. We find that without the rosette, the cells of the epithelial sheet migrate the same distance as they would have in the presence of the rosette. When cells of the epithelial sheet adjacent to the rosette are ablated, the rosette internalizes normally. Finally, when either Mav or g is ablated, the remaining portion of the rosette is able to internalize.

INTRODUCTION

In vivo, the cells in multicellular organisms are always parts of a whole. Therefore, studies of cellular behavior during morphogenesis must include how changes in behavior influence neighboring cells and cell populations. One line of investigation considers morphogenesis as a mechanical process where cells and cell movement are directly affected by changes in the physical properties of the cells and/or their relationship with neighbors. Another line of investigation considers morphogenesis from a molecular standpoint. Via cell-to-cell communication or intrinsic cues, molecules regulate cellular changes that govern cell shape, polarity, and migration. With both lines of thought, it is important to first observe and establish the extent of autonomy and cooperation between cells and cell populations.

Autonomous cell behavior implies that the mechanical and molecular events leading to morphological change are intrinsic to the cells. This scenario is most like envisioning morphogenesis as a puzzle board; each piece has its own unique property that, if removed, is not replaced but also does not change the shape of the other pieces. Autonomous cell behavior during early development is sometimes due to an early restriction of cell fate. This describes mosaic development where the fate of early cells is specified such that deletion of that cell removes its entire lineage. *C. elegans* development is a classic example of mosacism, and in fact, the gastrulation movements of the cells in this organism are autonomous (Nance et al., 2005).

On the other hand, a cell or groups of cells with mutual influence implies mechanical and molecular events that may be unique to each cell but that affect neighboring cells. This is the case for the invaginating cells during *Drosophila* gastrulation. Ectopic expression of ventralizing genes can cause a furrow to form anywhere on the *Drosophila* embryo, and disruption of genes that confer lateral and dorsal fate does not prevent ventral furrow formation (Anderson et al., 1985; Leptin and Grunewald, 1990; Leptin and Roth, 1994; Leptin, 1995). Therefore, the genes that confer ventral fate are sufficient and necessary to the cellular behavior that causes invagination and pulls the neighboring cells toward the ventral midline. Under this

molecular control, ventral cells enact their behavioral programming, which in turn drives the movements of adjacent cells.

A classic method of studying cellular interactions is through microsurgery techniques like isolation and ablation studies. The efficacy of these techniques is best shown in gastrulation work with *Xenopus laevis*. "Keller explants" are flat cultures of dorsal mesendoderm and ectoderm dissected directly from pre-gastrula *Xenopus* embryos. These explants enact complicated gastrulation movements outside of the embryo, careful and detailed analysis of which has revealed much about specific regional behavior and molecular determination of different zones in the *Xenopus* embryo (Keller and Danilchik, 1988; Winklbauer and Nagel, 1991; Keller and Shook, 2008).

Among invertebrates, as previously discussed, work with *C. elegans* gastrulation includes isolation experiments of dissected blastomeres. Culturing pre-gastrula blastomeres in isolation and with various cell pairings revealed that each is capable of going through gastrulation movements without cell-cell contact (reviewed in Nance et al., 2005). This indicates that *C. elegans* gastrulation proceeds through autonomous, intrinsic signaling and does not rely on an inductive mechanism. Similar work in the decapod crustacean *Sicyonia ingentis* suggests dependence on an inductive mechanism during gastrulation behavior. Hertzler et al. (1994) cultured blastomeres isolated from 2-, 4-, 8-, and 16-cell *S. ingentis* embryos found that the mesendodermal D blastomere undergoes gastrulation regardless of its cell-cell contacts. Moreover, without the D blastomere, the other blastomeres never progress beyond blastulae (Hertzler et al., 1994). This suggests that cells during gastrulation in *S. ingentis* rely on an inductive signal from the D blastomere to go through normal gastrulation movements. The nature of this signal remains unknown.

In *Parhyale*, isolation and ablation studies have revealed an interesting mix of autonomous and cooperative cellular interactions during development. Isolation of individual blastomeres at the 2-, 4-, and 8-cell stages indicates that germline identity is defined by segregation of specialized cytoplasmic determinants that occurs as early as the 2-cell stage(Extavour, 2005). Cytoplasmic segregation at such an early stage normally implies autonomous specification and by extension cell behavior. However, careful ablation and lineage tracing of different blastomeres at the 8-cell stage revealed that ablation of any blastomere that will give rise to the ectoderm or mesoderm can be compensated for by other cells of the same germ layer after gastrulation (Price et al., 2010). Furthermore, single cell laser ablations during germ band development revealed that different portions of the developing ectoderm vary from being completely autonomous to relying heavily on inductive molecular cues for appropriate positioning (Vargas-Vila et al., 2010). Cells during *Parhyale* morphogenesis are clearly influenced by both intrinsic, autonomous signals and extrinsic, cooperative relationships.

In this chapter, I investigate the extent of cooperation between the rosette and the epithelial sheet during gastrulation using manual and photoablation. I find that the cells of the rosette and the epithelial sheet are autonomous and that Mav and g descendants are able to gastrulate without each other.

MATERIALS AND METHODS

Photoablation

I performed photoablation of different cell populations as previously described (Table 1) (Price et al., 2010). Broods of *Parhyale* embryos develop near-synchronously. Embryos from a single brood were injected, allowed to develop to the desired stage, and then unhealthy or mis-injected embryos were discarded. Half of the remaining embryos were subject to photoablation, and the other half were used as controls that were microinjected but not photoablated. For filming, ablated embryos were re-embedded alongside control embryos.

Modifications were as follows: widefield ablations were carried out on an inverted scope (Zeiss Axiovert 200m or an AxioObserver.z1) in a glass-bottomed dish. To ensure maximum light exposure and to prevent movement, embryos were embedded and oriented such that FITC injected cells were against the glass. Embryos were then exposed to either 100% power from a mercury lamp at 10x or 5x through Zeiss filter set 17 (excitation: BP 485/20) for 30 min.

Specific cells within a FITC-labeled area were targeted for photoablation on a Zeiss 700 confocal using the "regions" and the "photobleaching" functions, which allows laser scanning of a specific region and over a specified depth (Fig. 3.6 A-A', within dotted line). Scanning proceeded at 100% laser power for 15 minutes. The defined region fell within cell boundaries to prevent accidental ablation of neighboring cells. The one drawback is that the field of view is smaller on a confocal, restricting the number of embryos that can be ablated at the same time. Thus, in any brood, only two embryos were subject to photoablation at a time to keep the stage of ablation consistent. The most immediate indicator of successful photoablation is photobleaching of FITC fluorescence (Price et al., 2010). We used photobleaching as a marker for ablation, and confirmed through filming that ablated cells no longer divide and eventually lyse and are extruded from the embryo or resorbed. We did not observe any difference in the behavior of remaining cells in embryos where the cells lysed or were resorbed.

Manual ablation

I manually ablated Mav at the 8-cell stage. I injected a relatively large amount (~520 picoliters) of a concentrated mixture of DNAse (10 units; Roche, # 04716728001), RNAse (RNAseA .01mg, Sigma # R-5000; RNAse T1 10 units, Sigma R-1003), and TRITC (10mg/ml; 22 μl), incubated the embryos at 31ºC for two hours, and then removed the contents of the dead cell using capillary action from a pulled glass needle broken to a wide bore (.024 mm). After the two-hour incubation, the injected cell had ceased dividing, lost integrity, and yolky cytoplasm was often spilling out of the injection site. I used the glass needle to remove all visible cell remains through the injection site, making new holes in the chorion if necessary. Embryos were then kept at 26º C.

Cell tracing and analysis

Cell tracing was done over 157 frames (13h) using Volocity Processing software (PerkinElmer, v. 5.4, "Track Objects Manually"), beginning with embryos approximately 12 hpf (soccerball stage, S6) and progressing through germ cap formation (25 hpf, S8). Tracing was only done on embryos that survived the entire period of filming (24 - 48 hours).

Different cells migrate different distances due to the migration of the rosette and epithelial sheet to one side of the egg. Therefore, I traced three cells in each embryo from different regions of the vegetal epithelial sheet (Fig. 3.3, 3.4). Two cells were in contact with the rosette; a "near" cell on the side toward which migration would occur, and a "far" cell on the opposite side. The third "farthest" cell was a cell one-cell width away from the rosette on the side away from which migration would occur (Fig. 3.3, 3.4). From my observations and based on previous work, all cells traced were progeny of either El or Er (Alwes et al., 2011). Cleavage during this time period is asynchronous and the spindles are randomly oriented(Alwes et al., 2011). In cases of cell division, the daughter closest to the rosette was traced. If the daughters were equidistant from the rosette, a daughter was chosen at random.

Manual tracking in Volocity software creates a track (see Fig. 3.3), and then Volocity provides data about track length and displacement. Length is equivalent to the total distance migrated. Displacement measures the shortest distance between the start and endpoint of a track. All measurements were calibrated to μm based on the lens used for the film (5x or 10x). An unpaired, 2-tailed, Student's T-test was used to look for significant differences between means. Statistical analysis and graphs were created using Microsoft Excel.

RESULTS

I performed various cellular manipulations and observations at different stages of development during *Parhyale* gastrulation. We refer to the 4-cell (S3, ~7 hpf) at 26ºC), 8-cell (S4, ~8 hpf), soccerball (S6, ~12 hpf), rosette (S7, ~18 hpf), germ cap stages (S8, ~25 hpf), and late appendage formation (S21, ~120hpf). All staging was done according to Browne et al. (2005). Soccerball marks the stage just before the rosette begins to form, the rosette stage is mid-rosette internalization, and the germ cap stage is ~ 5 hours after the rosette is completely internalized. Late appendage formation is approximately halfway until hatching at 10 days hpf.

Table 1. Summary of ablation experiments and results

Region	Stage	Replicates[1]	Total n[2]	Results
Photoablation				
Entire rosette	soccerball	6	14	Epithelial sheet migrates without the rosette
Entire rosette	8-cell	3	10	The ectoderm still aggregates into a germ cap without the rosette.
Portion of Ep	soccerball	1	3	Epithelial sheet migrates away from the ablated cells
Portion of El or Er	soccerball	3	5	Epithelial sheet migrates away from the ablated cells.
Leading edge	soccerball	3	6	Rosette internalization normal, epithelial sheet movement shows a range of phenotypes
Mav	soccerball	5	15	g unable to internalize
g	soccerball	4	10	Mav internalizes normally
Mav	8-cell	2	8	g unable to internalize
g	8-cell	3	8	Mav internalizes normally
Manual ablation				
Mav	8-cell	2	6	g internalizes and migrates

1. Experiments that were pooled to generate the final number included in analysis.
2. Total number of embryos included in analysis.

Mav and g can internalize independently

Although grouped together in the rosette, Mav and g descendants behave differently during gastrulation. We therefore investigated the extent to which Mav and g cells depend on each other for proper internalization. First, I ablated Mav at the 8-cell and soccerball stages. Photoablation of Mav at either the 8-cell or soccerball stage prevents normal internalization of g during rosette internalization (Fig. 3.1). Whether the germline in these embryos internalizes later remains unknown. To investigate whether g is simply unable to bypass the cellular debris left by photoablation of Mav, I manually ablated Mav at the 8-cell stage. Manual ablation results in normal migration of the germline, as confirmed by antibody staining for the germline marker Vasa late in development (Fig. 3.2). Vasa is a highly conserved transcriptional repressor restricted to the germline throughout metazoa and cross-reactive antibodies have previously been used to identify the germline in *Parhyale* (Extavour, 2005; Ozhan-Kizil et al., 2009). In normal embryos, g descendants appear as a cluster in the center of the developing germ band that then splits into two bilaterally symmetric groups as the cells migrate to their final location within the somatic gonads (Gerberding et al., 2002; Browne et al., 2005, Fig. 3.2).

These results indicate that germline migration requires a clear path to internalize, i.e. g descendants cannot bypass an obstruction along their normal inward migration. When the obstruction is removed, g has no problem internalizing, suggesting that the signal for g migration is intrinsic and does not rely on normal Mav development.

I also confirmed previous work that found that ablation of g at the 8-cell stage does not affect gastrulation (Table 1). This is also true for ablating g descendants just before gastrulation (Alwes et al., 2011).

Rosette and epithelial sheet migration are autonomous: Rosette ablation

If rosette internalization depends on cooperative behavior between the rosette and epithelial sheet, then ablation of either population should arrest gastrulation. When the rosette is photoablated just before gastrulation, cells in the epithelial sheet do not exhibit significant differences in migration length or overall displacement (a measure of the shortest distance from start to endpoint) (Figs. 3.3 and 3.4, Supplemental movie 2). P-values for all migration length comparisons were insignificant (near: .47, far: .42, farthest: .71). P-values for displacement comparisons were also insignificant (near: .31, far: .16, farthest: .10). I did observe that migrating epithelial sheet cells in control embryos turn toward the rosette, whereas cells in photoablated embryos travel in a relatively straight line (Fig. 3.3). In addition, the epithelial sheet appears to condense normally. These results suggest that the cue for migration and condensation of the epithelial sheet does not originate in the rosette, but is an intrinsic signal among ectoderm precursors. That the rosette has some directional control over the migration path of cells in the epithelial sheet is interesting, and may indicate that the rosette exerts some force on the ectoderm cells. The extent of the rosette's influence, however, governs only the direction of migration as ectoderm precursors still migrate the same distance without it.

When the rosette is photoablated or manually ablated at the 8-cell stage, approximately 8-hours prior to epithelial sheet formation, a normal-looking germ cap still forms (Fig. 3.5, Table 1). Confocal images of these embryos reveal that the ectoderm precursors appear to condense and migrate normally (Fig. 3.5). Because this ablation takes place so long before any putative signaling event, this supports the conclusion that no signaling from the rosette influences formation and migration of the epithelial sheet.

I performed two additional ablations as controls (Table 1). There is ample evidence in the literature that when an epithelium is scratched, cells adjacent to the wound can migrate to close it in a wound-healing response (for review see (Martin and Parkhurst, 2004). To test whether rosette ablation results in a wound response, we ablated a portion of the epithelial sheet adjacent to the rosette (n=6; Fig. 3.6; Table 1; supplemental movie 5) or a portion of epithelial cells at a distance from the rosette (i.e., descendents of Ep) (n=3; Table 1). If the epithelial sheet response to rosette ablation were a wound-response, then ablating another portion of the epithelial sheet should cause the cells adjacent to that site to migrate over it. When I ablated a portion of the epithelial sheet adjacent to and roughly the same size as the rosette, the rosette internalized normally and the remaining epithelial cells migrated to cover the rosette but not the ablated area (Fig. 3.6B). When we ablated a portion of Ep cells, the remaining epithelial sheet cells migrated away from the dead cells (Table 1). In each case, the remaining cells of the epithelial sheet did not obviously change their migration paths to compensate for the ablated cells. Taken with the observation that epithelial cells travel in a straight line and do not migrate to cover an ablated rosette,

these results indicate that epithelial sheet migration when the rosette is ablated is not a response to wounding.

Rosette and epithelial sheet migration are autonomous: Ablation of the leading edge of epithelial cells

Because ablation of the entire epithelial sheet just before gastrulation would likely be a lethal ablation, I focused on the epithelial sheet cells touching the rosette. This leading edge of cells is the most likely candidate for any interaction between the rosette and epithelial sheet because it comprises the first cells to cover the rosette.

When the leading edge of epithelial cells is killed just before gastrulation, condensation and inward migration of the rosette slows but occurs normally (Fig. 3.7). However, ablation of the leading edge results in various phenotypes in the remaining epithelial sheet cells (Fig. 3.7; 3.8; supplemental movies 3a and 3b). In some cases (2/6), the dead leading edge cells were absorbed into the embryo and the epithelial sheet condensed normally (Fig. 3.7, supplemental movie 3a). In the majority of cases (4/6) at least one row of ectoderm cells behind the ablated leading edge failed to condense and migrate and instead retained its yolky, pre-migration size and phenotype. In addition, in these embryos it appeared that the rosette remained at the point of internalization rather than migrating to one side of the embryo (Fig. 3.8, supplemental movie 3b).

First, these results show that inward migration of the rosette does not require viable leading edge cells. Therefore, the signal for rosette migration is intrinsic to rosette cells. Second, given that in the majority of cases the rosette appears to remain stationary after rosette internalization when the leading edge is ablated, migrating inward and moving toward one side of the egg appear mechanistically distinct. Migration after internalization may rely on viable leading edge cells, which is discussed below. Finally, viable leading edge cells may influence condensation of the remaining epithelial sheet cells and migration of the rosette and epithelial sheet to one side of the egg. The most straightforward explanation is that the bulk of cellular debris from dead leading edge cells prevents the condensation of neighboring epithelial sheet cells and, ultimately, the post-internalization migration of the rosette. The presence of some properly condensed ectoderm cells at the posterior-most end of the epithelial sheet implies that those cells have enough distance from the cellular debris of the leading edge to be unaffected (Fig. 3.8).

However, in our rosette ablation experiments, I never observed failure of neighboring epithelial cells to condense and migrate; even early ablation of Mav/g blastomeres, which at the eight-cell stage comprises approximately one fourth of the embryo, does not generate enough debris to prevent proper epithelial sheet condensation and migration. An alternative scenario is therefore that the leading edge of the epithelial sheet possesses a signaling center that induces or enables post-internalization migration of the rosette and/or condensation and migration of the remaining epithelial sheet cells. Based on lineage tracing, all of the cells we ablated were descendants of El and Er. It is possible that the cells in the leading edge have lineage specific signals. The presence of properly condensed cells may therefore be evidence for signaling among Ep daughters.

DISCUSSION

Parhyale is able to gastrulate without the rosette or epithelial sheet

This work shows that the gastrulation behaviors of the rosette and epithelial sheet are autonomous. This supports the hypothesis that early gastrulation movements rely on maternally provided determinants that are segregated via specialized cytoplasm rather than inductive signaling (Extavour, 2005; Alwes, 2011). The result that each population does not rely on the other is also consistent with the semi-autonomy of *Parhyale* morphogenesis revealed in previous work (Extavour 2005; Price et al., 2010; Vargas-Vila et al., 2010; Alwes et al., 2011). Blastomeres ablated at the 8-cell stage are capable of replacing each other within mesoderm and ectoderm "equivalency" groups (Price et al., 2010). In other words, ablation of a mesoderm blastomere (ml, mr, or Mav) triggers compensation from the remaining mesoderm blastomeres and ablation of an ectoderm cell (El, Er, or Ep) can trigger replacement from other ectoderm cells, but a mesoderm cell will never compensate for an ablated ectoderm cell. In these compensation studies, different aggregations of cells appear to work together to the exclusion of neighboring populations of cells. The same appears true for different populations of cells during gastrulation. The rosette acts separately from the epithelial sheet. It is important to note, however, that the rosette is comprised of two separate lineages that should also act independently of each other.

To further study this idea, one might expect ml and mr descendants to act autonomously from either the rosette or the epithelial sheet because their gastrulation behavior is distinct from either group. Cellular autonomy narrows the possibility for inductive signaling events and highlights the importance of maternally provided determinants. It is currently thought that zygotic transcription in *Parhyale* occurs during or just after gastrulation. The autonomy of cells through the initial phase of gastrulation indicates that their behavior is regulated by cytoplasm inherited from the mother, possibly segregated through stereotyped cleavage.

Finally, the presumptive endoderm of *Parhyale* has received little attention. Alwes et al. (2011) observe that during gastrulation en descendants assume a stereotypical arrangement and that several daughters spread into a more squamous phenotype. The contribution of these cells to the migration of the epithelial sheet and the rosette, if any, remains unknown.

Yolk condensation vs. a leading edge signaling center

Ablation of the leading edge of ectoderm cells affects the migration of the rosette to one side of the embryo and can also interfere with condensation and migration of the epithelial sheet. We hypothesize that this may be due to abnormal yolk condensation. The amount and location of yolk during embryogenesis has a profound influence on the evolution of development. For example, sea urchins in the genus *Heliocidaris* display both planktotrophic larva (larva that swim and feed; *Heliocidaris tuburculata*) and lecithotrophic larva (larva with a large amount of yolk and that are not free-swimming; *Heliocidaris erythrogramma). H. tuburculata* gastrulates through ingression of the primary mesenchyme and invagination of the gut. In contrast, presumably to accommodate a large amount of yolk, the embryos of *H. erythrogramma*

elongate and internalize their gut tissue through involution (Wray and Raff, 1991). Yolk can clearly act as a physical barrier during a process like gastrulation.

Conversely, yolk can also aid the migration of cells during gastrulation. In zebrafish, gastrulation occurs through the epiboly of several layers of cells over a large yolk cell. The yolk cell contains a syncytium of nuclei and a network of microtubules. These microtubules are essential to the completion of gastrulation movements (Krezel and Driever, 1994). Although we have not seen any evidence in the yolk of *Parhyale* for a similar mechanism of cellular migration, the interface between the yolk and the cells is worth examination. Specifically, adhesive molecules such as cadherins and integrins have not been examined in *Parhyale*. Additionally, there could be varying amounts of tension in different populations of cells due to the influence of yolk extrusion pushing or pulling groups of cells to their final locations. By using precise laser ablation and then analyzing recoil in surrounding tissues, it is possible to measure the amount of tension holding a cell or population of cells in position (Peralta et al., 2007). This could inform how the early yolk extrusion of some cells influences the positioning of other groups of cells. How the yolk influences and contributes to cell behavior during gastrulation in *Parhyale* may be a crucial part of understanding cellular morphogenetic movements and their evolution among arthropods.

An alternative hypothesis is that the leading edge of cells contributes to the normal development of nearby epithelial cells through an as yet undetermined signal. *Drosophila* dorsal closure is a well-understood invertebrate example of an epithelium with a leading edge that influences morphogenesis. Dorsal closure in *Drosophila* occurs late in development when the extended germ band retracts, causing a canoe-shaped interruption in the dorsal epidermis that is covered by the amnioserosa, a transient epithelium. Over the course of dorsal closure, the epidermis draws together over the amnioserosa, eventually zipping shut at the dorsal midline. The leading edge of the epidermis forms a contractile acto-myosin "purse string." Contraction of the purse string and elongation of the leading edge cells generates the force necessary for dorsal closure (Young et al., 1993; Kiehart et al., 2000). The TGF-β signaling factor decapentaplegic (dpp), Jun-Kinase signaling, and apical constriction in the amnioserosa have all been implicated in normal dorsal closure (for review, see Harden 2002 and Jacinto et al., 2002). Interestingly, in this example, as in *Parhyale*, neither population of cells (the amnioserosa and epidermis in *Drosophila,* or the rosette and epithelial sheet in *Parhyale*) is absolutely necessary for continued migration of the other population (Kiehart et al., 2000).The leading edge in *Parhyale* gastrulation appears important, but further research is necessary before its role, if any, during morphogenesis is understood.

Figure 3.1. The germline does not internalize when Mav is photoablated.
Brightfield, fluorescent, and overlay images of a 20 hpf embryo with Mav photoablated at the 8-cell (left) and soccerball (middle) stages. Control embryos that were microinjected but not ablated shown at the right. Mav was injected with FITC (green) and g was injected with dsRed-NLS mRNA (red). When Mav is photoablated, g does not migrate normally during gastrulation.

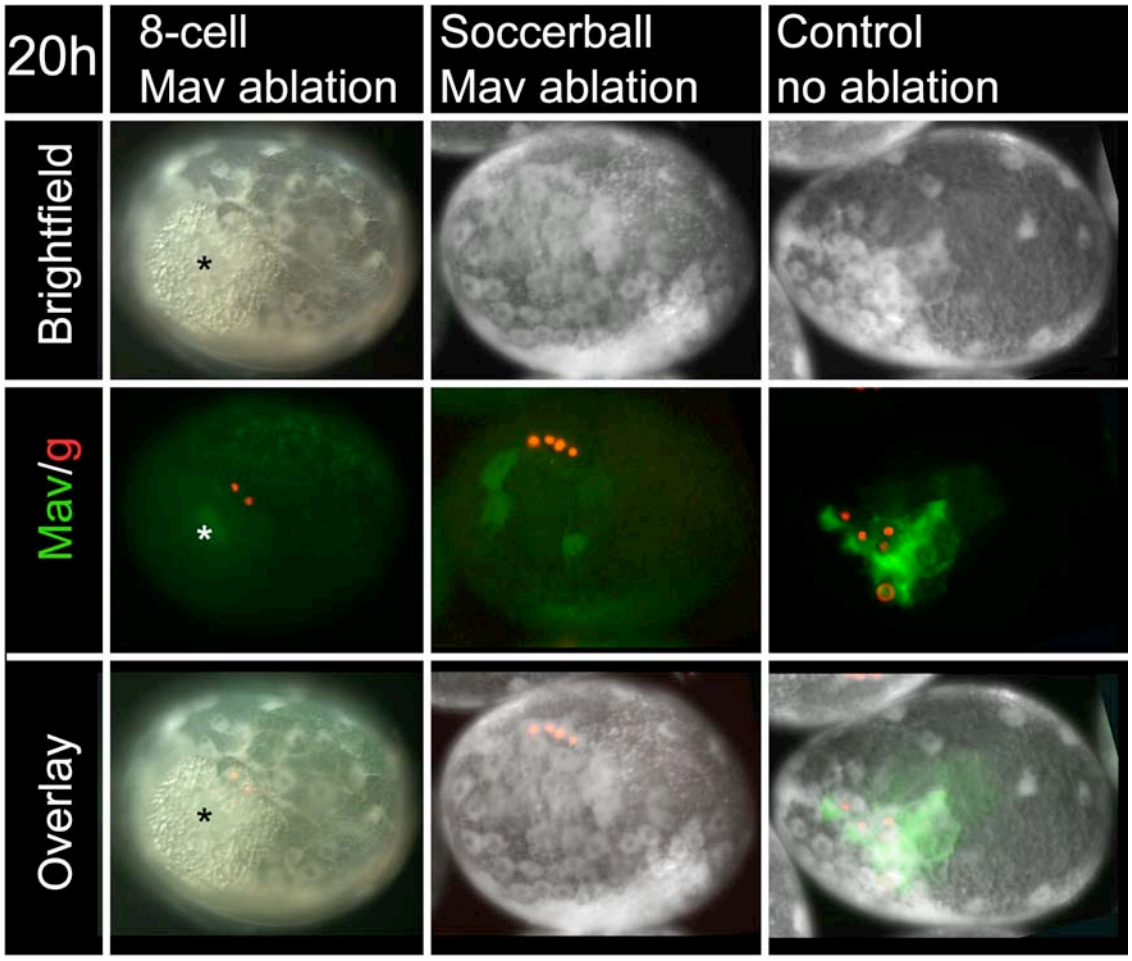
20h
8-cell
Mav ablation
Soccerball
Mav ablation
Control
no ablation
Brightfield
Mav/g
Overlay
*
*
*

Figure 3.2. The germline migrates normally when Mav is manually ablated. Confocal images of late appendage development (S21) embryos that were either unperturbed (A) or had Mav manually ablated (B). Nuclei are in blue (DAPI) and the germline marker Vasa is in red. Area in brackets is shown in higher magnification in the middle and right panels that are confocal stacks through the germline cells. In both animals, the germline is found in two bilaterally symmetric clusters, as in controls. Scale bars are 100 microns

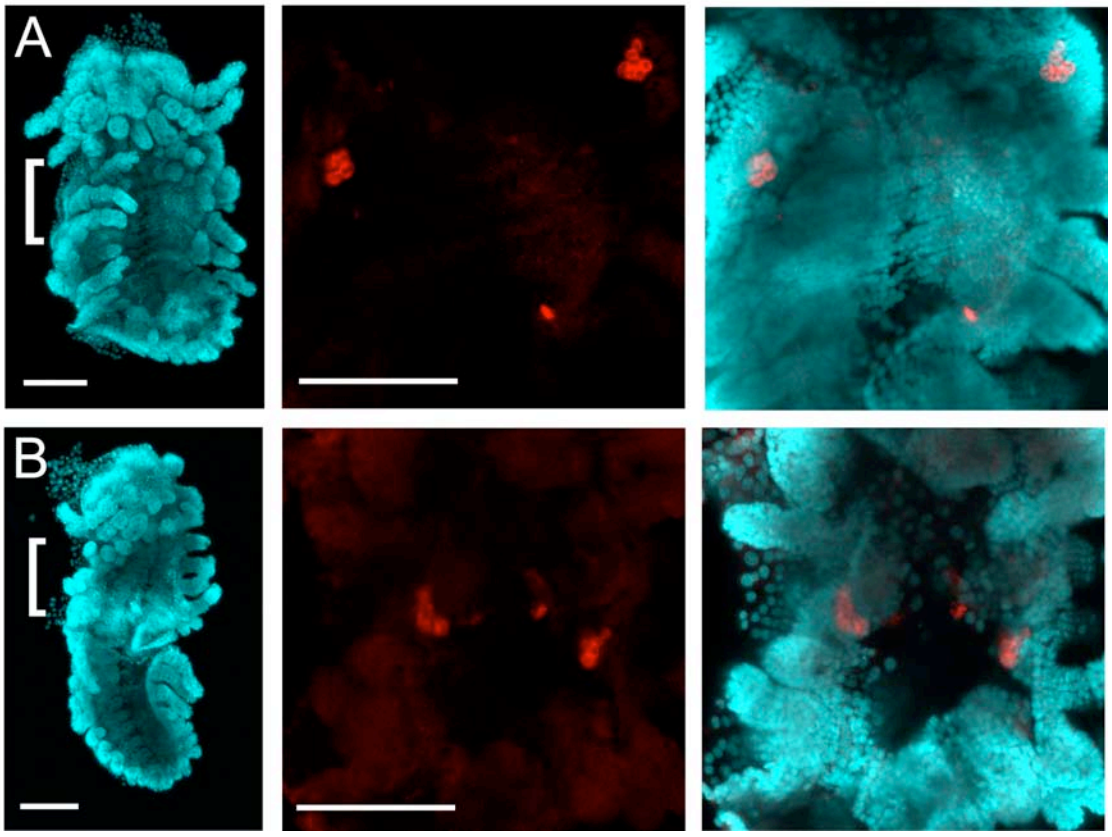
A
B

Figure 3.3. Manual tracking using Volocity software generates a track.
Stills of control (top) and photoablated (bottom) embryos from a timelapse video. The epithelial sheet is labeled with dsRed-NLS (red nuclei) and the rosette is labeled with FITC (green). Superimposed on the stills are the tracks generated by following the nuclei of three epithelial cells over 157 time points, a triangle marks the endpoint of each cell. Stills are oriented so that the direction of rosette and epithelial sheet migration is to the left. Time is shown in hours and is normalized to 0 h at the beginning of cell tracking. Lower left: Schematic of a vegetal view of a 13 hpf embryo (normalized to 0h). A red circle indicates examples of cells chosen for tracking. 1: near (blue track), 2: far (green track), 3: farthest (magenta track).

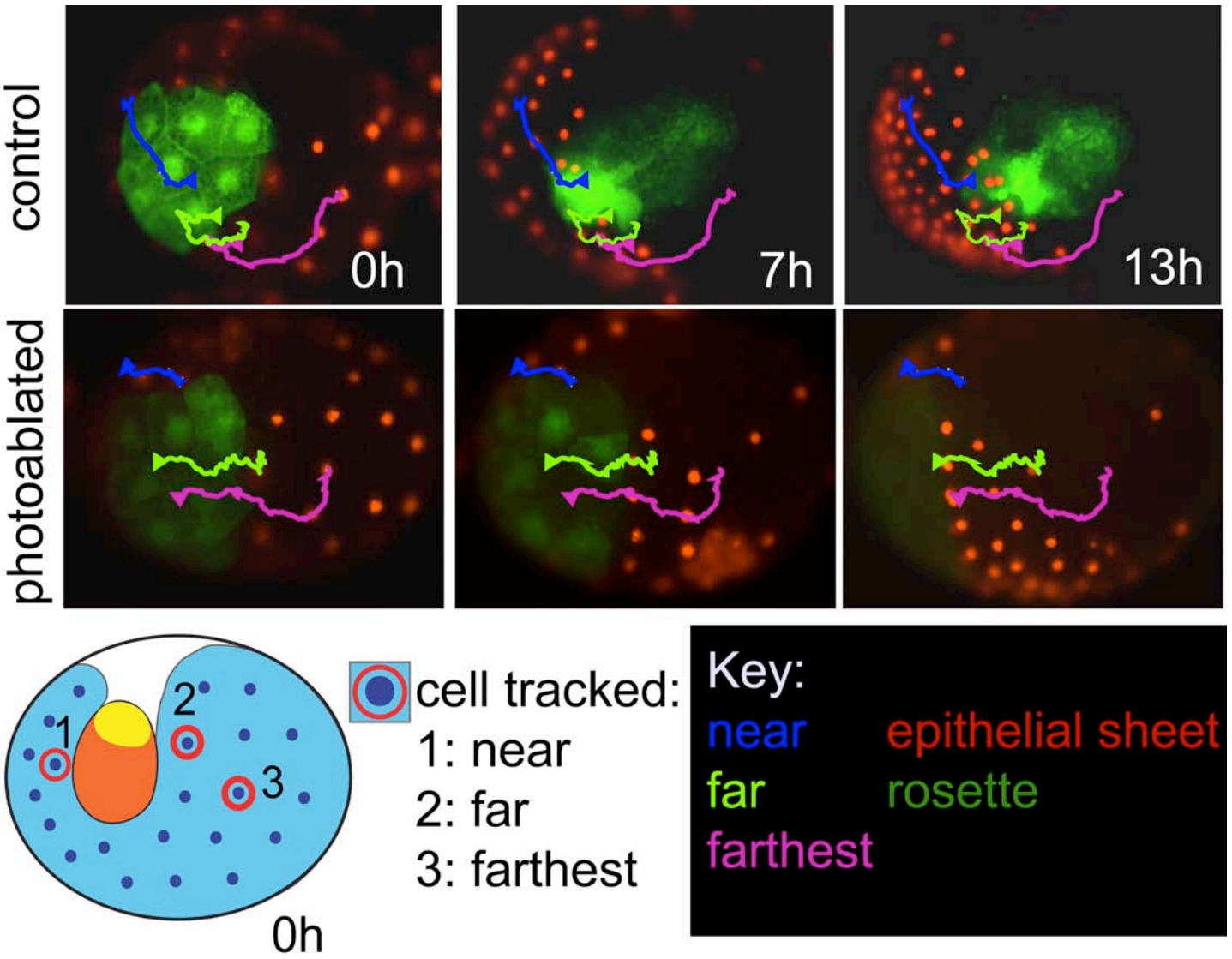
control
photoablated
0h
7h
13h
1
2
3
0h
cell tracked:
1: near
2: far
3: farthest
Key:
near
far
farthest
epithelial sheet
rosette

Figure 3.4. Photo-ablation of the rosette just prior to gastrulation has no significant effect on migration of the epithelial sheet.
Top: Graphs showing the average migration length and average displacement of cells in the epithelial sheet in control (non-ablated) and ablated groups. See methods and materials for further detail. Error bars indicate standard deviation. Difference is not significant in either the length migrated (left) or the displacement of cells (right) (p-value > .05 in each case). Bottom: Schematic of a vegetal view of a 13h embryo. A red circle indicates examples of cells chosen for tracking. 1: near, 2: far, 3: farthest.

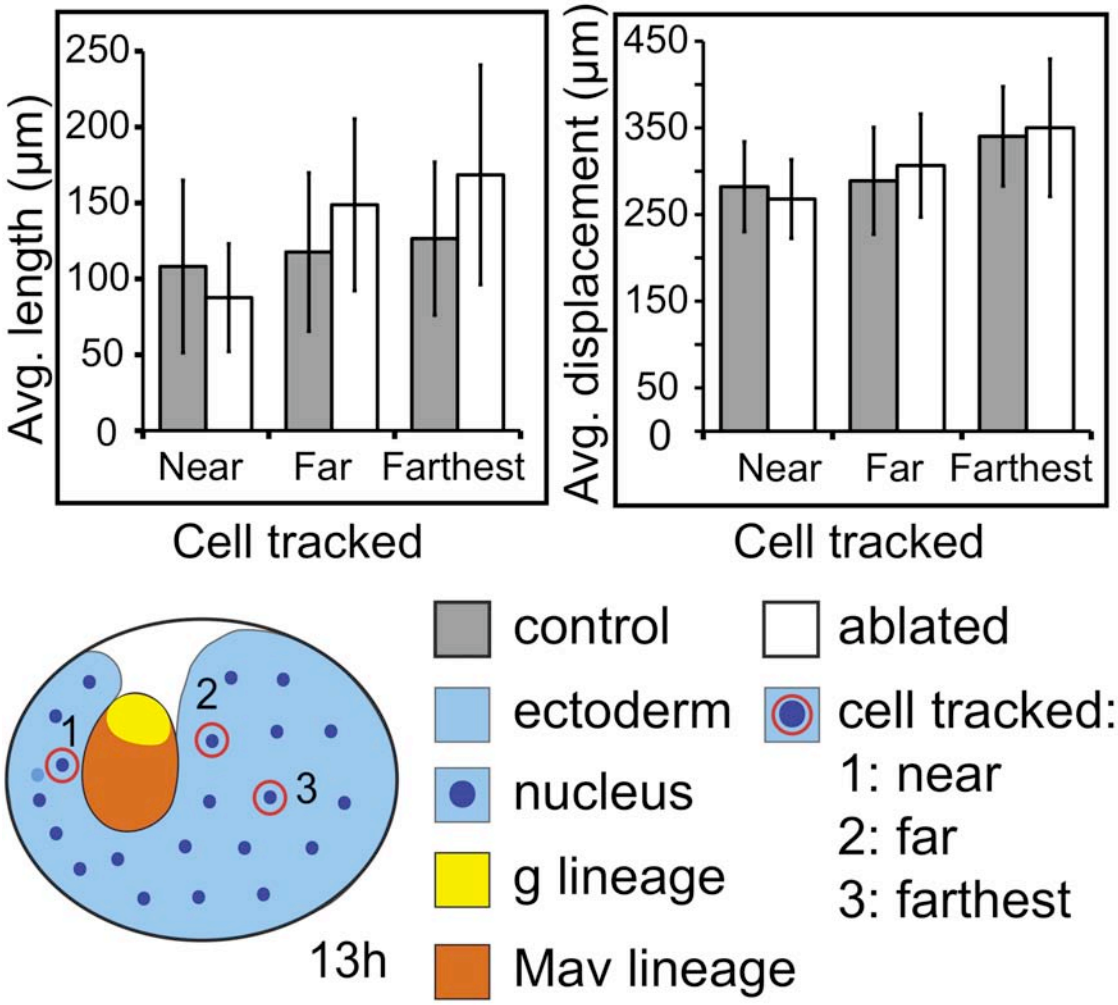
Avg. length (µm)
250
200
150
100
50
0
Near
Far
Farthest
Cell tracked
Avg. displacement (µm)
450
350
250
150
50
0
Near
Far
Farthest
Cell tracked
1
2
3
13h
control
ablated
ectoderm
cell tracked:
1: near
2: far
3: farthest
nucleus
g lineage
Mav lineage

Figure 3.5. Ablation of the rosette at the 8-cell stage does not hinder migration of the epithelial sheet.
A: Confocal stack of a control embryo at 20h of development. B: Confocal stack of an embryo with Mav and g photoablated at the 8-cell stage. The remains of the macro and micromeres are clearly visible. Arrowheads indicate epithelial sheet cells that have condensed and migrated. El or Er injected with TRITC (red) and El, Er, and Ep injected with dsRed-NLS (red nuclei). Nuclei in cyan (DAPI), actin in green (phalloidin).

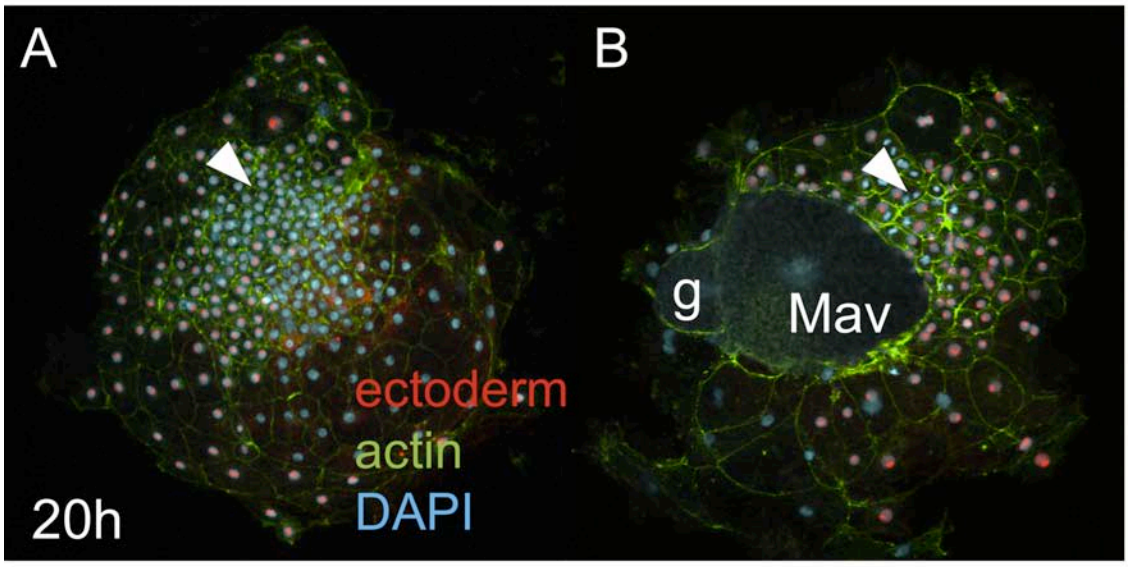
A
B
g
Mav
ectoderm
actin
DAPI
20h

Figure 3.6. Ablation of a portion of the epithelial sheet adjacent to the rosette does not affect rosette internalization.
Confocal stacks of a 13h embryo before (A) and after (A') confocal ablation. White dotted line indicates the region targeted for ablation. Note photobleaching from A to A'. (B) Stills from a timelapse video of ablated (top) and control (bottom) embryos. Stills are cropped and rotated to focus on a single embryo. Inset shows brightfield view just before the beginning of filming. Blue dotted line indicates the estimated area covered by ectoderm precursors. El and Er are labeled with dsRed-NLS (red nuclei), the rosette is labeled with TRITC (red), and El is labeled with FITC (green). Scale bars are 100μm.

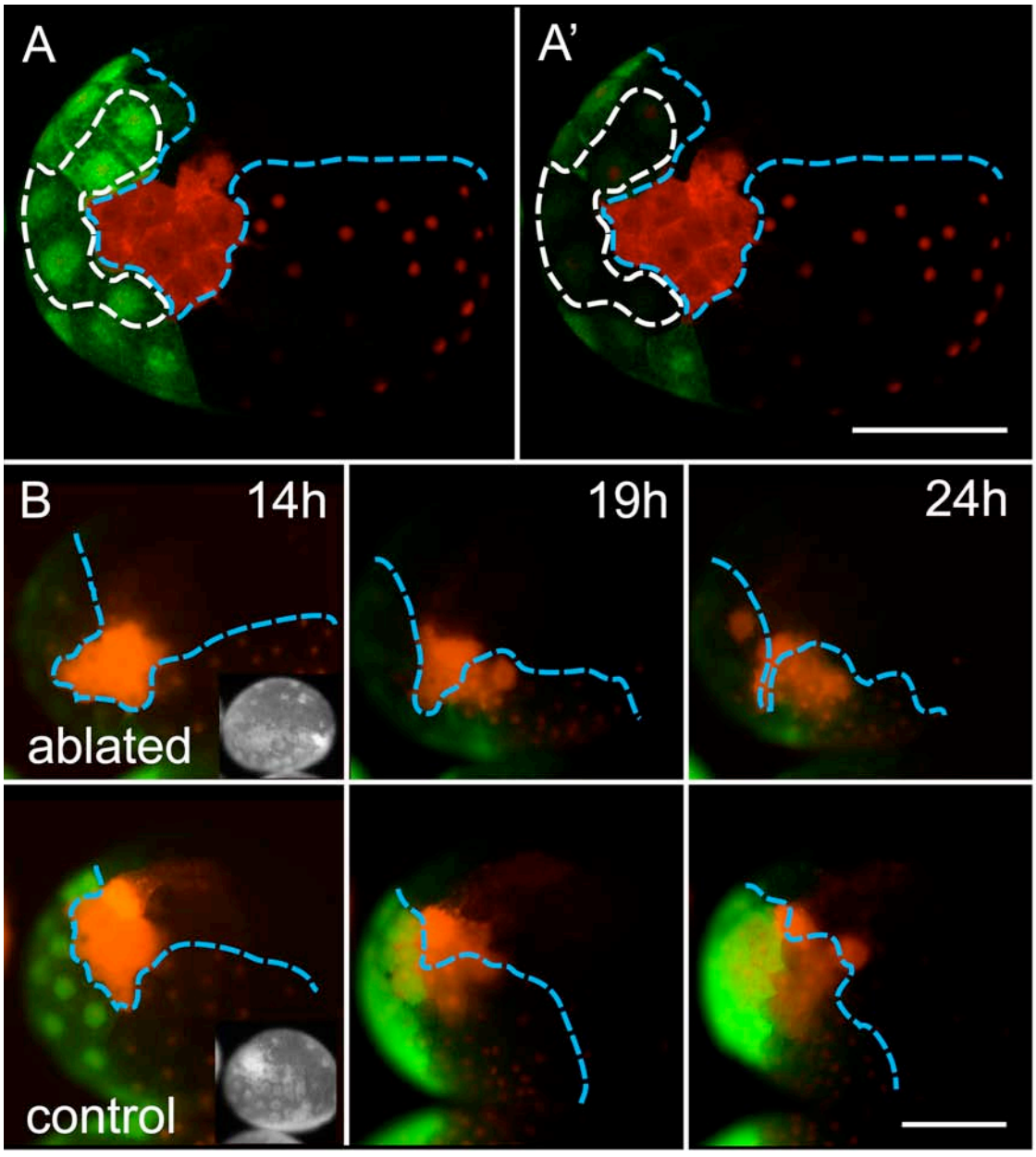
A
A'
B
14h
19h
24h
ablated
control

Figure 3.7. Ablation of the leading edge sometimes results in slowed internalization of the rosette and migration of the epithelial sheet.
Stills from a timelapse video of an embryo with the leading edge of ectoderm ablated (top) and a microinjected but unablated control (bottom). White dotted line outlines areas of photobleached, dead cells that are visible as the rosette internalizes. Arrowheads indicate ectoderm cells that migrate around the dead cells to close the epithelial sheet as the rosette internalizes. Rosette is labeled with TRITC (red), and the epithelial sheet is labeled with FITC (green).

0h
6h
13h
25h
Ablated
Control

Figure 3.8. Photoablation of all the ectoderm precursors adjacent to the rosette does not affect inward migration of the rosette, but arrests migration and condensation in some epithelial cells.

A: Confocal stacks of the vegetal view of a S6 embryo before and after confocal photoablation. Embryo is the same embryo as in B. Dotted line indicates region specified for laser scanning, note that this area is photobleached in the second image. El, Er: FITC, green. Mav, g: TRITC, red. Asterisk indicates g lineage, which marks the edge of the rosette and has a higher concentration of TRITC because it divides less. (B) The rosette internalizes, but does not migrate to one side of the embryo. Confocal stacks showing lateral views of a control and ablated embryo fixed and stained for actin (green) and nuclei (blue) after 30h of development. Ablated embryo is the same embryo as in A. Mav/g is labeled with TRITC (red haze, white asterisk) and El and Er progeny are labeled with dsRed-NLS (red nuclei). Small white arrowheads indicate approximate internalization site of the rosette. Arrow indicates direction of normal migration. In the ablated embryo, the rosette internalizes but does not migrate. Dashed line outlines an ectoderm cell that did not condense properly. Bracket indicates some ectoderm precursors that were able to migrate and condense.

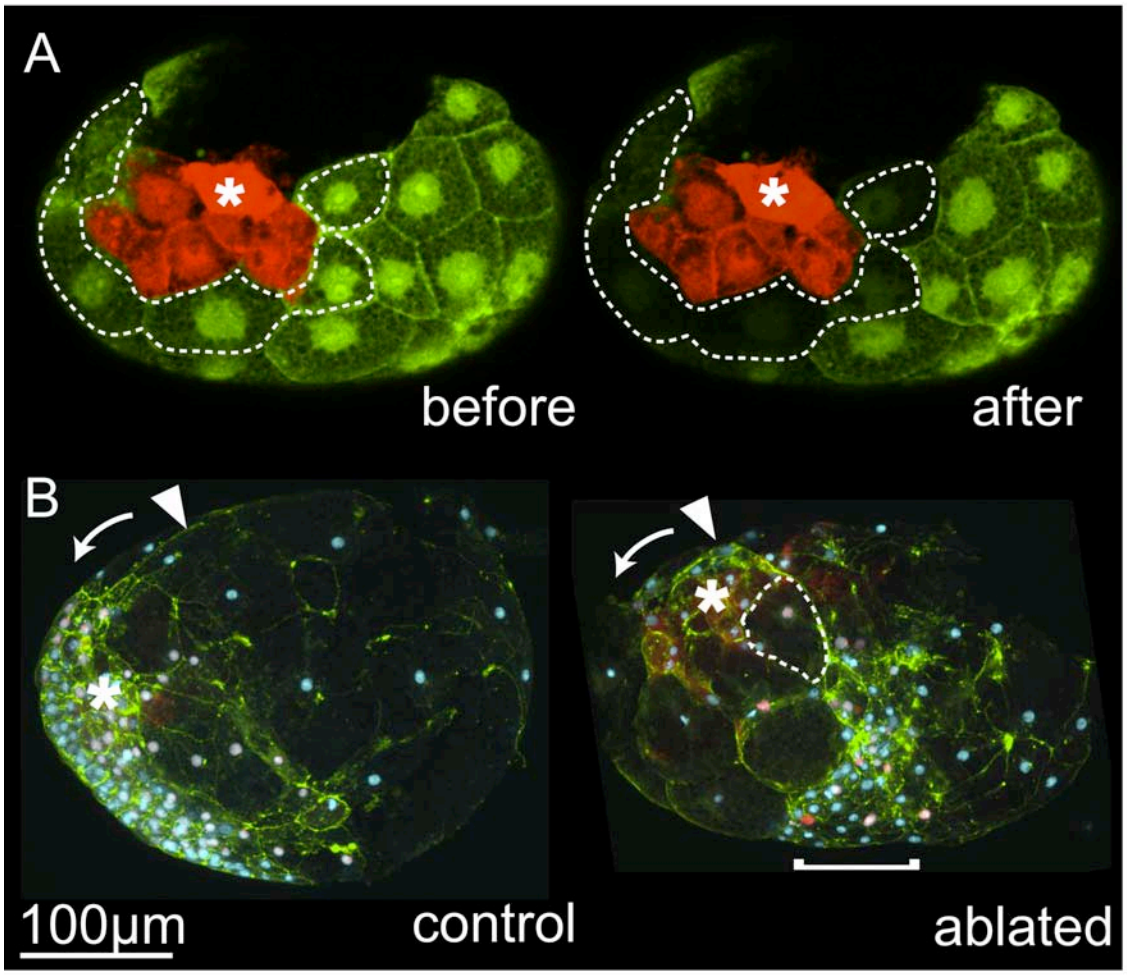
A
before
after
B
100µm
control
ablated

Chapter IV: Pharmacological inhibition of gastrulation

SUMMARY

During gastrulation, the cytoskeletal proteins actin and tubulin work together to reshape cells. Both actin and tubulin have been implicated in the apical constriction process. Furthermore, a highly conserved regulatory pathway through the small GTPase *rho* and its downstream effector *Rho-kinase* (Rock) has been implicated in apical constriction. In this chapter, I test the reliance of *Parhyale* gastrulation on actin, tubulin, and Rock by using the actin inhibitor Cytochalasin D, tubulin inhibitors Nocodazole and Taxol, cell cycle inhibitor Olomoucine, and the Rho-Kinase inhibitor ROCKOUT.

INTRODUCTION

Gastrulation is the rearrangement of an epithelial sheet into multiple layers. An epithelial sheet is defined as a laterally coherent sheet of cells with apical-basal polarity. The coherency of the sheet is maintained through cell-cell junctions that differ in connectivity, size, and components along the apical-basal axis. Differences in these junctions and in the meshwork of actin and tubulin that makes up the cell walls give the sheet its polarity (Schöck and Perrimon, 2002). Remodeling an epithelial sheet relies on cell migration and cell shape change. To accomplish this, cells rearrange their cytoskeleton and lose and/or remodel their contacts with their neighbors and the substratum. The actin cytoskeleton is the main focus of these changes, although in some cases microtubules also play a role (Schöck and Perrimon, 2002; Welch and Mullins, 2002).

In addition to polymers of actin and tubulin, the meshwork of proteins in cell walls also contains non-muscle myosin II. Myosin, when phosphorylated, slides actin filaments over one another. Myosin thereby mediates local contractions of actin filaments in shape changes like apical constriction and in group contractions such as the contractile acto-myosin purse string in the leading edge of epithelial cells during *Drosophila* dorsal closure (Small 1999, reviewed in (Schöck and Perrimon, 2002)(Harden, 2002).

Molecularly, the highly conserved Rho family of small GTPases regulate the actin cytoskeleton and associated myosins through several downstream targets (Ridley et al., 2003)(Raftopoulou and Hall, 2004). In particular, invertebrate homologs of rho-kinase have been shown to mediate actin localization and myosin phosphorylation during apical constriction in gastrulation and salivary gland formation and migration in *Drosophila* (the homolog is called Drok), and contraction of non-muscle cells in *C. elegans* (the homolog is called LET-502) (Riento and Ridley, 2003; Dawes-Hoang et al., 2005; Xu et al., 2008; Gally et al., 2009).

In this chapter, I use commercially available drug inhibitors to perturb assembly of actin and tubulin polymers. In addition, I use the pharmacological inhibitor Olomoucine as a control and ROCKOUT to test whether gastrulation in *Parhyale* depends on *rho-kinase* activity. I find that different phenotypes result from treatment

with actin, tubulin, and *rho-kinase* inhibitors. I also discover a phenotype that may be due to abnormal cell division.

MATERIALS AND METHODS

Microinjection

Microinjection for lineage tracing was done as previously described (Gerberding et al., 2002; Price et al., 2010). We injected an mRNA encoding a nuclear-localized dsRed protein (dsRed-NLS, Gerberding et al. 2002) at a concentration of 1μg/mL into the rosette at the 4- or 8-cell stage. Embryos were then allowed to recover for 1 hour at 26º C before drug treatment. In all cases, the injected amount was approximately 14 picoliters for micromeres or 143 picoliters for macromeres.

Drug treatment

Embryos were incubated in 50% - 80% ASW with one of the following inhibitors: Rho-Kinase Inhibitor III (ROCKOUT, EMD4Biosciences, #555553) at a final concentration of 100μM from a 50mM stock in DMSO; Taxol (Sigma) 15 μM from a 1mM stock in DMSO; Nocodazole (Sigma) 5μM from a 5mM stock in DMSO; Cytochalasin D (Sigma) 10 μM from a 1mM stock in DMSO; Olomoucine (TOCRIS #1284) 100μM from a 5mM stock in DMSO. Lower salinity prevents drug precipitation and does not affect normal development. Controls were from the same brood as treated embryos and were subject to equivalent concentrations of DMSO. Embryos were incubated in the drug for a minimum of 3 hours and a maximum of 72 hours beginning at the 8-cell or soccerball stage. For washout, embryos were removed at specific time points and rinsed into control conditions through 3 X 10 minute washes of control solution (50% ASW + DMSO).

This concentration of ROCKOUT was shown to halt wound-healing response in mammalian epithelial cells. ROCKOUT is a specific ATP competitor with ROCK (Yarrow et al., 2005). Controls were subject to the same conditions with equivalent concentrations of DMSO. For washout, embryos were removed at specific time points, and rinsed into control conditions through 3 X 10 minute washes of control solution (50% ASW + DMSO). Prior to fixation, embryos were washed 3 times over 15 minutes in 100% ASW.

Antibody and phalloidin staining

Antibody and phalloidin staining was performed as previously described in Chapter II.

RESULTS

Inhibition of microtubules with nocodazole, but not taxol, arrests gastrulation

To discern the importance of microtubules during gastrulation in *Parhyale,* and to test the efficacy of various microtubule inhibitors, I treated embryos with nocodazole and taxol. Table 2 and Figure 4.1 summarize our results. Nocodazole inhibits microtubule assembly, while taxol prevents microtubule disassembly. These

drugs had different effects on *Parhyale* gastrulation. In 2-cell nocodazole treated embryos, they were healthy looking 24 hours after treatment but had not progressed beyond the 4-cell stage (Fig. 4.1). This suggests that nocodazole penetrates the cell membrane in an hour or less since cell cycle length at this stage is roughly 1 hour at 26 ºC. Twenty-four hours after beginning treatment early in gastrulation (at 16 hpf), embryos were arrested at the rosette stage. Cell outlines were clear as in controls, with a slightly less compact and organized rosette. When treatment began at the rosette stage, development arrests and the embryos look disorganized and unhealthy (Fig. 4.1). If treatment began late in gastrulation (~19 hpf), embryos produced a normal looking germ cap (Fig. 4.1), but all died within 48 hours (Table 2).

Conversely, 24 hours after treatment with taxol, 2-cell embryos had progressed and arrested at the soccerball stage. Specimens treated at early gastrulation (16 hpf) progress to the germ cap stage after 24 hours. However, embryos have an abnormally raised germ cap, as though the cells of the epithelial sheet piled on top of one another. Furthermore, embryos that were treated at mid- or late-gastrulation showed completely normal looking germ caps (Fig. 4.1), however, none survive after 48 hours.

There are two explanations for the differences between nocodazole and taxol treatment. First, it is possible that taxol does not penetrate immediately. This lag time might account for the embryo's ability to accomplish several rounds of cell division before development is arrested. The different effects of the two drugs are also a plausible explanation. As a microtubule stabilizer, taxol arrests polymer formation by preventing the disassembly of tubulin monomers from microtubules. In this manner, taxol depletes the pool of tubulin available for use in the assembly of new microtubules. This process may require more time before resulting in a noticeable affect on development versus the direct inhibition of microtubule assembly from nocodazole.

To further test this difference, I performed a washout experiment where treated embryos were incubated with the drug and then moved into control conditions. Regardless of when treatment began with nocodazole, washout after 24 hours did not rescue any animals. All were dead within 48 hours of treatment. In taxol treated embryos, those that began treatment at the 2-cell or soccerball stages did not respond to washout of the drug and died within 48 hours. However, those that began treatment mid or late gastrulation recovered from washout and survived until hatching (Table 2).

These results could indicate that nocodazole treatment penetrates cell membranes more efficiently than taxol in *Parhyale* embryos. That *Parhyale* embryos are unable to recover from the effects of 24 hours in nocodazole indicates that its effects are also long lasting and debilitating to *Parhyale* development. It is possible that by the time washout begins, the cells have already started to die. Embryos that began treatment in taxol prior to the start of gastrulation are unable to recover, whereas embryos that begin taxol treatment after the beginning of gastrulation respond to a washout after 24 hours with 100% recovery. This could suggest that there is a checkpoint during gastrulation that the stabilization of microtubules interferes with. Presumably, beginning treatment after this checkpoint prevents cells from receiving the signal to halt development, which allows them to recover once the drug is washed out.

Table 2. Treatment and washout of taxol and nocodazole

	Total	To hatching	Survival (%)	Notes
Control				
2-cell	2	2	100	
Early-gastrulation	4	4	100	
Mid-gastrulation	2	2	100	
Late-gastrulation	2	2	100	
Taxol washout (24h)				
2-cell	4	0	0	All dead in 48h of washout
Early-gastrulation	4	0	0	All dead in 48h of washout
Mid-gastrulation	4	4	100	
Late-gastrulation	4	3	75	
Nocodazole washout (24h)				
2-cell	4	0	0	All dead in 24h of washout
Early-gastrulation	4	0	0	All dead in 48h of washout
Mid-gastrulation	4	0	0	All dead in 48h of washout
Late-gastrulation	4	0	0	All dead in 48h of washout

Cytochalasin D inhibits gastrulation in *Parhyale*

The actin cytoskeleton is central to many morphogenetic cellular behaviors. Inhibition of actin polymers is therefore expected to arrest gastrulation. We treated embryos with the drug Cytochalasin D, which binds to actin monomers, thereby preventing the formation of microfilaments (Goddette and Frieden, 1986). As expected, embryos that begin treatment at the soccerball stage never gastrulate. Instead, cells become disorganized and group together in cell "islands" that are clusters distributed around the embryo (Fig. 4.2, supplemental movie 4a and 4b). Phalloidin and tubulin staining reveal that tubulin is largely unaffected (not shown), but that the microfilaments have lost organizational integrity and are choppy in comparison to controls. Moreover, the majority of cells have two nuclei, indicating incomplete cytokinesis, which is a phenotype linked to actin inhibition (Fig. 4.2).

These results show that Cytochalasin D inhibits the formation of normal microfilaments that, in turn, is vital to normal *Parhyale* gastrulation. It is interesting that actin inhibition results in clusters of cells, suggesting that there is a difference to the importance of actin assembly between groups of cells. If microfilament assembly were uniformly important, than inhibition of actin polymerization should affect all cells similarly, arresting movements completely. Instead, some cells seem to pull together while losing contact with other cells (Fig. 4.2). This could indicate that the actin based cell junctions in some cells require more dynamic actin formation than in other cells.. Ultimately, these results confirm that actin polymerization plays a crucial role in *Parhyale* gastrulation.

Inhibition with Olomoucine does not prevent gastrulation

To test whether the inhibitory effect that Cytochalasin D has on gastrulation is due to its ability to inhibit the cell cycle, I treated embryos with the cyclin-dependent kinase inhibitor Olomoucine. *In vivo*, olomoucine arrests dividing cells at the G2/M phase transition in starfish embryos (Veselý et al., 1994) and slows cell division in brine shrimp (Annalisa VanHook, personal communication). When I treated soccerball *Parhyale* embryos, cell division appeared to continue unperturbed until the early formation of the germ cap. At this point, the cells were larger than they were in controls, suggesting slowed cell division. We did not assay with phalloidin or tubulin stain to quantify the extent of cell division arrest. Future work could assay with these stains or with markers for the G2/M transition because Olomoucine is supposed to arrest during this phase. The germ cap that formed was abnormal. It featured a large pit or furrow at what was presumably the gastrulation center. The epithelial cells also continued to migrate onto the germ cap, resulting in an abnormally large and protruding collection of cells (Fig. 4.3; supplemental movie 6). All embryos died within 48 hours of the beginning of treatment.

Our results confirm that arrest of gastrulation by Cytochalasin D is not due to its effects on cytokinesis, because perturbation of cell division by Olomoucine results in a completely different phenotype. This phenotype mimics that of the phenotype found by Alwes et al. (2011) using an inhibitor of RNA transcription. I also found that inhibition with Taxol mimics this phenotype (Fig. 4.4).

Pharmocological inhibition of rho-kinase arrests gastrulation

If gastrulation in *Parhyale* proceeds through Rho-kinase, then inhibition of *rho-kinase* should arrest gastrulation. I incubated embryos with the *rho-kinase* inhibitor ROCKOUT. We found that application of the inhibitor at the 8-cell or soccerball stage arrests development at gastrulation (Fig. 4.5). In embryos that began treatment at the soccerball stage, rosette and epithelial sheet formation appears normal after 6 hours. Later, 16 hours after the beginning of treatment, control embryos have a normal germ-cap but treated embryos have not completed rosette internalization. The rosette is less compact, and the epithelial sheet has formed but has not migrated over the rosette. In some cases, the rosette cells are no longer clustered. If the drug is washed out at 3 hours, prior to this phenotype, all embryos recover and develop normally (100% hatching, n=9; Table 3). If the drug is washed out at 8 hours, embryos attempt to recover, but give a range of phenotypes. Some appear to have normal rosettes but in others the rosette cells detach from each other and are scattered on the surface of the egg. In nearly all cases, the rosette cells internalize by 40 hours after washout, however, only 20% of embryos survive to hatching (Table 3). When compared to controls that have a normal germ cap 25 hours after the beginning of treatment, the epithelial sheet cells have lost their integrity and apico-basal polarity. Epithelial cells in treated embryos are no longer columnar and hexagonal, and do not have actin-rich cell-cell junctions. Some rosette cells have internalized, but some remain on the surface (Fig. 4.5). Rho-kinase may therefore play a role in regulating normal inward migration of the rosette, keeping rosette cells attached to each other, and regulating normal epithelial cell morphology during *Parhyale* gastrulation.

Table 3. Summary of embryo survival after treatment and washout with ROCKOUT.

	Total	Day 5	Hatching	Survival (%)	Notes
Treated	20	0	0	0	All embryos are dead 72 hours after treatment.
Control	17	16	16	94	
Washout (3h)	9	9	9	100	All embryos survive and develop normally.
Washout (8h)	17	8	3	18	Some embryos at day 5 have gut and appendage development defects.

DISCUSSION

Inhibition of actin and rho-kinase arrests gastrulation

Some cells in the rosette have bottle-cell morphology during gastrulation and an apico-lateral concentration of actin. In addition, Cytochalasin D and ROCKOUT arrest development at gastrulation. Taken together, these results suggest that apical constriction might play an important role during rosette internalization. Apical constriction relies on acto-myosin contractility. The primary function of rho-kinase during *Drosophila* development appears to be phosphorylation of myosin (Mizuno et al., 1999; Winter et al., 2001; Riento and Ridley, 2003; Dawes-Hoang et al., 2005; Xu et al., 2008). Therefore, it is possible that ROCKOUT acts as an indirect myosin inhibitor in *Parhyale*, and that acto-myosin contractility is an important part of *Parhyale* gastrulation. Future work should focus on inhibiting actin and myosin in Mav descendants alone to test whether bottle cells are still able to form and whether inhibiting actin and *rho-kinase* in these cells prevents their internalization.

Alternatively, it is possible that ROCKOUT's effect is due to Rho-kinase's part in regulating cell polarity. This is supported by the change from cuboidal cells with putative apical actin-based junctions to rounded cells with no apico-basal polarity. Future work could investigate the extent of the difference between cells by describing cell-cell junctions and through an analysis of potential differences in cell size and/or volume. The upstream triggers of the Rho – Rock – myosin II pathway are varied, but include non-canonical and canonical Wnt signaling (Strutt, 2002; Schlessinger et al., 2009; Zimmerman et al., 2010). As suggested by Alwes et al. (2011), cell polarity is a likely factor during gastrulation in *Parhyale,* and it is a central part of recruiting actin and myosin to the apical domain of constricting cells. Components of this pathway, such as Frizzled, Disheveled, and PAR proteins, are highly conserved and are attractive candidates for study in *Parhyale*.

A common phenotype

We noticed that inhibition of *Parhyale* development with Taxol and Olomoucine gives a phenotype that mimics the one reported by Alwes et al. (2011) from inhibition with the transcriptional repressor alpha-amantin (Fig. 4.4). It may therefore be the case that this phenotype is a result of inhibiting cell division. This

raises several questions about development post-gastrulation in *Parhyale*. In normal embryos, gastrulation ends with a transition into the beginning of germ band formation and elongation with the formation and organization of the head. After this, cells are recruited to the posterior of the germ band and segmentation proceeds through a highly regimented division pattern (Gerberding et al., 2002; Browne et al., 2005).

In embryos treated with Olomoucine or Taxol, head lobes never form. Instead, a raised germ cap forms with an abnormally large groove at what appears to be the original gastrulation center. If this phenotype is due to abnormal cell division, some part of the regulatory machinery of cell division may also regulate migration and cell positioning. Again, promising candidates appear in molecules that control cell polarity. For example, during zebrafish development, non-canonical Wnt signaling through the planar cell polarity pathway (PCP) is linked to cell division during gastrulation and neurulation (Gong et al., 2004; Ciruna et al., 2006). During gastrulation, the PCP pathway instructs cells to divide along the animal-vegetal axis to extend the embryo (Gong et al., 2004). During neurulation, the PCP pathway functions after mitosis to instruct daughters to intercalate with cells across the midline during closure of the neural tube (Ciruna et al., 2006). Genetic perturbation of components of the non-canonical Wnt pathway prevents daughter cells from migrating across the midline during neural tube closure. Imaging of these cells reveal that the cells never regain polarity after cell division, causing them to amass in disorganized concentrations (Ciruna et al., 2006).

It is possible that cell division combined with a polarity cue is responsible for normal formation of the head and germ band in *Parhyale* embryos. It appears that inhibiting cell division in *Parhyale* disrupts this combination and results in the amassment of disorganized cells. If polarity and division are linked in *Parhyale,* it is likely different than the one in zebrafish. Inhibition of cell division during neurulation in zebrafish rescues genetic perturbation of Wnt signaling (Ciruna et al., 2006). Instead, the mechanism might be more similar to the function of the PCP pathway during zebrafish gastrulation where it serves to orient and position cells (Gong et al., 2004). To investigate this, future work could ask whether oriented cell division occurs during formation of the head. This might include description of spindle orientation post gastrulation, as well as description and knockdown of the *Parhyale* orthologs of PCP pathway members.

Drug specificity

An issue with using pharmacological inhibition of cytoskeletal components on whole embryos is that perturbation is not specific to any one population of cells. Future work could address this problem by investigating the possibility of using heat shock constructs to knockdown specific pathway components in sub-populations of cells. Heat-shock hairpin constructs are currently being developed in the lab for *Parhyale*. Another approach could be to culture and drug treat cells in isolation. Previous work has successfully cultured blastomeres for up to 24 hours (Extavour, 2005).

Figure 4.1. Embryos after 24h of treatment in Taxol and Nocodazole.
Brightfield images of embryos after 24 hours in control or drug treatment with two different microtubule inhibitors at different stages of early *Parhyale* development. Stages when treatment began (2-cell, ~7 hpf; early gastrulation, ~16 hpf; rosette ~18 hpf; and late gastrulation, ~19 hpf) are listed across the top. Treatment with Nocodazole at the 2-cell, early gastrulation, or mid-gastrulation stages arrests development, but treatment of late gastrulation embryos results in a germ cap. Taxol only arrests 2-cell embryos. Treatment with Taxol during early, middle, or late gastrulation results in the formation of germ caps. When present, germ cap in a representative embryo is indicated by a white arrowhead. Scale bar is 100μm.

24h
2-cell
16h
18h
19h
Control
Nocodazole
Taxol

Figure 4.2. Treatment with Cytochalasin D arrests gastrulation.
(Left) Stills from a timelapse video of untreated (top) and Cytochalasin D treated (bottom) embryos. Time is across the top, with the beginning of filming normalized to 0h. Rosette and epithelial sheet were labeled with FITC and TRITC, respectively. (Right) Cells from untreated (top) and Cytochalasin D treated (bottom) embryos stained with phalloidin after gastrulation. Phalloidin is green, DAPI is blue. Scale bar is 100μm.

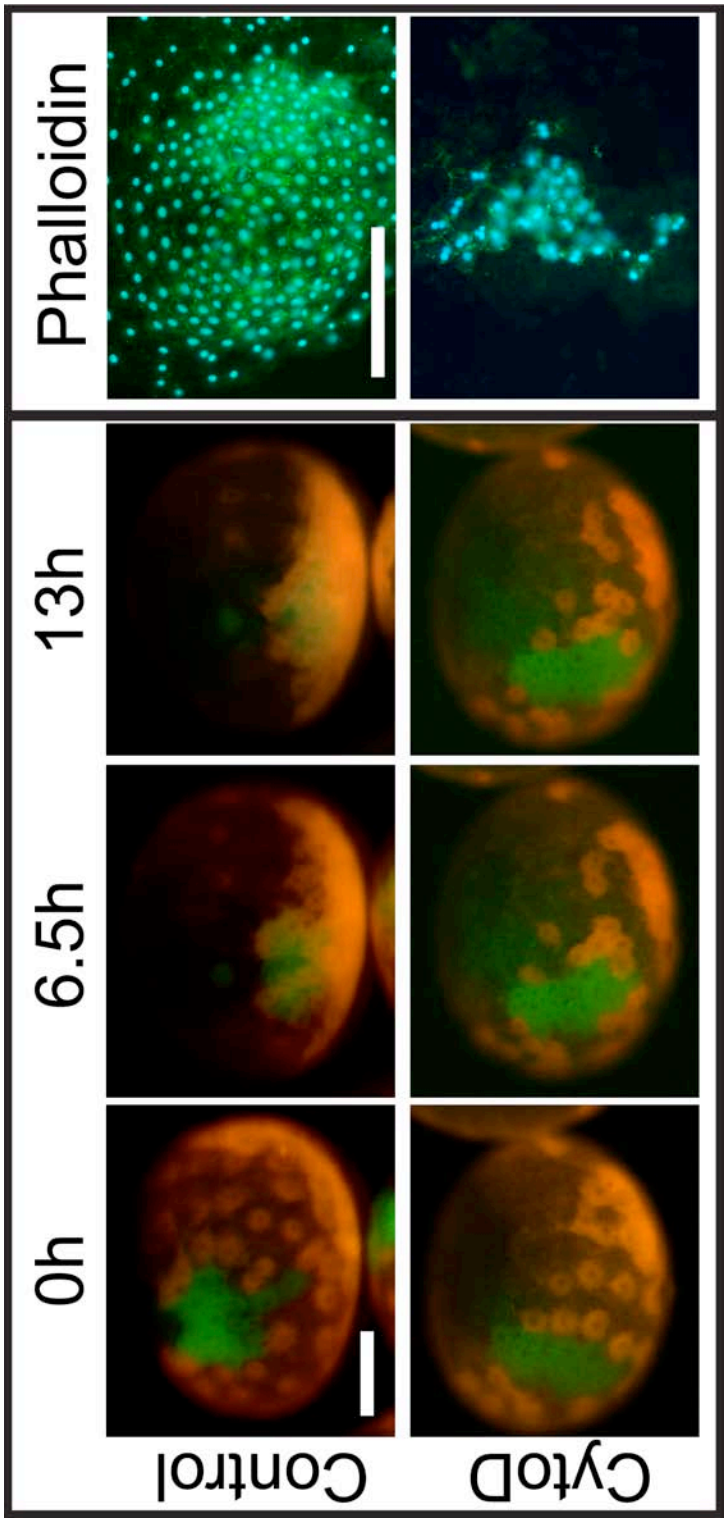
Phalloidin
13h
6.5h
0h
Control
CytoD

Figure 4.3. Treatment with olomoucine results in an abnormal germ cap.
Stills from a timelapse video of embryos treated with olomoucine. The beginning of the film is normalized to 0h. Embryos develop normally for 6.5 hours (middle) but then cells appear to continue to pile onto the germ cap, creating an abnormal cleft (right, blue arrowheads). Scale bar is 100μm.

Olomoucine
0h
6.5h
13h

Figure 4.4. Similarity of phenotypes between taxol, olomoucine, and alpha-amantin treated embryos.
Comparison of phenotypes in embryos treated with taxol, olomoucine and alpha-amantin (Alwes et al., 2011). Treatment of taxol and olomoucine embryos began early gastrulation (16 hpf) or pre-gastrulation (12 hpf). Embryos are shown 24 hours after the beginning of treatment. Image of alpha-amantin embryo is from Alwes et al., 2011, The embryo was continuously treated, and is shown after a normal germ cap formed and then development continued abnormally for 24 hours. Arrows indicate unusual furrow.

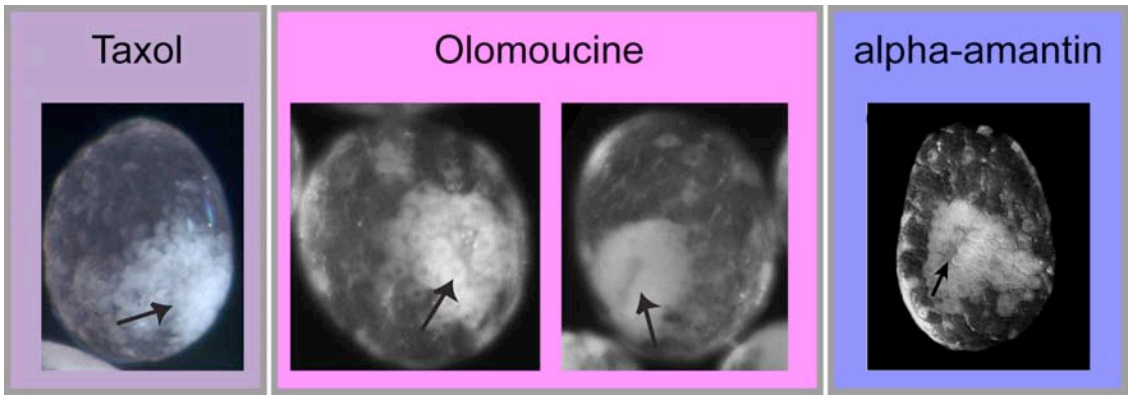
Taxol
Olomoucine
alpha-amantin

Figure 4.5. Treatment with a Rho-kinase inhibitor arrests development at gastrulation and affects normal epithelial morphology.
Confocal images of the germ cap region of whole embryos at the germ cap stage 12 hours after the start of a ROCKOUT washout experiment. Cells from control embryos are shown in (A) and cells from embryos subject to 8-hours of ROCKOUT treatment then washed into control conditions are in (B). ROCKOUT treatment began at soccerball stage. (A) Overlay of tubulin antibody (magenta), actin (phalloidin, green), rosette cells (dsRed-NLS, red nuclei), and nuclear staining (DAPI, cyan). Cells in the epithelial sheet are hexagonal, and cell boundaries well defined. Rosette cells are completely internalized. Arrowheads indicate an apical concentration of actin, possibly indicating cell-cell junctions, which confirms apico-basal polarity in the epithelial sheet. (B) Cells have lost all polarity and shape. Cells appear larger because they have lost the regimented geometery of those in control embryos; a volumetric analysis was not done. Some rosette cells have internalized, but many remain on the surface. Green line in (A) and (B) indicates the position of the XZ section. The blue line indicates the position of the YZ section. Scale bar is 50μm.

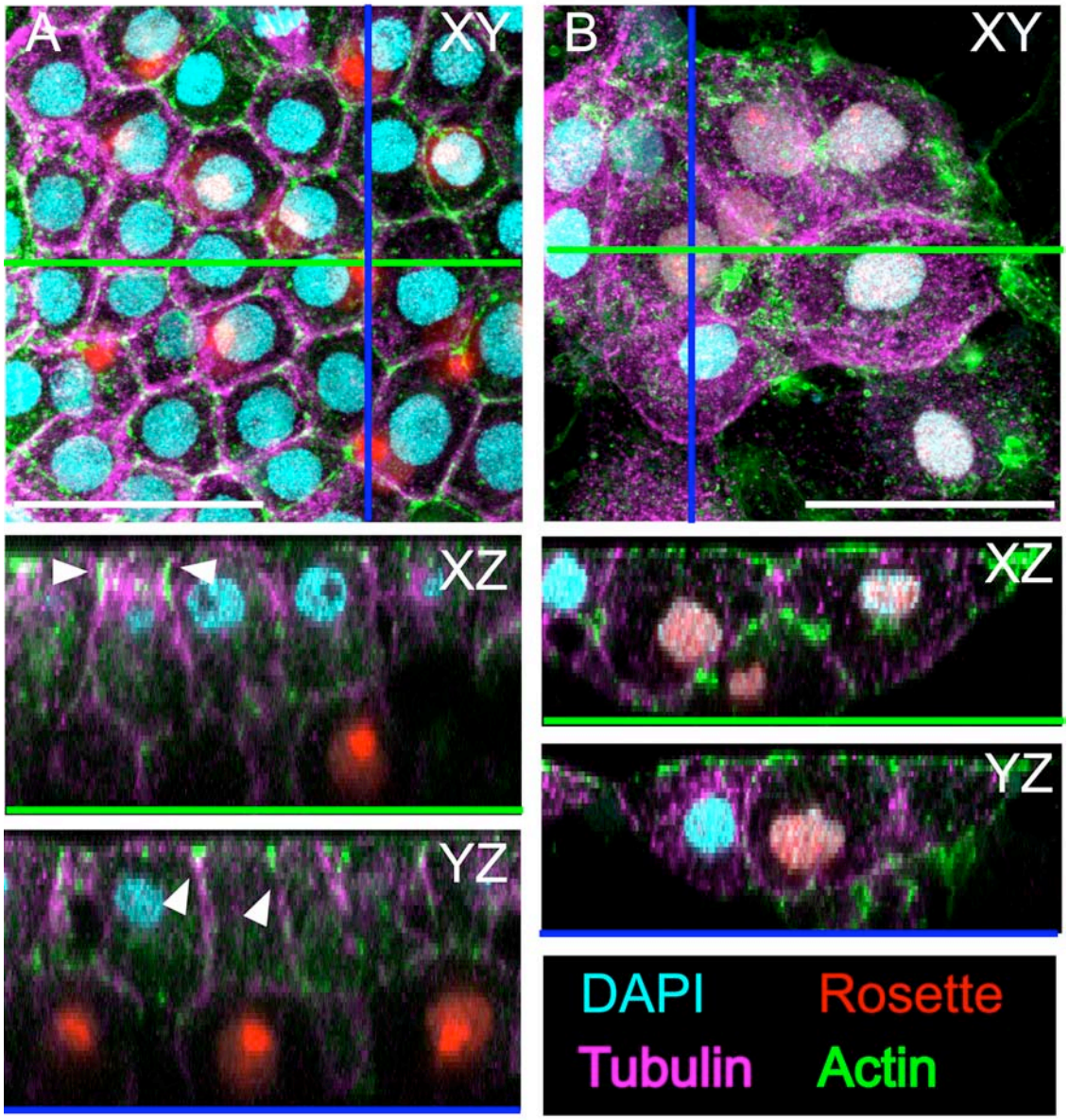
A
XY
B
XY
XZ
XZ
YZ
YZ
DAPI
Rosette
Tubulin
Actin

Chapter V: Candidate signaling pathways during rosette internalization

SUMMARY

Upstream of genes that directly regulate the cytoskeleton during morphogenesis are genes that confer cell fate and determine cell identity. In early *Parhyale* development, no genes conferring mesoderm and ectoderm identity have been found prior to gastrulation. In this chapter, I investigate the *Parhyale* homologs of several candidate genes that were previously cloned: Snail, Decapentaplegic, and Notch/Delta. In all cases, these genes belong to signaling pathways that are highly conserved players during fate determination and morphogenesis across taxa.

INTRODUCTION

Molecular signals during morphogenesis serve three main functions– establishment of cell identity, establishment of cell polarity, and programming cell behavior (Davidson, 2008). Often, the genes regulating these functions fall into two main categories: those regulating changes in the cytoskeleton i.e. cell polarity and behavior, and those conferring cell fate/ cell identity (Dawes-Hoang et al., 2005; Leptin, 2005). In *Parhyale*, no early molecular markers for mesoderm or ectoderm identity have been identified. However, some interesting candidates have been previously cloned, including the Transforming Growth Factor-β (TGF-β) ligand, *decapentaplegic,* members of the *Snail* superfamily of transcriptional repressors, and the transmembrane receptor *Notch* and its ligand *Delta*.

Transforming Growth Factor-β signaling: Decapentaplegic

Members of the Transforming Growth Factor-β (TGF-β) superfamily of secreted proteins are multi-potent signaling factors involved in a wide variety of morphogenetic events across nearly all animal phyla (Sporn, 2006). In many species, a gradient of TGF-β signaling along with specific inhibitors and modulators set up cell fate and/or dorsal-ventral polarity. This conserved cassette of molecular pathways was first discovered in *Xenopus* and *Drosophila* (De Robertis and Sasai, 1996; Holley and Ferguson, 1997). In *Xenopus,* Bone Morphogenetic Protiens-2 and -4 (BMP-2/4) work with the inhibitors chordin and noggin to establish dorsal/ventral polarity in the embryo. BMP-2/4 are ventralizing factors that induce the ventral mesoderm and non-neurogenic ectoderm (Jones et al., 1996; Dale and Jones, 1999). The invertebrate homolog of BMP-2/4 is decapentaplegic (dpp). Unlike BMP 2/4, dpp works as a dorsalizing factor. Prior to gastrulation in *Drosophila, dpp* expression is repressed ventrally by the maternal transcription factor *dorsal*. *Dorsal* up regulates the *Drosophila* homolog of *chordin, short gastrulation (sog)*. Sog antagonizes *dpp* activity on the ventral side of the embryo. (Ferguson and Anderson, 1992; De Robertis and Sasai, 1996). In *Drosophila,* Dpp is a main component in defining the orientation of the embryo.

Dpp also plays a role in the definition of dorsal-ventral polarity in other arthropods. In the beetle *Tribolium casteneum, dpp* and *sog* are present in a similar

pattern as *Drosophila*; *sog* is expressed ventrally and confines *dpp* to the dorsal area of the embryo. When expression of *Tc-sog* is lost, D/V polarity in the developing embryo is lost (van der Zee et al., 2006) . In the spider *Achaearanea tepidariorium* (reclassified to *Parasteatoada* (Saaristo, 2006)), *dpp* signals from the first group of internalizing cells to an overlying population of ectoderm cells. This may play a role in defining the dorsal zone of the developing spider. Reduction in *dpp* signal prevents dorsal and ventral patterning (Akiyama-Oda and Oda, 2003; Akiyama-Oda, 2006).

Defining D/V polarity in a developing organism confers cellular identity that is important to the gastrulation process. In *Drosophila,* it is the ventral cells that first undergo internalization, while in *Achaearanea* the first group of internalizing cells actively breaks the symmetry of the embryo. In *Tribolium*, the dynamic interaction between *dpp* and *sog* is apparent in their expression patterns before, during, and after gastrulation. Through degenerate PCR, a *Parhyale* homolog of *dpp* has been cloned, but its expression and function, if any, during early development remains unknown.

The *snail* superfamily of transcription factors

Snail genes are well-studied because of their roles in inducing epithelial to mesenchymal transitions (EMT) and as mesoderm determinants (Barrallo-Gimeno and Nieto, 2005). *Snails* are zinc-finger transcription factors that mainly function as repressors. During EMT, *snail* family genes down regulate E-cadherin, a protein that is central to maintaining cell-cell adhesion and therefore epithelial integrity (Thiery and Sleeman, 2006). As a mesoderm determinant, *snail* was first observed in the developing mesoderm of *Drosophila* where it represses mesectodermal and neuroectodermal regulatory genes (Nambu et al., 1990; Kosman et al., 1991; Rao et al., 1991; Ip and Gridley, 2002). Since then, *snail* family members have been found in a wide variety of organisms including a number of diploblasts, where it appears in the endoderm just prior to gastrulation and may therefore be crucial to the initial gastrulation movements in these animals. Thus, Snail appears to have an ancient role in defining populations of cells that will internalize (Fritzenwanker et al., 2004; Martindale et al., 2004).

Among arthropods, *snail* homologs have been studied in several insects outside of *Drosophila* and in chelicerates and myriapods. In *Tribolium* and in the mosquito *Anopheles gambiae, snail* appears in the ventral mesoderm (Sommer and Tautz, 1994; Goltsev et al., 2007). In the two chelicerates examined (*Cupiennius salei* and *Achaearanea tepidariorium;* both arachnids), *snail* was found in the developing nervous system or in the ectoderm during gastrulation (Weller and Tautz, 2003; Yamazaki et al., 2005). In the one myriapod examined (*Glomeris marginata*, a diplopod (millipede)), *snail* genes appear during neurogenesis (Pioro and Stollewerk, 2006).

In *Parhyale,* one copy of *snail*, *Ph-sna1,* is expressed in the mesoderm at germ band stages (Price, 2005; Hannibal, 2010), and may be instrumental during migration of the mesoteloblasts (Hannibal, 2010). Two other copies of *snail*, *Ph-sna2* and *Ph-sna3,* and a related gene, *Ph-scratch,* show no expression during segmentation. The early expression patterns and functions of these genes, if any, remain unknown.

Notch signaling

Short-range signaling through the transmembrane receptor Notch and its ligands is fundamental to developmental events such as cell identity, proliferation, and apoptosis (Artavanis-Tsakonas, 1999; Bray, 2006). Of particular interest to this study is Notch/Delta signaling as an inducer of mesenchyme in sea urchins. In the urchin *Lytechinus variegatus,* the vegetal micromeres have powerful inductive abilities. Transplantation experiments show that the micromeres are able to ectopically induce mesendoderm cells and invagination in the animal hemisphere of developing embryos (Hörstadius, 1973; Ransick and Davidson, 1993; Ettensohn and Sweet, 2000). Notch is located in the early secondary mesenchyme cells (SMCs) that give rise to non-skeletogenic mesoderm and ingress as the archenteron elongates during gastrulation (Sherwood and McClay, 1997). Notch signaling proceeds through the ligand Delta produced from the vegetal micromeres (Sweet et al., 2002), making Notch/Delta signaling a key component to mesoderm induction (Sweet et al., 2002; Peter and Davidson, 2011).

During morphogenesis in arthropods, Notch/Delta signaling has been most extensively examined in *Drosophila* where it determines, among other things, cell fate in the neurogenic ectoderm through a process called lateral inhibition (Kooh et al., 1993; Axelrod, 2010). Notch/Delta homologs play an important role during segmentation in the *C. salei* (Stollewerk et al., 2003), and during the production of the posterior region of the embryo in the *A. tepidariorium* (Oda et al., 2007).

During *Parhyale* development, previous work using cloned orthologs of *Notch* and *Delta* along with DAPT, a drug that inhibits Notch signaling, indicate that it functions to define segments during germ band and appendage formation. Embryos treated with DAPT exhibit a range of phenotypes including fused and/or missing segments, antennae, appendages, and/or segments of appendages (O'Day, 2006). Drug treatment sometimes resulted in lethality prior to the formation of the germ band, indicating a possible function for Notch/Delta signaling during early development. However, all previous work did not investigate whether Notch and Delta transcripts appeared before gastrulation.

Molecular signals during gastrulation in *Parhyale*

To investigate whether the *Parhyale* homologs of *dpp* (*Ph-dpp*), Snail family genes *(Ph-sna1, -sna2, -sna3, and Ph-scrt)*, and Notch and Delta *(Ph-notch and Ph-delta)* are expressed during gastrulation stages, I performed in situ hybridization during early cleavage and gastrulation. I also attempted to confirm my results through RT-PCR. This is the first analysis of a *dpp* ortholog during *Parhyale* development. I show its phylogenetic relationship to other TGF-β genes and the percentage of similarity and identity to orthologs from other species (Fig 5.1 and 5.2). The phylogenetic positions and similarity/identity of the other *Parhyale* genes have been discussed in previous work (O'Day, 2006; Hannibal, 2010). I find that the cloned copy of *dpp* groups with BMP-4 and other arthropod dpps. Surprisingly, I was unable to find convincing expression of any of the candidate genes during early cleavage and gastrulation stages. *Ph-notch* and *Ph-delta* were the only transcripts that manifested during early development

MATERIALS AND METHODS

Fixation and dissection of animals

Fixation and dissection of embryos was carried out as previously described in Chapter 2 with the modification that the timing of fix ranged from 20 minutes to an hour. Post-germ band embryos were not immersed in high salinity pre-fix because the second, inner membrane negates the positive effects of a hypersaline treatment.

Ph-dpp, *Ph-Snail* family members, and *Ph-notch* and *–delta*

With the exception of *Ph-dpp,* cloning of the genes used for this work has been previously described (Hannibal, 2010; O'Day, 2006). *Ph-dpp* was provided by Dr. Ron Parchem, a former member of the lab. A fragment of *Ph-dpp* was previously cloned by Dr. Matthias Gerberding. Parchem used that fragment to perform 5' and 3' race with the Firstchoice RLM-RACE kit. The full sequence he obtained is provided in Appendix A.

Phylogenetic analysis and similarity/identity matrices

For the phylogenetic analysis of *Ph-dpp,* amino acid sequences from NCBI were collected with the help of Dr. Cristina Grande. Sequences were trimmed to the highly conserved ligand domain of TGF-β family members (approximately 100 amino acids from the C-terminus). Alignment was performed using MUSCLE software and then corrected by eye. The alignment was then used to create a maximum likelihood tree with 100 bootstrap replicates using PhyML software online (phylogeny.fr/)(Castresana, 2000; Dereeper et al., 2008; 2010).

For comparison of percent amino acid sequence identity/similarity of *Parhyale hawaiensis dpp* with sequence of *Drosophila* and *Tribolium,* MacVector software running CLUSTAL W (alignment) and BLOSUM (identity/similarity matrices) was used. The *D. melanogaster* propeptide domain has an N-terminal region of 82 amino acids that was not used in the comparison (white box, Fig. 5.2).

In situ hybridization

Digoxygenin (DIG) or Fluorescein (FL) labeled antisense and sense riboprobes for each gene were synthesized using SP6, T7, and T3 polymerases (Roche) and then diluted and stored in hybridization buffer. Probes were used at a final concentration of 0.5ng/ml to 3 ng/ml. Multiple probes from various regions that ultimately spanned the entire transcript were used for each gene. In situs were carried out as previously described (Rehm et al., 2009c).

Sense probes were used as negative controls. Positive controls were either the gene *ph-Pax 3/7* or *ph-β–catenin*. Both are expressed pre-and post-gastrulation. *Pax 3/7* is perinuclear and ubiquitous early, and is then restricted to a subset of the developing germband (Melinda Modrell, personal communication; and(Parchem, 2008)). β-*catenin* expression is restricted to cytoplasm surrounding the nucleus in the germline during cleavage stages and is then restricted to the anterior portion of certain segments during germ band development (Modrell, 2007).

Cloning and preparation of probes was done according to published protocols with minor modifications (Rehm et al., 2009c). Briefly, after cloning into pBluescript vector, the plasmid DNA with the piece of the gene of interest was linearized into a template for transcription using PCR with universal probes M13 forward and reverse.

RT PCR

Total RNA was isolated from 1-, 2-, 4-, and 8-cell embryos and soccerball, germ cap, and appendage bud (S17, ~87 hpf) embryos using TRIzol Reagent (Sigma). Synthesis of cDNA proceeded according to manufacturer's instructions using the SuperScript® Synthesis System for first-strand cDNA kit (Invitrogen). Gene specific *Ph-Notch* primers (forward primer 5'-CGC TAA GAA CTT TTC AAA TGC TAA C-3'; reverse primer 5'-TAT GCC TCC ATT ATA CCG TCA CAT T-3') and *Ph-Delta* primers (forward primer 5'-GGC ATT AAT TCT TTC AAG TGT CAG T-3'; reverse primer 5'-AGA GCT CCG TAA ATA ATA AAT GTC G-3') were used. Positive controls were *Pax 3/7* and *tubulin*.

RESULTS

Ph-dpp groups with BMP-4 and other dpp, but is not expressed before gastrulation.

To confirm that the cloned *Parhyale* gene was an ortholog of decapentaplegic, Dr. Cristina Grande, a postdoc in the lab at the time, and I created a phylogeny of TGF-β family members. *Ph-dpp* groups with BMP-4, the vertebrate homolog of decapentaplegic, with high confidence (bootstrap value: 91%; Fig. 5.1). Furthermore, I compared the amino acid sequence of Ph-dpp to that of dpp from *Drosophila* and *Tribolium*. TGF-β family members are secreted in an immature form that consists of a propeptide N-terminal sequence and a highly conserved C-terminal domain that features 7-9 cysteines. For signaling to occur, the cysteine-rich domain is cleaved and acts in its mature form as a ligand for specific receptors (Massague, 1990). In our comparison, similarity in the propeptide domain suggests that it is considerably less well conserved than the ligand domain. Between Drosophila and Parhyale, sequence similarity in the propeptide region is 39.1% versus 76.5% in the ligand. Between Tribolium and Parhyale, sequence similarity in the propeptide is 40.1% versus 76.5% in the ligand. A similar disparity is apparent in sequence identity. Between Drosophila and Parhyale, sequence identity in the propeptide region is 22.5% versus 65.7% in the ligand; between Tribolium and Parhyale, identity in the propeptide is 21.1% versus 61.8% in the ligand. This difference is expected because the propeptide domain, as an inactive part of the protein, is less well conserved (Massague, 1990; Fig. 5.2). Our tree of TGF-β family members and comparison of related sequences indicate that *Ph-dpp* is indeed a *Parhyale* ortholog of *decapentaplegic*. Whether it is the only copy of *decapentaplegic* in the *Parhyale* genome remains unknown.

If *Ph-dpp* functions to define of dorsal-ventral polarity, we would expect it to have differential expression during early gastrulation and possibly early cleavage stages. Because cell behavior during gastrulation is autonomous, it is reasonable to assume that determinants for cell-location and ultimate fate are present at the time of

gastrulation. *Ph-dpp*, if it functions as *dpp* in *Drosophila*, might be segregated to descendants of the blastomere en, as they are the dorsal most cells of the embryo during rosette internalization. Alternatively, if *dpp* expression were in the cells that first break the symmetry of early cleavages, as in *Achaearanea,* then *dpp* expression would appear in the cells of the rosette.

We preformed in-situ hybridization with various *Ph-dpp* riboprobes on 2-cell, 4-cell, 8-cell, and early-, mid-, and late-gastrulation stages. Despite repeating the experiment with various probes encompassing portions of or the entire length of the UTRs and the coding region, no conclusive early expression during these stages was detected. Six replicates were performed and positive and negative controls in each case worked to expectations. This result indicates that transcripts of this version of *dpp* are not present during early embryogenesis. It is highly unlikely that TGF-β signaling would be absent from early embryogenesis. A more likely explanation is that this copy of TGF-β is not functioning at these stages, and that a different copy or a different family member is present.

Previous work by Parchem using this copy of *Ph-dpp* during late segementation/early appendage development suggested that it might have an expression pattern specific to neural development. However, this pattern was only detected once, and I was unable to replicate it.

Snail family members are not expressed during gastrulation stages

If *Parhyale* development relies on *Snail* family members as either mesoderm determinants or as regulators of migration, we would expect to see differential expression of transcript in either mesoderm cells or in migrating cells. Through in situ hybridization, we found that the current *Snail* family members we have in the lab are not expressed during early cleavage or gastrulation stages. Together with Roberta Hannibal, a graduate student in the lab at the time, four replicates were performed at the 2-cell, 4-cell, 8-cell, soccerball, and early-, mid-, and late-gastrulation stages for each gene. Positive and negative controls and older embryos all had expected expression patterns. These results indicate that the present copies of *Snail* family genes are not present during early embryogenesis. It is possible that *Parhyale* uses other mechanisms to regulate mesoderm determination and cell migration.

Notch/Delta expression during early cleavage and gastrulation stages

If *Ph-notch* is signaling with its ligand *Ph-delta*, and this is an early mesoderm determinant like in urchins, we expect differential expression of *Ph-notch* and *Ph-delta* transcripts during gastrulation stages and possibly early cleavage stages. Expression of *Ph-notch* transcript might be ubiquitous but transcript of the ligand *Ph-delta* might only appear in cells adjacent to those intended to have active *Ph-notch* signaling. As a mesoderm determinant, it is therefore possible that *Ph-delta* transcript would be apparent in the epithelial cells adjacent to Mav and ml/mr descendants.

Under my supervision, an undergraduate named Evie Huang performed in situ hybridization for *Ph-notch* and *Ph-delta* on early cleavage stages (4-, 8-, 16-, and 32-cells), soccerball (S6), rosette (S7), and germ cap (S8) stages. *Ph-notch* expression is ubiquitous and perinuclear at the 8-cell and 16-cell stages, but is absent from 32-cell

specimens. Unfortunately, 4-cell specimens were lost during the *in situ* procedure. *Ph-notch* transcript is also absent from soccerball, rosette, and germ cap stages (Fig. 5.3).

Expression of *Ph-delta* transcript is also ubiquitous and perinuclear during early cleavage. At the 4-cell stage, expression appears offset and to one side of the nucleus (Fig. 5.3). At 8-, 16-, and 32-cells, soccerball and rosette, *Ph-delta* transcripts are located in the cytoplasm immediately surrounding the nucleus (Fig. 5.3). During the germ cap stage, *Ph-delta* expression narrows to a strip of cells that will become the first cells to divide during the formation of the germ band (O'Day, 2006).

To confirm these results, we performed RT PCR on cDNA made from total mRNA collected from various stages. *Ph-delta* transcripts were present in all the stages we used (Fig. 5.3). *Ph-notch* transcripts are present during early cleavage stages, but are absent from soccerball and germ cap stages. Both *Ph-notch* and *Ph-delta* transcripts are present at Stage 17 as expected from their roles during segmentation (O'Day, 2006).

Unfortunately, we were only able to produce these *in situ* results once. I attempted two replicates after Huang left the lab and was unable to reproduce the expression patterns.

These results, if accurate, indicate that *Ph-notch* and *Ph-delta* transcripts are present during pre-gastrulation stages in *Parhyale.* Furthermore, they have different temporal expression patterns. Because the onset of zygotic transcription is thought to occur sometime after the initiation of gastrulation, the transcript present in pre-gastrulation stages must be maternally provided. The lack of *Ph-notch* transcript from the 32-cell, soccerball, and rosette stages indicates a degradation of maternal transcript. Previous work reports that the earliest expression of *Ph-notch* is at stage 11 (~60 hpf), when head lobes are fully formed and germ band segmentation begins (O'Day, 2006). This late expression of *Ph-notch* is probably zygotic. Whether the early expression of *Ph-notch* that we observed is crucial to early development remains to be seen. Previous work with DAPT, a pharmacological inhibitor of Notch/Delta signaling, found that treatment with DAPT can result in lethality prior to the formation of the germ cap. The reason for this phenotype remains unknown.

DISCUSSION

The absence of *Ph-dpp* and *Ph-Snail* family members from early embryogenesis

That *Ph-dpp* and *Ph-Snail* family members we investigated are not used to confer cell identity or to regulate cell migration in *Parhyale* is not necessarily surprising. Although every effort was made with degenerate PCR to pull all possible family members from each group, it is entirely possible that alternate copies or members of each signaling family exist in *Parhyale* and are functioning in the stead of the copies we tested in this study.

Future work could take advantage of a recently annotated and easily searchable *Parhyale* EST database (http://genome.jgi-psf.org/parha/parha.home.html). Preliminary work using this database from a current student in the lab, Angela Kaczmarczyk, has uncovered a TGF-β family member that BLASTS to *Drosophila glass-bottom-boat* (aka 60A). Glass bottom boat more closely resembles vertebrate BMP-5 and BMP-7

versus dpp's resemblance to BMP-4. It is thought that the divergence between the two lineages occurred well before the divergence of insects and mammals (Wharton et al., 1991). Functionally, 60A appears to work synergistically with Dpp during several events during *Drosophila* development, making it an interesting candidate for study in *Parhyale*.

Searching the EST database may also be fruitful for determining whether another *Snail* family member exists. Another approach may be to study the proteins and junctions that are known to regulate and to be regulated by *Snail*. Downstream of *Snail,* changes in proteins that comprise cell-cell junctions would mark cells enacting migratory behavior. Among these, β-catenin is a promising candidate that has been previously cloned and for which commercially available cross-reactive antibodies appear to work (Modrell, 2007). β-catenin is also a part of the canonical Wnt-signaling pathway that has been found upstream of Snail in sea urchins (Wu et al., 2007; Oliveri and Tu, 2008; Thiery et al., 2009). Other adhesion proteins in *Parhyale* have not received any attention. In particular, cadherins, integrins, and their associated proteins might provide a rich area for study.

Upstream of *Snail,* fibroblast and epidermal growth factors (FGF and EGFs), TGF-β, Notch, and Wnt signaling have all been implicated in the pathway that leads to mesenchymal behavior (Thiery and Sleeman, 2006). Aside from this study, the possible functions of these signaling pathways have not been investigated in *Parhyale* at pre-gastrulation or during gastrulation stages.

Notch and Delta during gastrulation in *Parhayle*

We found the presence of maternal *Ph-notch* and *Ph-delta* transcript in early cleavage stages. Furthermore, the *Ph-delta* transcript persists throughout early development and into germ band formation and segmentation, but the *Ph-notch* transcript ceases to appear prior to gastrulation until the head lobes appear in the developing germ band. That the two have different temporal expression patterns could indicate that they have some functional significance during early cleavage stages. The loss of *Ph-notch* transcript after the 16-cell stage until the beginning of segmentation could indicate that *Ph-notch* is a transcript targeted for active degradation by maternal factors. As described by Tadros and Lipshitz (2009), the first step of the transition from maternal to zygotic transcription is the destabilization and elimination of a subset of maternal transcripts. This occurs through both maternally and zygotically controlled processes, and could serve to make way for patterned zygotic transcription to organize the embryo (Tadros and Lipshitz, 2009). It is possible that transcript for the *Ph-notch* receptor is depleted after it is no longer functionally important, while ligand transcript is allowed to persist because the ligand is useless without a receptor. Replication of our results combined with a fine-scale description of *Ph-notch*/*Ph-delta* transcript during rosette internalization would further our understanding of these potentially important temporal differences.

To truly assess the importance of Notch and Delta during *Parhayle* development, it will be necessary to develop methods for studying protein expression and function. The development of *Parhyale* specific antibodies to Ph-notch and Ph-delta would allow the analysis of temporal and spatial differences in protein

expression. Through the use of immunohistochemistry, antibodies would not only be a descriptive tool but would also provide an assay for functional studies. Previous functional work has included perturbation of Notch/Delta signaling with the commercially available inhibitor DAPT. O'Day (2006) successfully assayed the efficacy of this method through phenotypic analysis combined with in situ hybridization of *Ph-notch* and *Ph-delta* and a downstream target of *notch* signaling, *suppressor of hairless*. However, possession of antibodies would greatly streamline this process.

Finally, O'Day (2006) also observed a lethality phenotype from drug inhibition of Notch/Delta signaling that appeared to kill embryos prior to formation of the germ cap. This work also noted that drug penetration was difficult to control due to precipitation issues that persist even at lower salinity. Future work could focus on characterizing the lethality phenotype and developing novel methods for more focused and easily controlled inhibition of Notch/Delta signaling. Currently, techniques for the molecular knockdown of transcripts including siRNA and hairpin constructs are gaining ground in the lab. These would be useful in significantly lowering the amount of maternally transmitted *Ph-notch*/*Ph-delta* RNA. Combined with an assay for protein expression, these techniques would be a powerful way to learn more about the role of Notch/Delta signaling during early embryogenesis in *Parhyale*.

Early ecto- and mesoderm determinants in *Parhyale*

Defining tissue layers and embryo orientation is vital to proper morphogenesis. In addition, the creation of cellular identity is the first step toward the specific and individual cell behaviors that will drive gastrulation.

A clear candidate for defining early ectoderm and mesoderm fate during *Parhyale* development remains to be found. Discovery of such a molecule would further our understanding of fate determination and the establishment of dorsal/ventral and anterior/posterior axes in *Parhayle* development as well as contributing to our understanding of the evolution of these different processes.

Figure 5.1. Ph-dpp groups with BMP-4 and other dpps.
Maximum likelihood cladogram of the TGF-b ligand domain of representatives from various subfamilies in the TGF-b superfamily. Bootstrap values for 100 replicates are shown in red. *Ph-dpp* and group are highlighted in blue. Abbreviations are used: Xl (*Xenopus laevis*, African clawed frog); Xt (*Xenopus tropicalis*, Western clawed frog); Dr (*Danio rerio*, zebrafish); Mus (*Mus musculus*, mouse); Ur (sea urchins); Gal (*Gallus gallus*, chick); Ag (*Anopholes gambiae*, mosquito); Dm (*Drosophila melanogaster*, fruit fly); Ph (*Parhyale hawaiensis,* sand scud); At (*Achaeranea tepidariorium*, spider); Tc (*Tribolium castaneum*, flour beetle); Bm (*Bombyx mori*, silk moth); Dp (*Daphinia pulex*; water flea).

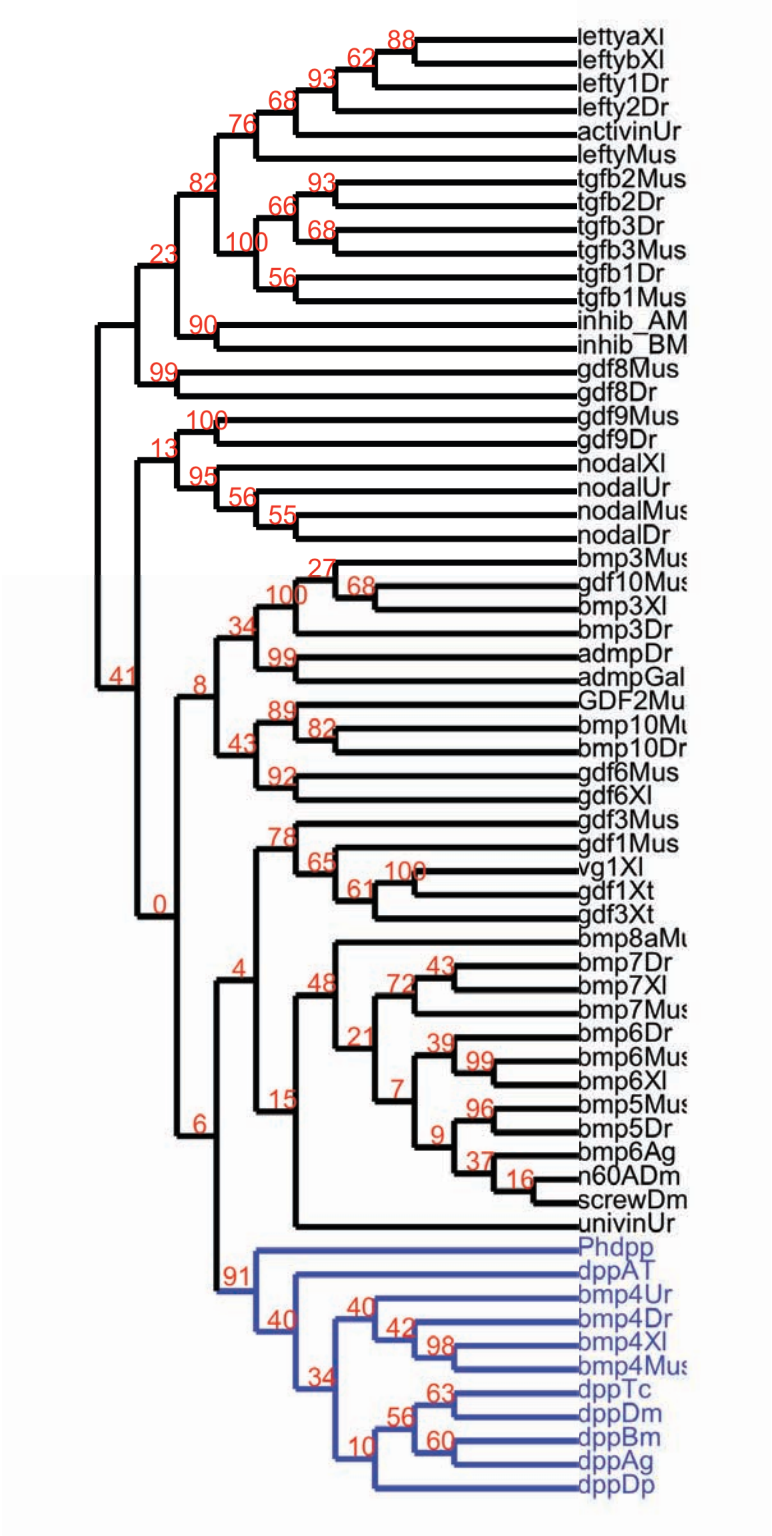
lefty1Dr
lefty2Dr
activinUr
leftyMus
tgfb2Mus
tgfb2Dr
tgfb3Dr
tgfb3Mus
tgfb1Dr
tgfb1Mus
inhib_AM
inhib_BM
gdf8Mus
gdf8Dr
gdf9Mus
gdf9Dr
nodalXl
nodalUr
nodalMus
nodalDr
bmp3Mus
gdf10Mus
bmp3Xl
bmp3Dr
admpDr
admpGal
GDF2Mu
bmp10Mu
bmp10Dr
gdf6Mus
gdf6Xl
gdf3Mus
gdf1Mus
vg1Xl
gdf1Xt
gdf3Xt
bmp8aMu
bmp7Dr
bmp7Xl
bmp7Mus
bmp6Dr
bmp6Mus
bmp6Xl
bmp5Mus
bmp5Dr
bmp6Ag
n60ADm
screwDm
univinUr
Phdpp
dppAT
bmp4Ur
bmp4Dr
bmp4Xl
bmp4Mus
dppTc
dppDm
dppBm
dppAg
dppDp

Figure 5.2 Ph-dpp identity and similarity with Drosophila and Tribolium.

(A) Comparison of percent amino acid sequence identity/similarity of *Parhyale hawaiensis dpp* with related sequences. Propeptide: the first amino acid after the putative signal peptidase cleavage site to the first cysteine of the mature domain. Length of propeptide domain (green) used for comparison is indicated. The *D.melanogaster* propeptide domain has an N-terminal region of 82 amino acids that was not used in the comparison (white box). Ligand: the mature, ligand domain (blue) from the first cysteine to stop. Ligand domain is 102 amino acids in all organisms. Yellow lines indicate the seven conserved cysteine (C) residues of TGF-β family members. MacVector software running CLUSTAL W and BLOSUM was used to generate alignments and identity/similarity matrices. Sequence accession numbers: *D.melanogaster :* NP_477311, *T.castaneum:* AAB38392 (B) Schematic of phylogenetic relationships between *D. melanogaster, T. castaneum, and P.hawaiensis*. Estimated divergence time of two nodes are shown in millions of years ago (mya), based on (Ponting, 2008). (C) Alignment of mature ligand domain between the three amino acid sequences. phmat = *Parhyale* mature ligand, tcmat.prot = *Tribolium* mature ligand, dppmat = *Drosophila* mature ligand.

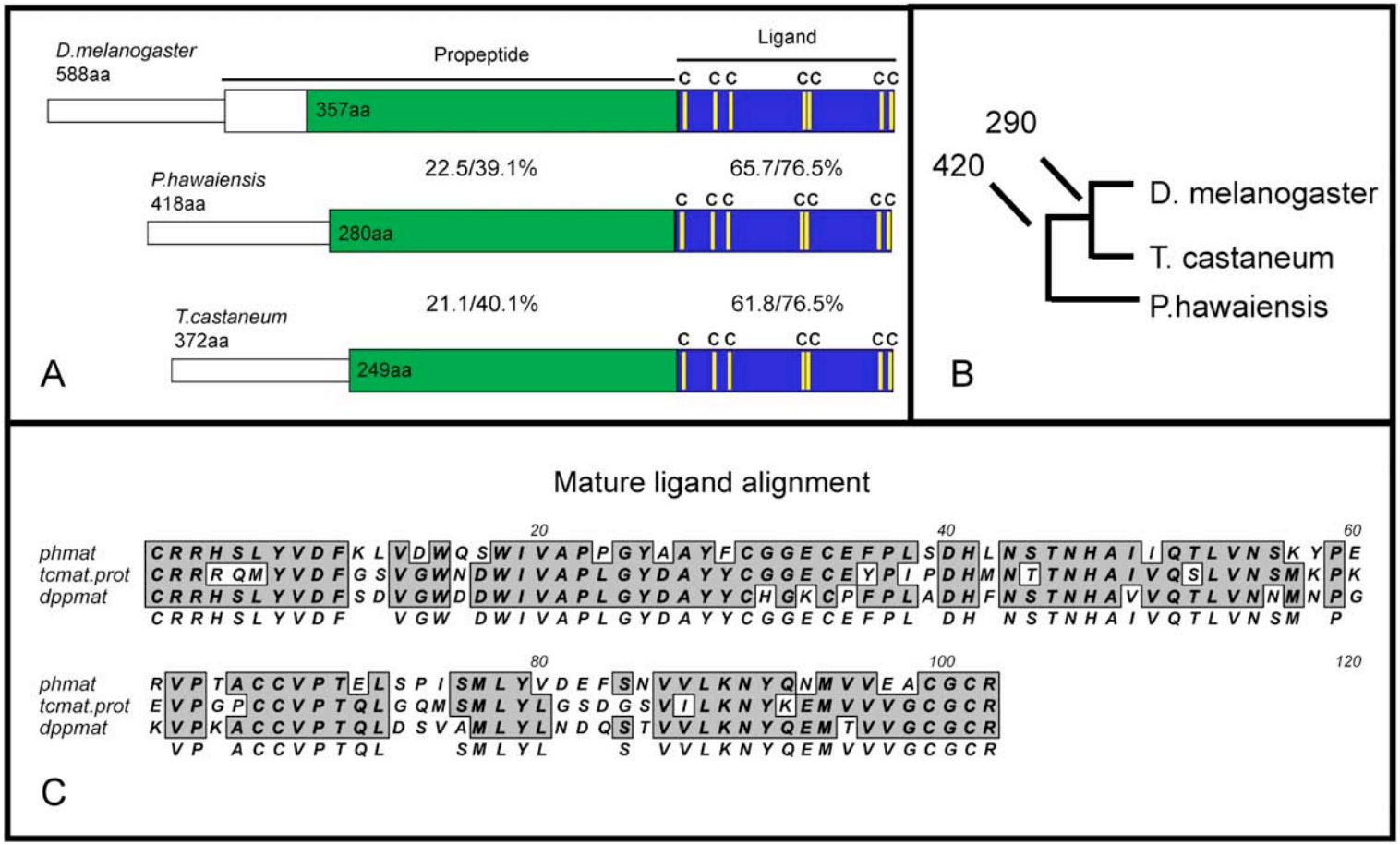
D.melanogaster
588aa
Propeptide
Ligand
357aa
22.5/39.1%
65.7/76.5%
P.hawaiensis
418aa
280aa
21.1/40.1%
61.8/76.5%
T.castaneum
372aa
249aa
A
290
420
D. melanogaster
T. castaneum
P.hawaiensis
B
Mature ligand alignment
phmat
tcmat.prot
dppmat
C

Figure 5.3. RT PCR and expression of *Ph-notch* and *Ph-delta* during early embryogenesis.
(A) RT PCR results for various stages during development. Brackets represent lanes loaded with PCR from different stages. Red: 1 cell ; Orange: 2 cell ; Yellow: 4 cell; Green: 8 cell; Blue: Soccerball; Purple: Germ cap; Beige: Appendage bud. At each stage we amplified (product size): *Ph-notch* (526bp), *-delta* (547bp), *-pax3/7* (437bp), and *-tubulin* (200bp). *Ph-pax 3/7* and *tubulin* were used as positive controls. Ladder band sizes are shown down the left. (B). *Parhyale Notch* expression in 8 and 16 cell embryos. *In situ* hybridization of *Ph-notch* reveals ubiquitous signal. Top; brightfield, Bottom: DAPI (C) *Parhyale Delta* expression in 4-cell embryos is to one side of the nucleus. Top: brightfield image. Bottom: DAPI (blue) and false color overlay of *Ph-Ph-delta* expression (red). Levels were significantly altered to reduce background for the bottom image. (D) *Parhyale Delta* expression from 8-cell through soccerball**.** Top: brightfield image. Bottom: DAPI (blue). (E) *Parhyale Delta* expression at the rosette stage. Left: Brightfield view. The rosette is visible as a cluster for darker cells. Middle: DAPI (blue). Right: Overlay of brightfield and DAPI stain.

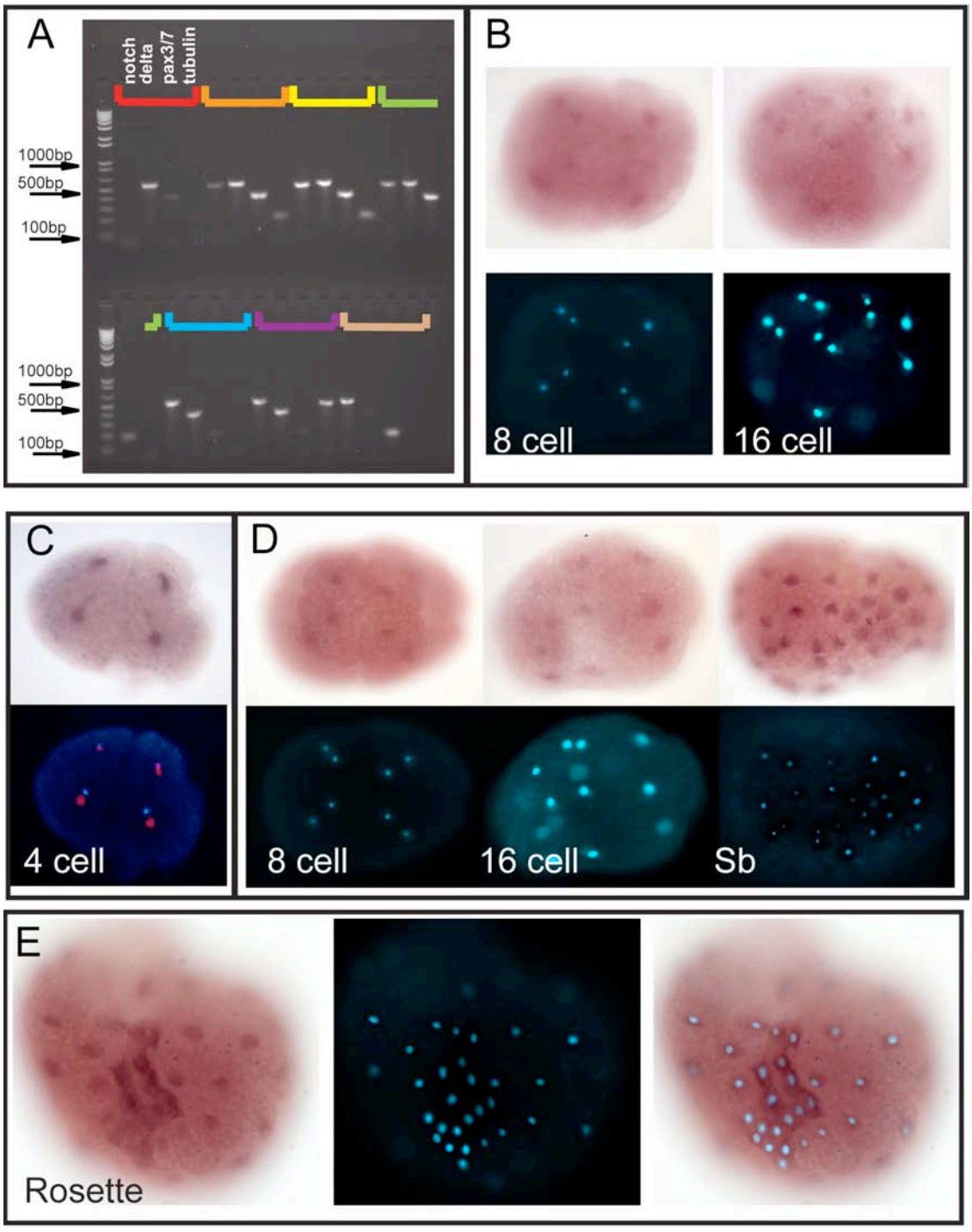
A
notch
delta
pax3/7
tubulin
1000bp
500bp
100bp
1000bp
500bp
100bp
B
8 cell
16 cell
C
4 cell
D
8 cell
16 cell
Sb
E
Rosette

Chapter VI: Conclusions and future directions

This dissertation represents several novel contributions to our growing understanding of cell behavior during *Parhyale* gastrulation. I found cell shape change in the rosette that confirms previous hypotheses suggesting that gastrulation in *Parhyale* proceeds through ingression or invagination. I also found that the rosette and epithelial sheet act autonomously, and that the descendants of different lineages within the rosette are able to internalize independently. Using drug inhibition, I identified *rho-kinase* as important to epithelial integrity during gastrulation, and discovered a phenotype that may be associated with abnormal cell division. Finally, I investigated several candidate genes in an effort to discover a molecular marker for early mesoderm and ectoderm fate. This study provides valuable information about the process of cell internalization, cell autonomy during gastrulation, and suggests potential highly conserved mechanisms for cell behavior during *Parhyale* gastrulation.

Blastopores and gastrulation

In the second chapter of this dissertation, we conclude that the presence of bottle cells in the rosette combined with the movement of germline descendants and epithelial cells toward a single internalization site suggests two things: 1. That internalization proceeds through ingression or invagination and 2: that a blastopore, although not necessarily visible with brightfield microscopy, does exist in *Parhyale*. Blastoporal positioning is important for at least three reasons. First, the blastopore marks the region that will give rise to the internalizing tissues. Second, the position of the blastopore in relation to the site of meiotic division varies between Bilaterians and radial animals like Cnidarians and Ctenophores. In Bilaterians, the blastopore occurs on the vegetal half of the embryo versus its position on the animal half in Cnidarians and Ctenophores. This deep evolutionary variation in blastoporal positioning may indicate a fundamental difference in the Bilateran body plan. Finally, as the locus for cell internalization, the blastopore often indicates a signaling center for molecules regulating cell fate and migration (Martindale and Hejnol, 2009).

Amphipod blastopores are different from those found in other malocostraca because they mark the anterior portion of the germ band rather than forming at the presumptive posterior of the animal (Gerberding and Patel, 2004). In many triploblasts, the embryo develops in an anterior to posterior fashion. This means that the head and anterior structures are born first and then further tissue is added to the developing animal posteriorly. This is true in *Parhyale* and many insects outside of *Drosophila* (Davis and Patel, 2002; Browne et al., 2005). In this regard, moving the normally posterior blastopore to an anterior location may increase developmental efficiency, or it could reflect an overlap between signals directing cell internalization and the initiation of head lobe formation and development. There is a significant lag time between the completion of rosette internalization (~20 hpf) and the formation of the head lobes (~87 hpf). Future work could focus on the surely complex morphological and molecular rearrangements that occur during this time period.

Uncovering the timing and regulation of internalization, head lobe formation, and the extent to which the two are linked might explain why amphipods exhibit a derived blastopore position during gastrulation.

The relationship of the putative *Parhyale* blastopore to the later internalization of the somatic mesoderm and then endoderm remains unclear. In many arthropods, internalization of the meosoderm and endoderm is separated spatially and temporally. *Drosophila* gastrulation is an example. After the internalization of the mesoderm as discussed in the introduction, endoderm internalizes through anterior and posterior midgut invaginations. Definition of the endoderm is regulated by the zinc finger transcription factors *huckebein* and *tailless* that are expressed in the anterior and posterior domains of the *Drosophila* blastula (for review, see Leptin, 1995). It will be interesting to discover how the later phases of *Parhyale* gastrulation occur compared to rosette internalization and to the later phases of *Drosophila* gastrulation.

Cellular interactions, polarity, and Rho-kinase

Chapters three, four, and five focus on discerning potential mechanisms for cell internalization during early *Parhyale* gastrulation. To this end, chapter three asks whether cells are interdependent during *Parhyale* gastrulation. In other words, is there a group of cells generating molecular or mechanical cues that instruct or permit the other cells to complete their gastrulation programs? We conclude that the cells of the rosette and epithelial sheet act autonomously, and that the two lineages of the rosette are able to internalize independently.

Among other arthropods, gastrulation often depends more closely on cellular interactions. For example, in spiders, gastrulation in many species begins with the internalization of a small group of mesendodermal cells called the cumulus. When these cells are ablated, the embryo is unable to complete development and develops radial instead of bilateral symmetry. Moreover, transplanting the cumulus cells can induce twinned embryos (Holm, 1940). As discussed in chapter three, the D blastomere of the decapod shrimp *S. ingentis* also has inductive abilities. When cultured with other cells, it enables the progression of development into gastrulation stages. This makes the autonomy of *Parhyale* cells appear to be a unique, possibly derived state.

In chapters four and five, we investigate cytoskeletal and molecular candidates for the regulation of cell behavior. We find that *Parhyale* gastrulation requires *rho-kinase* and that Notch/Delta signaling has some promise for future investigation. Rho GTPases are found regulating the actin cytoskeleton in all known taxa, so to find evidence of downstream effectors of Rho signaling in *Parhyale* is expected. What differs between taxa are the varied purposes for and ways in which *Rho-kinase* is deployed (Riento and Ridley, 2003). For example, in *Drosophila*, Rho-kinase acts to phophorylate myosin during apical constriction, but during zebrafish gastrulation it regulates cytokinesis and cell migration (Riento and Ridley, 2003; Lai et al., 2005).

As an effector of *Rho* signaling, *rho-kinase* also functions downstream of non-canonical *wnt* signaling through the planar cell polarity pathway (*wnt*-PCP) to regulate cell polarity in epithelial sheets (Schlessinger and Hall, 2009). The phenotype we observe in this study after treating embryos with the *rho-kinase* inhibitor ROCKOUT is consistent with *rho-kinase* having a role in regulating cell polarity during gastrulation.

Namely, epithelial cells lose their cuboidal shape and actin-rich apical junctions are missing. Some controversy exists over whether *wnt*-PCP signaling directly activates Rho-kinase activity or whether a novel pathway exists (Lapébie et al., 2011). Futher work investigating the molecular regulation of cell polarity will illuminate how *Parhyale* utilizes the versatile Rho-ROCK pathway during development.

Our conclusion that Notch/Delta signaling is important to gastrulation is tentative because we were unable to replicate our results more than once. However, Notch/Delta signaling is common and pleiotropic during development in all known taxa (Wang, 2011). Its involvement in *Parhyale* development is expected, but our study is the first to find evidence for it in pre-gastrulation embryos. During early developmental stages, Notch/Delta signaling can confer endomesodermal cell fate. As discussed in chapter five, sea urchin cell fate specification is a classic example. Among arthropods, Notch/Delta signaling often functions post-gastrulation during germ band formation and segmentation (Kooh et al., 1993; Stollewerk et al., 2003; O'Day, 2006; Oda et al., 2007; Mito et al., 2011). The use of Notch/Delta signaling during pre-gastrulation stages in *Parhyale* may prove to be an unusual function. To understand how Notch/Delta signaling is utilized in various arthropods, further characterization of its use during *Parhayle* embryogenesis will be illuminating. To this end, as discussed in Chapter V, the development of specific molecular knockdown and overexpression constructs is key because drug inhibition has previously proven to be difficult to control (O'Day, 2006).

The autonomy of cells during gastrulation movements implies an early restriction of cell fate over a later inductive event. This aligns *Parhyale* development with lophotrochozoan systems that employ similar cell-autonomous determination events like *C. elegans* and mollusks. The mechanisms governing patterning in mollusks are less well understood than those in *C. elegans*. However, recent work shows that some mRNAs are localized to the centrosome in the snails *Ilyannasa obsoleta* and *Crepidula fornicata*, and that these mRNAs are subsequently segregated to a single daughter cell. This implies that these mRNAs could play a role in early fate determination (Lambert and Nagy, 2002; Kingsley et al., 2007; Henry et al., 2010). This method of segregation of specific mRNAs for early fate determination is also used in other metazoans, including arthropods such as wasps and *Drosophila* (Lasko, 1999; Lécuyer et al., 2007; Olesnicky and Desplan, 2007). In this study, we observed that early *Ph-delta* expression appears to one side of nucleus in 4-cell embryos, however it is ubiquitous at the 8-cell stage. Previous work in *Parhayle* has observed that *β-catenin* transcripts localize to the germ cell up to gastrulation (Modrell, 2007). Future work could look for further evidence of asymmetrically localized mRNAs that are segregated to a single daughter. It might also be interesting to investigate whether cell autonomy is common in the amphipod lineage by repeating our ablation experiments in a relatively closely related species such as *O. cavimana*.

Final Thoughts

My work with *Parhyale* integrates a variety of cell-biological and molecular tools to address two broad areas of concern in evolutionary developmental biology: 1) the cellular basis of morphogenesis and 2) the need for an understanding of

development in a variety of organisms. As discussed throughout this dissertation, an understanding of how, when, and where cells move provides a vital and fundamental context for understanding how morphogenesis occurs. Previous work regarding *Parhayle* includes work that is descriptive (Gerberding et al., 2002; Browne et al., 2005), focused on fate determination (Price and Patel, 2008; Price et al., 2010), or that investigates the evolution of molecular pathways important to segmentation and polarity in the germ band (Liubicich et al., 2009; Pavlopoulos et al., 2009; Vargas-Vila et al., 2010). Recent work describes the movement and relationships of blastomeres pre-gastrulation with some description of the movements when a micromere is deleted (Alwes et al., 2011). The present study is the first to focus on and directly manipulate populations of cells during gastrulation. This kind of experimentation is an avenue toward realizing the importance of specific cell populations during gastrulation and therefore understanding how cells build the *Parhyale* body plan during morphogenesis.

Current developmental model systems are marked by considerable knowledge of both the cellular and molecular mechanisms at work during all stages of development. Knowledge of cellular mechanisms during early *Parhyale* development furthers this organism's status as a crustacean model system by establishing a basis for comparisons with other organisms. This knowledge informs the organized investigation of the origin of homologous genes and gene pathways as well as morphological characteristics. A contextual understanding of cellular interactions during early *Parhyale* development broadens it relevancy to evolutionary comparisons and provides an important additional data point for comparative analyses.

Finally, this study raises at least as many questions as it answers. It is my hope that a better understanding of cell behavior and gastrulation in *Parhyale* will inspire future work.

Bibliography

Akiyama-Oda, Y., 2006. Axis specification in the spider embryo: dpp is required for radial-to-axial symmetry transformation and sog for ventral patterning. Development 133, 2347–2357.

Akiyama-Oda, Y., Oda, H., 2003. Early patterning of the spider embryo: a cluster of mesenchymal cells at the cumulus produces Dpp signals received by germ disc epithelial cells. Development 130, 1735.

Alwes, F., Hinchen, B., Extavour, C.G., 2011. Patterns of cell lineage, movement, and migration from germ layer specification to gastrulation in the amphipod crustacean Parhyale hawaiensis. Developmental Biology 359, 110–123.

Alwes, F., Scholtz, G., 2006. Stages and other aspects of the embryology of the parthenogenetic Marmorkrebs (Decapoda, Reptantia, Astacida). Development Genes and Evolution 216, 169–184.

Anderson, K.V., Jürgens, G., Nüsslein-Volhard, C., 1985. Establishment of dorsal-ventral polarity in the Drosophila embryo: Genetic studies on the role of the Toll gene product. Cell 42, 779–789.

Arendt, D., Technau, U., Wittbrodt, J., 2001. Evolution of the bilaterian larval foregut. Nature 409, 81–85.

Artavanis-Tsakonas, S., 1999. Notch Signaling: Cell Fate Control and Signal Integration in Development. Science 284, 770–776.

Axelrod, J.D., 2010. Delivering the lateral inhibition punchline: it's all about the timing. Science signaling 3, pe38.

Barrallo-Gimeno, A., Nieto, M.A., 2005. The Snail genes as inducers of cell movement and survival: implications in development and cancer. Development 132, 3151–3161.

Beane, W.S., Gross, J.M., McClay, D.R., 2006. RhoA regulates initiation of invagination, but not convergent extension, during sea urchin gastrulation. Developmental Biology 292, 213–225.

Bolker, J., 1995. Model systems in developmental biology. Bioessays 17, 451–455.

Bray, S.J., 2006. Notch signalling: a simple pathway becomes complex. Nature Reviews Molecular Cell Biology 7, 678–689.

Browne, W.E., Price, A.L., Gerberding, M., Patel, N.H., 2005. Stages of embryonic

development in the amphipod crustacean, Parhyale hawaiensis. Genesis 42, 124–149.

Castresana, J., 2000. Selection of conserved blocks from multiple alignments for their use in phylogenetic analysis. Mol. Biol. Evol. 17, 540–552.

Ciruna, B., Jenny, A., Lee, D., Mlodzik, M., Schier, A.F., 2006. Planar cell polarity signalling couples cell division and morphogenesis during neurulation. Nature 439, 220–224.

Costa, M., Wilson, E., Wieschaus, E., 1994. A putative cell signal encoded by the folded gastrulation gene coordinates cell shape changes during Drosophila gastrulation. Cell 76, 1075–1089.

Dale, L., Jones, C., 1999. BMP signalling in early Xenopus development. Bioessays 21, 751–760.

Darwin, C., 1855. On the origin of species by means of natural selection. Odhams Press limited.

Davidson, L.A., 2008. Integrating morphogenesis with underlying mechanics and cell biology. Curr Top Dev Biol 81, 113–133.

Davis, G.K., Patel, N.H., 2002. Short, Long, and Beyond: Molecular and Embryological Approaches to Insect Segmentation. Annu. Rev. Entomol. 47, 669–699.

Dawes-Hoang, R.E., Zallen, J.A., Wieschaus, E.F., 2003. Bringing classical embryology to C elegans gastrulation. Developmental cell 4, 6–8.

Dawes-Hoang, R.E., Parmar, K.M., Christiansen, A.E., Phelps, C.B., Brand, A.H., Wieschaus, E.F., 2005. folded gastrulation, cell shape change and the control of myosin localization. Development 132, 4165–4178.

De Robertis, E.M., Kuroda, H., 2004. Dorsal-Ventral Patterning and Neural Induction in Xenopus Embryos. Annu Rev Cell Dev Biol 20, 285–308.

De Robertis, E.M., Sasai, Y., 1996. A common plan for dorsoventral patterning in Bilateria. Nature 380, 37–40.

Dereeper, A., Guignon, V., Blanc, G., Audic, S., Buffet, S., Chevenet, F., Dufayard, J.-F., Guindon, S., Lefort, V., Lescot, M., Claverie, J.-M., Gascuel, O., 2008. Phylogeny.fr: robust phylogenetic analysis for the non-specialist. Nucleic Acids Res 36, W465–9.

Dereeper, A., Audic, S., Claverie, J.-M., Blanc, G., 2010. BLAST-EXPLORER helps you building datasets for phylogenetic analysis. BMC Evol. Biol. 10, 8.

Ettensohn, C., Sweet, H., 2000. Patterning the early sea urchin embryo. Curr Top Dev Biol 50, 1–44.

Extavour, C.G., 2005. The fate of isolated blastomeres with respect to germ cell formation in the amphipod crustacean Parhyale hawaiensis. Developmental Biology 277, 387–402.

Ferguson, E.L., Anderson, K.V., 1992. Localized enhancement and repression of the activity of the TGF-beta family member, decapentaplegic, is necessary for dorsal-ventral pattern formation in the Drosophila embryo. Development 114, 583–597.

Fritzenwanker, J.H., Saina, M., Technau, U., 2004. Analysis of forkhead and snail expression reveals epithelial-mesenchymal transitions during embryonic and larval development of Nematostella vectensis. Developmental Biology 275, 389–402.

Gally, C., Wissler, F., Zahreddine, H., Quintin, S., Landmann, F., Labouesse, M., 2009. Myosin II regulation during C. elegans embryonic elongation: LET-502/ROCK, MRCK-1 and PAK-1, three kinases with different roles. Development 136, 3109–3119.

Gerberding, M., Browne, W.E., Patel, N.H., 2002. Cell lineage analysis of the amphipod crustacean Parhyale hawaiensis reveals an early restriction of cell fates. Development 129, 5789–5801.

Gerberding, M., Patel, N.H., 2004. Gastrulation: from cells to embryo, Gastrulation in Crustaceans: Germ Layers and Cell Lineages. Cold Spring Harbor Laboratory Press, Cold Spring Harobor, NY.

Gerson, E., 2007. The juncture of evolutionary and developmental biology. From Embryology to Evo-Devo: A History of Developmental Evolution (Laubichler M, Maienschein J, eds) 435–463.

Giribet, G., Edgecombe, G.D., Wheeler, W.C., 2001. Arthropod phylogeny based on eight molecular loci and morphology. Nature 413, 157–161.

Goddette, D.W., Frieden, C., 1986. Actin polymerization. The mechanism of action of cytochalasin D. J Biol Chem 261, 15974–15980.

Goltsev, Y., Fuse, N., Frasch, M., Zinzen, R.P., Lanzaro, G., Levine, M., 2007. Evolution of the dorsal-ventral patterning network in the mosquito, Anopheles gambiae. Development 134, 2415–2424.

Gong, Y., Mo, C., Fraser, S.E., 2004. Planar cell polarity signalling controls cell division orientation during zebrafish gastrulation. Nature 430, 689–693.

Grobben, K., 1908. Die systematische Einteilung des Tierreiches. Verhandlungen Zoolog Botan Gesellschaft Wien.

Haeckel, E., 1866. Generelle Morphologie der Organismen. G. Reimer, Berlin.

Hannibal, RL., 2010. Mesoderm Segmentation in the Amphipod Crustacean *Parhyale hawaiensis*. UC Berkeley.

Harden, N., 2002. Signaling pathways directing the movement and fusion of epithelial sheets: lessons from dorsal closure in Drosophila. Differentiation 70, 181–203.

Hardin, J., 1996. The Cellular Basis of Sea Urchin Gastrulation. Curr Top Dev Biol 33, 159–262.

Hardin, J., Keller, R., 1988. The behaviour and function of bottle cells during gastrulation of Xenopus laevis. Development 103, 211–230.

Hejnol, A., Martindale, M.Q., 2008. Acoel development indicates the independent evolution of the bilaterian mouth and anus. Nature 456, 382–386.

Henry, J.J., Perry, K.J., Fukui, L., Alvi, N., 2010. Differential localization of mRNAs during early development in the mollusc, Crepidula fornicata. Integrative and Comparative Biology 50, 720–733.

Hertzler, P.L., Wang, S.W., Clark, W.H., 1994. Mesendoderm cell and archenteron formation in isolated blastomeres from the shrimp Sicyonia ingentis. Developmental Biology 164, 333–344.

Hertzler, P.L., Clark, W.H., 1992. Cleavage and gastrulation in the shrimp Sicyonia ingentis: invagination is accompanied by oriented cell division. Development 116, 127–140.

Holley, S.A., Ferguson, E.L., 1997. Fish are like flies are like frogs: Conservation of dorsal-ventral patterning mechanisms. Bioessays 19, 281–284.

Holtfreter, J., 1943. A study of the mechanics of gastrulation. Part I. Journal of Experimental Zoology.

Hörstadius, S., 1973. Experimental embryology of echinoderms. Clarendon Press.

Ip, Y., Maggert, K., Levine, M., 1994. Uncoupling gastrulation and mesoderm differentiation in the Drosophila embryo. EMBO J 13, 5826.

Ip, Y., Gridley, T., 2002. Cell movements during gastrulation: snail dependent and independent pathways. Curr Opin Genet Dev 12, 423–429.

Ip, Y.T., Park, R.E., Kosman, D., Yazdanbakhsh, K., Levine, M., 1992. dorsal-twist interactions establish snail expression in the presumptive mesoderm of the Drosophila embryo. Genes Dev 6, 1518–1530.

Jaffe, A., Hall, A., 2005. RHO GTPASES: Biochemistry and Biology. Annu Rev Cell Dev Biol 21, 247–269.

Jenner, R.A., Wills, M.A., 2007. The choice of model organisms in evo–devo. Nature Reviews Genetics 8, 311–314.

Jones, C., Dale, L., Hogan, B., Wright, C., 1996. Bone morphogenetic protein-4 (BMP-4) acts during gastrula stages to cause ventralization of Xenopus embryos. Development.

Keller, R., 1981. An experimental analysis of the role of bottle cells and the deep marginal zone in gastrulation of Xenopus laevis. The Journal of Experimental Zoology 216, 81–101.

Keller, R., Danilchik, M., 1988. Regional expression, pattern and timing of convergence and extension during gastrulation of *Xenopus laevis*. Development 103, 193–209.

Keller, R., Shook, D., 2008. Dynamic determinations: patterning the cell behaviours that close the amphibian blastopore. Philosophical Transactions B 363, 1317.

Keller, R.E., 1996. Holtfreter Revisited: Unsolved Problems in Amphibian Morphogenesis. Dev Dyn 205, 257–264.

Kiehart, D.P., Galbraith, C.G., Edwards, K.A., Rickoll, W.L., Montague, R.A., 2000. Multiple forces contribute to cell sheet morphogenesis for dorsal closure in Drosophila. J Cell Biol 149, 471–490.

Kimberly, E.L., Hardin, J., 1998. Bottle cells are required for the initiation of primary invagination in the sea urchin embryo. Developmental Biology 204, 235–250.

Kimelman, D., Kirschner, M., 1987. Synergistic induction of mesoderm by FGF and TGF-β and the identification of an mRNA coding for FGF in the early xenopus embryo. Cell 51, 869–877.

King, N., 2004. The unicellular ancestry of animal development. Developmental cell 7, 313–325.

Kingsley, E.P., Chan, X.Y., Duan, Y., Lambert, J.D., 2007. Widespread RNA segregation in a spiralian embryo. Evol Dev 9, 527–539.

Knoll, A.H., Carroll, S.B., 1999. Early animal evolution: emerging views from comparative biology and geology. Science 284, 2129–2137.

Kooh, P.J., Fehon, R.G., Muskavitch, M.A., 1993. Implications of dynamic patterns of Delta and Notch expression for cellular interactions during Drosophila development. Development 117, 493–507.

Kosman, D., Ip, Y.T., Levine, M., Arora, K., 1991. Establishment of the mesoderm-neuroectoderm boundary in the Drosophila embryo. Science 254, 118–122.

Kölsch, V., Seher, T., Fernandez-Ballester, G.J., Serrano, L., Leptin, M., 2007. Control of Drosophila gastrulation by apical localization of adherens junctions and RhoGEF2. Science 315, 384–386.

Kurth, T., Hausen, P., 2000. Bottle cell formation in relation to mesodermal patterning in the Xenopus embryo. Mechanisms of Development 117–131.

Lai, S.-L., Chang, C.-N., Wang, P.-J., Lee, S.-J., 2005. Rho mediates cytokinesis and epiboly via ROCK in zebrafish. Mol. Reprod. Dev. 71, 186–196.

Lambert, J.D., Nagy, L.M., 2002. Asymmetric inheritance of centrosomally localized mRNAs during embryonic cleavages. Nature 420, 682–686.

Lane, M.C., Koehl, M.A., Wilt, F., Keller, R., 1993. A role for regulated secretion of apical extracellular matrix during epithelial invagination in the sea urchin. Development 117, 1049–1060.

Lapébie, P., Borchiellini, C., Houliston, E., 2011. Dissecting the PCP pathway: One or more pathways? Bioessays, Does a separate Wnt-Fz-Rho pathway drive morphogenesis? 33, 759–768.

Lasko, P., 1999. RNA sorting in Drosophila oocytes and embryos. The FASEB journal 13, 421–433.

Lee, J.-Y., Marston, D.J., Walston, T., Hardin, J., Halberstadt, A., Goldstein, B., 2006. Wnt/Frizzled signaling controls C. elegans gastrulation by activating actomyosin contractility. Curr Biol 16, 1986–1997.

Lee, J.-Y., Goldstein, B., 2003. Mechanisms of cell positioning during C. elegans gastrulation. Development 130, 307–320.

Lee, J.-Y., Harland, R., 2007. Actomyosin contractility and microtubules drive apical constriction in Xenopus bottle cells. Developmental Biology 311, 40–52.

Lee, J.-Y., Harland, R.M., 2010. Endocytosis is required for efficient apical constriction during Xenopus gastrulation. Curr Biol 20, 253–258.

Leptin, M., 1995. Drosophila gastrulation: from pattern formation to morphogenesis. Annu Rev Cell Dev Biol 11, 189–212.

Leptin, M., 2005. Gastrulation movements: the logic and the nuts and bolts. Developmental cell 8, 305–320.

Leptin, M., Grunewald, B., 1990. Cell shape changes during gastrulation in Drosophila.

Development 110, 73–84.

Leptin, M., Roth, S., 1994. Autonomy and non-autonomy in Drosophila mesoderm determination and morphogenesis. Development 120, 853–859.

Lécuyer, E., Yoshida, H., Parthasarathy, N., Alm, C., Babak, T., Cerovina, T., Hughes, T.R., Tomancak, P., Krause, H.M., 2007. Global analysis of mRNA localization reveals a prominent role in organizing cellular architecture and function. Cell 131, 174–187.

Liubicich, D.M., Serano, J.M., Pavlopoulos, A., Kontarakis, Z., Protas, M.E., Kwan, E., Chatterjee, S., Tran, K.D., Averof, M., Patel, N.H., 2009. Knockdown of Parhyale Ultrabithorax recapitulates evolutionary changes in crustacean appendage morphology. Proceedings of the National Academy of Sciences 106, 13892–13896.

Martin, P., Parkhurst, S.M., 2004. Parallels between tissue repair and embryo morphogenesis. Development 131, 3021–3034.

Martindale, M.Q., Pang, K., Finnerty, J.R., 2004. Investigating the origins of triploblasty: "mesodermal" gene expression in a diploblastic animal, the sea anemone Nematostella vectensis (phylum, Cnidaria; class, Anthozoa). Development 131, 2463–2474.

Martindale, M.Q., Hejnol, A., 2009. A developmental perspective: changes in the position of the blastopore during bilaterian evolution. Developmental cell 17, 162–174.

Massague, J., 1990. The Transforming Growth Factor-beta Family. Annu Rev Cell Biol 6, 597–641.

McDonald, K., 1999. High-Pressure Freezing for Preservation of High Resolution Fine Structure and Antigenicity for Immunolabeling. Methods in Molecular Biology 117.

Mito, T., Shinmyo, Y., Kurita, K., Nakamura, T., Ohuchi, H., Noji, S., 2011. Ancestral functions of Delta/Notch signaling in the formation of body and leg segments in the cricket Gryllus bimaculatus. Development 138, 3823–3833.

Mizuno, T., Amano, M., Kaibuchi, K., Nishida, Y., 1999. Identification and characterization of Drosophila homolog of Rho-kinase. Gene 238, 437–444.

Modrell, M., 2007. Early Cell Fate Specification in the amphipod crustacean, *Parhyale hawaiensis*. UC Berkleey.

Morize, P., Christiansen, A.E., Costa, M., Parks, S., Wieschaus, E., 1998. Hyperactivation of the folded gastrulation pathway induces specific cell shape

changes. Development 125, 589–597.

Nambu, J.R., Franks, R.G., Hu, S., Crews, S.T., 1990. The single-minded gene of Drosophila is required for the expression of genes important for the development of CNS midline cells. Cell 63, 63–75.

Nance, J., Munro, E.M., Priess, J.R., 2003. C. elegans PAR-3 and PAR-6 are required for apicobasal asymmetries associated with cell adhesion and gastrulation. Development 130, 5339–5350.

Nance, J., Lee, J.-Y., Goldstein, B., 2005. Gastrulation in C. elegans. WormBook 1–13.

Nance, J., Priess, J., 2002. Cell polarity and gastrulation in C. elegans. Development 129, 387–397.

Nikolaidou, K.K., Barrett, K., 2004. A Rho GTPase signaling pathway is used reiteratively in epithelial folding and potentially selects the outcome of Rho activation. Curr Biol 14, 1822–1826.

O'Day, K., 2006. Notch signaling and segmentation in *Parhyale hawaiensis*. UC Berkeley.

Oda, H., Nishimura, O., Hirao, Y., Tarui, H., Agata, K., Akiyama-Oda, Y., 2007. Progressive activation of Delta-Notch signaling from around the blastopore is required to set up a functional caudal lobe in the spider Achaearanea tepidariorum. Development 134, 2195–2205.

Odell, G., Oster, G., Burnside, B., Alberch, P., 1980. A mechanical model for epithelial morphogenesis. Journal of Mathematical Biology 9, 291–295.

Odell, G., Oster, G., Alberch, P., Burnside, B., 1981. The mechanical basis of morphogenesis I. Epithelial folding and invagination. Developmental Biology 85, 446–462.

Olesnicky, E.C., Desplan, C., 2007. Distinct mechanisms for mRNA localization during embryonic axis specification in the wasp Nasonia. Developmental Biology 306, 134–142.

Oliveri, P., Tu, Q., 2008. Global regulatory logic for specification of an embryonic cell lineage, in: Proceedings of the …. Presented at the Proceedings of the ….

Ozhan-Kizil, G., Havemann, J., Gerberding, M., 2009. Germ cells in the crustacean Parhyale hawaiensis depend on Vasa protein for their maintenance but not for their formation. Developmental Biology 327, 230–239.

Parchem, R.J., Poulin, F., Stuart, A.B., Amemiya, C.T., Patel, N.H., 2010. BAC library for the amphipod crustacean, *Parhyale hawaiensis*. Genomics 95, 261–267.

Parchem, R.J., Jr, 2008. Segmentation in Parhyale hawaiensis. University of California, Berkeley.

Parks, S., Wieschaus, E., 1991. The drosophila gastrulation gene concertina encodes a Gα-like protein. Cell 64, 447–458.

Pavlopoulos, A., Kontarakis, Z., Liubicich, D.M., Serano, J.M., Akam, M., Patel, N.H., Averof, M., 2009. Probing the evolution of appendage specialization by Hox gene misexpression in an emerging model crustacean. Proceedings of the National Academy of Sciences 106, 13897–13902.

Pawlak, J.B., Sellars, M.J., Wood, A., Hertzler, P.L., 2010. Cleavage and gastrulation in the Kuruma shrimp Penaeus (Marsupenaeus) japonicus (Bate): A revised cell lineage and identification of a presumptive germ cell marker. Dev Growth Differ, Kuruma shrimp development 52, 677–692.

Peralta, X.G., Toyama, Y., Hutson, M.S., Montague, R., Venakides, S., Kiehart, D.P., Edwards, G.S., 2007. Upregulation of forces and morphogenic asymmetries in dorsal closure during Drosophila development. Biophysical Journal 92, 2583–2596.

Peter, I.S., Davidson, E.H., 2011. A gene regulatory network controlling the embryonic specification of endoderm. Nature 474, 635–639.

Pioro, H.L., Stollewerk, A., 2006. The expression pattern of genes involved in early neurogenesis suggests distinct and conserved functions in the diplopod Glomeris marginata. Development Genes and Evolution 216, 417–430.

Ponting, C.P., 2008. The functional repertoires of metazoan genomes. Nature Reviews Genetics 9, 689–698.

Price, A.L., Modrell, M.S., Hannibal, R.L., Patel, N.H., 2010. Mesoderm and ectoderm lineages in the crustacean Parhyale hawaiensis display intra-germ layer compensation. Developmental Biology 341, 256–266.

Price, A.L., Patel, N.H., 2008. Investigating divergent mechanisms of mesoderm development in arthropods: the expression of Ph-twist and Ph-mef2 in Parhyale hawaiensis. J Exp Zool B Mol Dev Evol 310, 24–40.

Raftopoulou, M., Hall, A., 2004. Cell migration: Rho GTPases lead the way. Developmental Biology 265, 23–32.

Ransick, A., Davidson, E., 1993. A complete second gut induced by transplanted micromeres in the sea urchin embryo. Science 259, 1134–1138.

Rao, Y., Vaessin, H., Jan, L.Y., Jan, Y.N., 1991. Neuroectoderm in Drosophila embryos is dependent on the mesoderm for positioning but not for formation.

Genes Dev 5, 1577–1588.

Regier, J.C., Shultz, J.W., Zwick, A., Hussey, A., Ball, B., Wetzer, R., Martin, J.W., Cunningham, C.W., 2010. Arthropod relationships revealed by phylogenomic analysis of nuclear protein-coding sequences. Nature 463, 1079–1083.

Rehm, E., Hannibal, R., Chaw, R.C., Vargas-Vila, M.A., Patel, N.H., 2009a. Antibody Staining of Parhyale hawaiensis Embryos. Cold Spring Harb Protoc, Emerging Model Organisms: A Laboratory Manual.

Rehm, E., Hannibal, R., Chaw, R.C., Vargas-Vila, M., Patel, N., 2009b. Fixation and Dissection of *Parhyale hawaiensis* Embryos. Cold Spring Harb Protoc, Cold Spring Harbor Protocols.

Rehm, E., Hannibal, R., Chaw, R.C., Vargas-Vila, M., Patel, N., 2009c. In situ hybridization of labeled RNA probes to fixed *Parhyale hawaiensis* embryos. Cold Spring Harb Protoc, Cold Spring Harbor Protocols.

Rehm, E., Hannibal, R., Chaw, R.C., Vargas-Vila, M., Patel, N., 2009d. Injection of Parhyale hawaiensis blastomeres with fluorescently labeled tracers. Cold Spring Harb Protoc, Cold Spring Harbor Protocols.

Ridley, A.J., Schwartz, M.A., Burridge, K., Firtel, R.A., Ginsberg, M.H., Borisy, G., Parsons, J.T., Horwitz, A.R., 2003. Cell migration: integrating signals from front to back. Science 302, 1704–1709.

Riento, K., Ridley, A., 2003. Rocks: Multifunctional kinases in cell behaviour. Nature Reviews Molecular Cell Biology 4, 446–456.

Saaristo, M., 2006. Theridiid or cobweb spiders of the granitic Seychelles islands (Araneae, Theridiidae). Phelsuma 14, 49–89.

Sander, K., 2002. Ernst haeckel's ontogenetic recapitulation: irritation and incentive from 1866 to our time. Annals of Anatomy - Anatomischer Anzeiger 184, 523–533.

Sasai, Y., Lu, B., Steinbeisser, H., Geissert, D., Gont, L., DeRobertis, E., 1994. Xenopus chordin: A novel dorsalizing factor activated by organizer-specific homeobox genes. Cell 79, 779–790.

Sawyer, J.M., Harrell, J.R., Shemer, G., Sullivan-Brown, J., Roh-Johnson, M., Goldstein, B., (null), (null), (null), (null), (null), 2010. Apical constriction: a cell shape change that can drive morphogenesis. Developmental Biology 341, 5–19.

Schlessinger, K., Hall, A., Tolwinski, N., 2009. Wnt signaling pathways meet Rho GTPases. Genes Dev 23, 265–277.

Schlessinger, K., Hall, A., 2009. Wnt signaling pathways meet Rho GTPases. Genes Dev.

Schöck, F., Perrimon, N., 2002. Molecular Mechanisms of Epithelial Morphogenesis. Annu Rev Cell Dev Biol 18, 463–493.

Sherwood, D.R., McClay, D.R., 1997. Identification and localization of a sea urchin Notch homologue: insights into vegetal plate regionalization and Notch receptor regulation. Development 124, 3363–3374.

Sommer, R.J., Tautz, D., 1994. Expression patterns of twist and snail in Tribolium (Coleoptera) suggest a homologous formation of mesoderm in long and short germ band insects. Developmental genetics 15, 32–37.

Sporn, M., 2006. The early history of TGF-β, and a brief glimpse of its future. Cytokine & Growth Factor Reviews 17, 3–7.

Stein, P., Musci, T., Kirschner, M., 1993. FGF signalling in the early specification of mesoderm in Xenopus. Development.

Stetina, Von, S., Watson, J., Fox, R., Olszewski, K., Spencer, W., Roy, P., Miller, D., III, 2007. Cell-specific microarray profiling experiments reveal a comprehensive picture of gene expression in the C. elegans nervous system. Genome Biology R135.

Stollewerk, A., Schoppmeier, M., Damen, W.G.M., 2003. Involvement of Notch and Delta genes in spider segmentation. Nature 423, 863–865.

Strutt, D.I., 2002. The asymmetric subcellular localisation of components of the planar polarity pathway. Semin Cell Dev Biol 13, 225–231.

Sweet, H.C., Gehring, M., Ettensohn, C.A., 2002. LvDelta is a mesoderm-inducing signal in the sea urchin embryo and can endow blastomeres with organizer-like properties. Development 129, 1945–1955.

Sweeton, D., Parks, S., Costa, M., Weischaus, E., 1991. Gastrulation in Drosophila: the formation of the ventral furrow and posterior midgut invaginations. Development 112, 775–789.

Tadros, W., Lipshitz, H., 2009. The maternal-to-zygotic transition: a play in two acts. Development 136, 3033–3042.

Thiery, J., Sleeman, J., 2006. Complex networks orchestrate epithelial–mesenchymal transitions. Nature Reviews Molecular Cell Biology 7, 131–142.

Thiery, J.P., Acloque, H., Huang, R.Y.J., Nieto, M.A., 2009. Epithelial-mesenchymal transitions in development and disease. Cell 139, 871–890.

van der Zee, M., Stockhammer, O., Levetzow, von, C., Nunes da Fonseca, R., Roth, S., 2006. Sog/Chordin is required for ventral-to-dorsal Dpp/BMP transport and head formation in a short germ insect. Proc Natl Acad Sci USA 103, 16307–16312.

Vargas-Vila, M.A., Hannibal, R.L., Parchem, R.J., Liu, P.Z., Patel, N.H., 2010. A prominent requirement for single-minded and the ventral midline in patterning the dorsoventral axis of the crustacean Parhyale hawaiensis. Development 137, 3469–3476.

Veselý, J., Havlicek, L., Strnad, M., Blow, J.J., Donella-Deana, A., Pinna, L., Letham, D.S., Kato, J., Detivaud, L., Leclerc, S., 1994. Inhibition of cyclin-dependent kinases by purine analogues. Eur. J. Biochem. 224, 771–786.

Wang, M.M., 2011. Notch signaling and Notch signaling modifiers. Int. J. Biochem. Cell Biol. 43, 1550–1562.

Welch, M.D., Mullins, R.D., 2002. Cellular control of actin nucleation. Annu Rev Cell Dev Biol 18, 247–288.

Weller, M., Tautz, D., 2003. Prospero and Snail expression during spider neurogenesis. Development Genes and Evolution 213, 554–566.

Wharton, K., Thomsen, G., Gelbart, W., 1991. Drosophila 60A gene, another transforming growth factor beta family member, is closely related to human bone morphogenetic proteins, in: Proc. Natl. Acad. Sci. Presented at the Proc. Natl. Acad. Sci, pp. 9214–9218.

Willmer, P., 1990. Invertebrate relationships: patterns in animal evolution. Cambridge University Press, Cambridge.

Winklbauer, R., Nagel, M., 1991. Directional mesoderm cell migration in the Xenopus gastrula. Developmental Biology 148, 573–589.

Winter, C., Wang, B., Ballew, A., Royou, A., Karess, R., Axelrod, J.D., Luo, L., 2001. Drosophila Rho-Associated Kinase (Drok) Links Frizzled-Mediated Planar Cell Polarity Signaling to the Actin Cytoskeleton. Cell 105, 81–91.

Wolff, C., 2009. The embryonic development of the malacostracan crustacean Porcellio scaber (Isopoda, Oniscidea). Development Genes and Evolution 219, 545–564.

Wolff, C., Scholtz, G., 2002. Cell lineage, axis formation, and the origin of germ layers in the amphipod crustacean Orchestia cavimana. Developmental Biology 250, 44–58.

Wray, G., Raff, R., 1991. Rapid Evolution of Gastrulation Mechanisms in a Sea Urchin with Lecithotrophic Larvae. Evolution 45, 1741–1750.

Wu, L.H., Lengyel, J.A., 1998. Role of caudal in hindgut specification and gastrulation suggests homology between Drosophila amnioproctodeal invagination and vertebrate blastopore. Development 125, 2433–2442.

Wu, S.-Y., Ferkowicz, M., McClay, D.R., 2007. Ingression of primary mesenchyme cells of the sea urchin embryo: a precisely timed epithelial mesenchymal transition. Birth defects research. Part C, Embryo today: reviews 81, 241–252.

Xu, N., Keung, B., Myat, M.M., 2008. Rho GTPase controls invagination and cohesive migration of the Drosophila salivary gland through Crumbs and Rho-kinase. Developmental Biology 321, 88–100.

Yamazaki, K., Akiyama-Oda, Y., Oda, H., 2005. Expression patterns of a twist-related gene in embryos of the spider Achaearanea tepidariorum reveal divergent aspects of mesoderm development in the fly and spider. Zool. Sci. 22, 177–185.

Yarrow, J.C., Totsukawa, G., Charras, G.T., Mitchison, T.J., 2005. Screening for cell migration inhibitors via automated microscopy reveals a Rho-kinase inhibitor. Chemistry & Biology 12, 385–395.

Young, P.E., Richman, A.M., Ketchum, A.S., Kiehart, D.P., 1993. Morphogenesis in Drosophila requires nonmuscle myosin heavy chain function. Genes Dev 7, 29–41.

Zimmerman, S.G., Thorpe, L.M., Medrano, V.R., Mallozzi, C.A., McCartney, B.M., 2010. Apical constriction and invagination downstream of the canonical Wnt signaling pathway require Rho1 and Myosin II. Developmental Biology 340, 54–66.

Appendix A: *Ph-dpp* sequence

Sequence, 5' to 3', 2.2kb.
Untranslated sequence
Coding region, 1.2kb.

CGCGGATCCAGACGCTGCGTTTGCTGGCTTTGATGAAAAGTTTGCAGGAAG
CTGCCGTCGTCTGTGGATGTGTGTGTCTGTGTCGTGCGTGTGCAACTGCCCT
TCTACAGTTTCATTAAGCTAATTTTTCTCCCTTTTCCTCAAACTGTTGCGTGT
GTTGTAGCTACTGCCACTGAAAAATTCTCATTACGATAACTGCAGAACAGT
AAGCCGAAGTGAAGCAGTTGTGCAGTATCTCGTGCAATCATCTCATGCTAT
TGAAGTGAGTCGTTCAATAGGCAACTTCTCTAACCGGTTGCTGGCCCAAGA
AACAACCCACTTCGGAATTCTTCAAATTGTTACTTTACTTTTTCGAAACTCG
GTGATGCTCCTAAATTGTGAAATTGTATCGTTATAAGCAAATACGATGAAG
TGTCGAGACTGTTCCATACACCTGGACGCCCCTGTACCATGAGGGTGTGCC
TGTGTGTCCACACGTGCCCTGTCACCACCCCAACCACGGTAGAAGCTACAT
CGCTTTCAAAGCGACGCCTCAGAATCAACTTCAACTTGTCTCAGCTCGTCAT
TAGCTAACTTTTTAAGGTGGCCTACGCAGCGAGAGCAGGACAGCATCGGGC
CACCACCATGAGGCGACTGCACGCTCGCTATTGGAGCTCGCGGCAGCACCA
GTCTAGTGTACTGTTCTGGTTACTTTGGTTCATTCTGCTACTTCATACGAGA
TCCTGCTTGGCTACTTCCTCTACCGATGATCTACAAGAAGAGTTACTAAAGT
TCCTGGGGATGAAGCGCCCCAGTCACACCACGGCCCCGCATGTGCCGTCCT
ACATGCATCAGCTTTACAAGGATCAGCAAATCTTCAACTATGGATCTGACA
GCGGGAGCCATGATGGTGGCTTTCGGTACAGTCACTTCGGACCTCCTGACA
CTGTGCGCAGCATAGCCAACATAACTGAAATCAGCGATGTGAGCGAAGTTC
GTCCGGGCGTTGGACGAATTCGCGTCCAATTCGCGCTTGACGGCCTAGCGT
CGGACGAACGACTCCACACGGCCCAGCTGCGGGTAACCCACGCGCCCTCC
ACACCCCAAGGCGACCTCGTCAGCAGAACCTCCCACCACCCCAACAGTGTC
ACTGGTGACTTTGAAGACTATGGACACAATAATAAATACAAGAAAGATCA
ACTTCCCTACGTGAACTATATCAGAGTGTACGATGTCGTGCGGACTCTGGA
CGACGGTGACTCAGTGCTTCGGTTGCTGGACACAGCGCTTGTAGACCGACG
ACAGTCCGGTGTGTTGAAACTGGACGTCGGTCCCGCGGTCCAGCGCTGGGT
TAAAAAACCTCACACCAACAACGGGCTCGTTCTCGAAATGGATCCTTTCAA
TAAGAACCACCATCAACAGTCCCGGTCTGGGGGCGACACGCCAGACATGT
CCCATCTGCGCATTAGACGAAGCGCAGACGTGGACGACGCCACATGGCAG
GACGTTCGACCGTCCGTCGYGGTGTACAGTGACGATGGCAAGCCTAAGCA
ARGAGTAAAGAGAGCCAAACCTTCTGCTCCTTACGAACAGTGCCGTCGCCA
CTCGCTCTATGTCGACTTCAAATTAGTCGACTGGCAGAGCTGGATAGTCGC
GCCCCCGGGCTACGCAGCCTATTTCTGTGGTGGGGAGTGTGAGTTTCCTCTC
AGTGACCATCTCAATTCCACCAACCACGCTATAATCCAAACGCTTGTCAAT
TCCAAATATCCGGAACGAGTCCCGACGGCCTGTTGCGTACCGACGGAGCTG
TCGCCGATATCCATGCTCTATGTTGACGAATTTTCCAATGTCGTTTTGAAAA
ATTATCAGAATATGGTAGTGGAAGCGTGTGGGTGCCGGTAAATAACTCACA
AGTTTTTAAATTGAAACTAGCAATAAATTTTGTGTATAGGATTCTATGAAA
GCCCCGTGTGCGAGGGTAGAACATACAAGACTTTTATATTTCTTGGTAGCT

GATCTTTGCAGCTAAATGTTTGTTTGTGATGATGAATAGTGATAGCTGATTG
TACTATAGCTTTCTATGAAGATTTGTAGCGTATATGTAGTTGAAGAATGTAC
GTATTTTGTTATAGTGAAAGGTGCTGCTTCTTAACTCTGTACAGTTTGAATA
ATATTTGATTTAAGTAAATCCCCTGTTGGTGCTTAAAAAAAAAAAAAAAAAA
AAAAAAAAAAAAAAAAAAAAAAAMAAWAAAAAAAAAAAAAAAAAAAAAAAA
AAAAAAAAAAAACACTGTCATGCCGTTACGTAGCG

Appendix B: Accession Numbers

Table D.1 NCBI accession numbers for phylogenetic analysis of Ph-dpp (Fig. 5.1).

Name	Accession #	Name	Accession #
admpDr	AAL49502.1	gdf3Xl	AAH73508
admpGal	NP_990153.1	gdf6mus	AAA18779.1
antivinUr	AAS00535.1	gdf6Xl	AAI69872.1
bmp10Dr	NP_001124072.1	gdf8Dr	NP_571094.1
bmp10mus	AAC77461.1	gdf8mus	NP_034964
bmp3Dr	NP_001071233.1	gdf9Dr	AAI08014.1
bmp3mus	NP_775580.1	inhib_Amus	CAJ18587
bmp3Xl	XP_002934044.1	inhib_Bmus	CAA49326.1
bmp4Dr	AAB49985.1	lefty1Dr	NP_571035.1
bmp4mus	NP_031580.2	lefty2Dr	NP_571036.1
bmp4Ur	AAD28038.1	leftyaXl	NP_001079214.1
bmp4Xl	AAB27336.1	leftybXl	NP_001082043.1
bmp5Dr	AAH54647	leftymus	2211405A
bmp5mus	AAI00754.1	60ADm	NP_477340.1
bmp6Ag	XP_320599.3	nodalCi	NP_001072000.1
bmp6Dr	NP_001013357.1	nodalDr	AAH97089.1
bmp6mus	NP_031582.1	nodalmus	AAI28019.1
bmp6Xl	NP_001089390.1	nodalUr	AAS00534.1
bmp7Dr	AAH54647	nodalXl	AAI69925.1
bmp7mus	NP_031583	screwDm	AAA56872.1
bmp7Xl	NP_001080866.1	tgfb1Dr	NP_878293.1
BMP8amus	AAH52168.1	tgfb1mus	EDL24239
gdf9mus	AAH52667.1	tgfb2Dr	NP_919366.1
dppAt	BAC24087.1	tgfb2mus	AAG02247.1
dppDm	AAC47552.1	tgfb3Dr	NP_919367.2
dppTc	NP_001034540.1	TGFb3mus	AAH05513.1
gdf10mus	AAH22669.1	univinUr	ABG00200.1
gdf1mus	NP_032133.2	vg1Xl	AAW30007.1
gdf1Xt	AAI61554		
gdf2mus	NP_062379.3		
gdf3mus	NP_032134.2		

Appendix C: BAC library screen for *Ph-caudal*

This appendix contains information on the Bacterial Artificial Chromosome (BAC) sequence for *Ph-caudal,* an ortholog of a gene that establishes the posterior domain of the *Drosophila* embryo (Wu and Lengyel, 1998). The function of *Ph-caudal* is currently unknown, but *in situ* expression patterns show that it is confined to the posterior region of the germ band during segmentation (Julia Serano, personal communication). *Ph-caudal* is not discussed elsewhere in this dissertation.

MATERIALS AND METHODS

Screening the BAC library was done as described in (Parchem et al., 2010). Briefly, BAC filter sets were screened for *Ph-caudal* through hybridization with radioactively labeled probes. Positives were characterized with cloning, PCR, and restriction enzymes. A single sample was sent for sequencing to the Department of Energy Joint Genome Institute. With the help of Dr. Julia Serano, this sequence was analyzed using Sequencher software (gene tools) and MacVector (MacVector, Inc.).

RESULTS:

One BAC was characterized through PCR as having the entire *caudal* transcription unit (Filter position; plate:row:column; 51:O:6). Sequencing was done by the U.S. Department of Energy Joint Genome Institute. Like other genes analyzed, *Ph-caudal* has a high proportion of intronic sequences (Parchem, 2010). There are four exons and five introns. Of the 137kb, 3.6kb are coding region and 133.4kb are intron sequence (Fig. C.1).

Sequence of exons

caudal exon 1

ATTTTCGTGCAGCTCTTCGTTAGTGCGTGGTGTGATGTAGTAGTGTGTGTTC
TTCAGTAGTTAACGTCTTCTTATATCCTTCCAATAGTGGTTAACTATGTCTT
AAAAGTGAAAATGTATTGATAATGAAATTGAAATTATATTGTTACTTTTCG
TGAAAATCTAAGAAGTGATCGATGTGAACTTTGTTGCTAATTCTTCAAAGG
CAATGAAAATGTGGAACTTCTCAACTCAAAACACAGTTTTTTGGTTCGGTG
TATACTGAAATGTTTAAAAAGTCTATTGAATTTTGTTACAGTGGCTATTATT
CGTAGTTTACTTCTGCATGTGCCGTCTACAAATAATTTATATCTAGTGTGGA
CATATATTTGGTGCAAACATGGCGTAGATAGCATATATTTTTTGCTTAGATT
TTAGTTGAGCTGGGTACCTCGAAACATCAAGTTACGTTATTCAATTGTGTGT
CGTGGAGCTCAGAAGGACTTGGTGACGTAATATTTAAAACAATAATATTTT
TGTTAGAAACTCAATAATGTTTGGAGTTGGTCGTGAAGACCATTACTTGAA
AGATGATTTAACGATGTACCACGCTCCAGCACCTCAGTATTTTCACCAATC
GTACGGTAACCACGCATCAACGATGCAGAGACACGACTACAACCAATACT
ATTTGCCAAGTGAACCTTATTATACGTCATTGCCCAACCTAACGCGCAATG
AAAACTCTCCACCGCTCTCTGTGACGTCTCAAACTCCCTCTACTTCTTCTCC
AGCCACTTCAGCCCATACTTCTTCGCCGGCAGTGATCGGCCACCGCGCCTT
GCCGACACCTCCGCATCTGTCACCAGACGCTTCTCCTTCGACGTCCTCTGCT

GGGGCTTCAGTCGTGCCCTCCAACAGAAACGAATATGCTAGTCATTATTCG
GCGTATCCAAGCCAGGCATTGCATTCTGGACTGTCGGCGAATGGTCACGGC
TTCATGCCGAATAATGTGGCCGGAGCTCTCTATCCGCCATCACCAGCCATC
AACCATCCCGCCAGCGTCTATGCTCTGGGCGGTCGGGAGTCGCTGCCGATC
CCCAACTTGCCCACAACCGTCCAGCAACATGAGATAGACGCCCAGAGAAA
TGTCGTCCGCGCTGACTACCAGTGGATGAAGAAGGAAACTACATCTGCAG

caudal exon 2
GGTCCAATGCCAATCGAGCTCGGAATGAAG

caudal exon 3
GTCGGACCAGAACGAGGGACAAGTACCGTGTGGTGTACAGCGAACACCAA
AGGCTGGAGCTGGAGAAAGAGTATTCATTCAATCGCTACATCACCATCAAA
AGGAAGACAGAGTTGGCCGATGCGCTGTCACTTTCTGAACGTCAG

caudal exon 4
ATCAAGATATGGTTCCAGAACCGGCGAGCCAAGGATAGGAAAACACTCAT
CAAGAAGAAAGGTGAAACGAAGGTGTCCTCCTCATCCTCGCAAATGGACG
CTTCTGCACAGCCTAGTCAATCCCACGTGCATGAACACAATGGCATCAACA
CACGCATGCCACCTATACCTCATGGCCAGCAGGCTTTGAGTACCTCCGGTA
CGAATGATTCTTCCAGCCAAGCGGCCCAGCACTACGGCGCTGCTGAAAATT
CTAGAATGCTACCGAGTGAAGAATTCCAGAACCAGATCGCCATGGCCGAC
AATTCACAAGGGCAAGCCATACTTCCTGATCATGGCCACATGCCTCCTGAA
GCTTTGCAATTGATGCAGCTTCAGCAGTTTCCAGGTCATCAACCCAATAGT
CATAGCAACTCTTACCCGTTGGGTCATCATTCTGAGTACTCGCCAACTTTCA
TGCACGGCCACAATCCATTCTTATCTACCAATCCTTTCTTGCACCACGAAAT
GTCTCAGGAGTTTCGTTTCCAGCAACAAATGCACAACATCACTTACATCGA
TGCTTATCAGCAACATGCCGCTGCTGCTCATATTAATCATCAAAATCAGCA
TCTGCAGCATCATCATCAGCAGCAGCAACAGCAGCACCATCAAAATGGCCC
TCAGCAACCTCAATCTTCCAGTCTTCAGCAATCGTCGACCGATGCTCAAGG
CTCCCTAACTTCTCCACAGATTCCCCTCACAGTAACATCCCTTGAGAAACCA
AAAAGAGAAATCAGTCCGAACGTAAAGGCCGAAAGTTCCCCTTGATGGTA
GTGCATAGCATGTATTTGAAAAGTTTGTAAGAACTTAGCTCTACATAGGTT
ATAGTTGGTTATTTCTTTTTAGTGATACTCTTGGGAAGGGCATTTGTTTTTAT
TTCTTAGCGTGGTTACGGGTGATTATTATCAGTTTTGAGTTTTGTTGAAGAT
ATGTATAGAAAGCATGATCTTGACTGCCGATGTTGACCTAAATATTGCTTTT
TAATCAAAATTGATCTGATTTTTACTGAATTCTTATGAAAATATAGATTGTA
AGCTGCAACATTTTACTTTCAATTAAGTTCAAAGTTTTATGGTGTAAATTTA
AAGCAAGTTAGGTTTTTATGGCTTTGTTCTTACTTCCTCAGACCGTACGTGA
CGTTGTTTTTTGACTTGAGGGTCCGCAGTCTATTCTTATGTTCGATGCTTTGC
AAAACTTATAAGTTCAAAACTATGAAGAAAAATATTATTTCAATGCTTCAC
CAGCTGCCTATCTCGAAAAGCTGCTCCTAATTGCATTATTTCCACAGCATAC
TGATCGTACTGCTGCAGATATCGACATCACAGCTTACTGGCTTAATTATAG
AAAATAATTTTTTTTTGCTTAAAGTACTGCTTCCAATAACAATGTTGTAGAC
ATATCCTGTCTAAATAGACTTTCACCCTCTGGATTTGTGAGCGCAACACTTA

CTTCTGTTCTCTCTCCCTCTGATCCTTTTGCATTAACCTTAATGTATAAATAG
ATCTCTCATATAATTACGTTTCAAATGATCACGAGATAAAGTCTCCGAAAA
TAATAATAACTAGCCAAGACCTGTTGATGTTTCAAAATTAAACTATAATTTT
TCGTTGACACCCGGACCAATATTACCATGATGCTATTTTTCTTCTATGTACG
TATTTCTGAAATCTATATATACCCAGTAGAGCCGAACTGACCTCAAGCAGA
ATGATGCCACTAATAATTTTCCTATCTATGTATTGTGTACTTCTATATTTATT
GTGGACCAAAAAATCCTCCAATTTATTATTCTGAAAAGTCACTACGTAATT
ATTATTGCCATAATTTAAATGCATTTGTCTGTTGCGATTTCACTTGGCCACC
ACAAACTTCAATCAATAATTGTGTCAACTCATTGGGTTGTGTTAGGGAAAT
ATTCTTTCGTCTGCTTATATTTCGCTATGCATCGTTAAGTCCATTCCCTCGCC
CAGTTCATCTGACTGGATTTTGAATGCAATACGTGTACAACGCCCGTATCA
TTGAAAACTCGTTTTGGTTATGATTGTAATTACTGGTTTAAAGTGGTTATAG
ACCTGGTTTTGTCGGTCCTGTTCATCCCTAACCTGTTGTTTCTATGCTTAGTG
TCTATTGACTCATGGGTTTTACATTTATCGCGGTAAGCTGTTATCTTGAACA
AGCTACCGAGAAATTGGCTAGGAAAAATG

Figure C.1. Schematic of full length caudal transcript from BAC library screening.
Sequence is shown 5'-3', introns are in cyan, exons in blue. Numbers indicate basepairs in consensus sequence, exons are given with basepair position in consensus sequence. Diagram is not to scale.

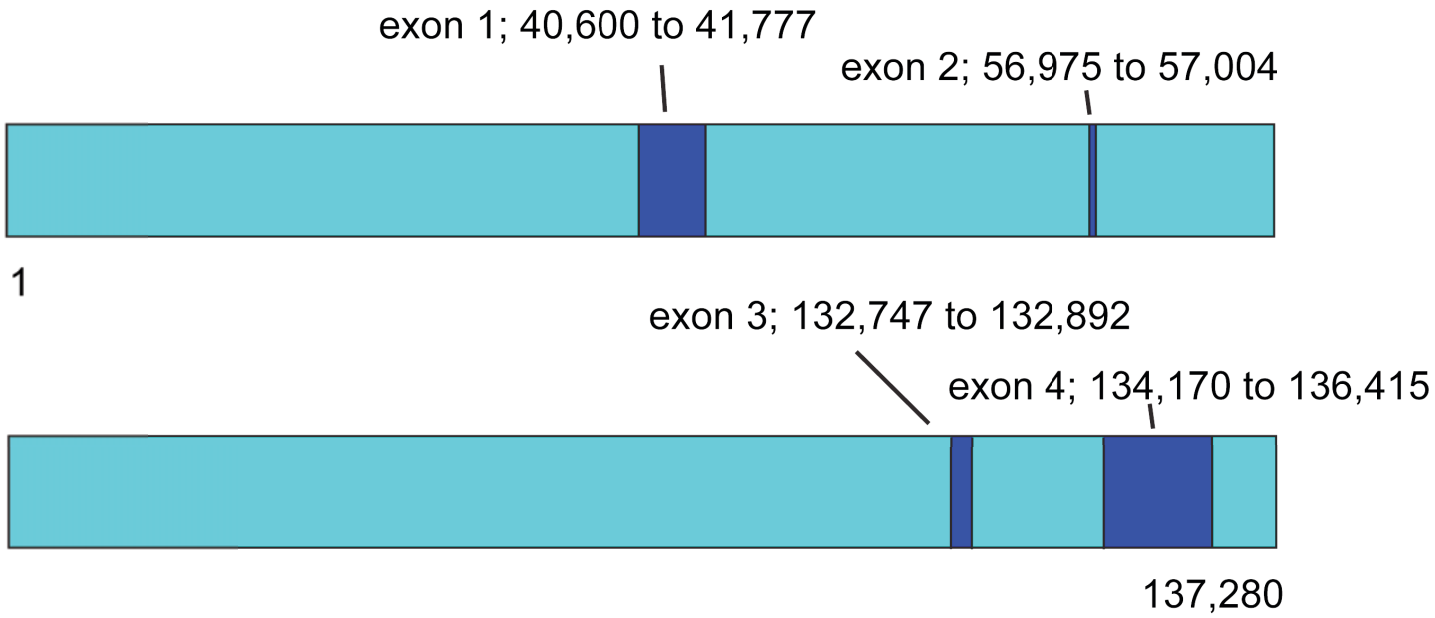
exon 1; 40,600 to 41,777
exon 2; 56,975 to 57,004
1
exon 3; 132,747 to 132,892
exon 4; 134,170 to 136,415
137,280

Appendix D: Cloning of Parhyale Poly-A binding protein (PAB)

In trying to realize a forward-genetic approach for identifying molecular markers for early identification of ectoderm and mesoderm, I began attempts to tag the poly-A tail of active transcripts during *Parhyale* development. By epitope-tagging the poly-A tail of transcripts, I hoped to make them easily separable for pull-down during RNA sequencing. In *C.elegans* this approach was successfully used to identify lineage-specific gene expression in the nervous system in embryonic and larval transgenic animals (Stetina et al., 2007).

Progress stalled for several reasons, including lack of an appropriate control for assaying the efficacy of epitope tagging. I did, however, successfully acquire the full-length coding region for the gene encoding *Parhyale* poly-A binding protein (*Ph-PAB)*. This appendix describes the process of cloning *Ph-PAB* through degenerate PCR and gives the acquired sequence of untranslated and coding regions. The coding region aligns with other PAB proteins (Fig. D.1). Poly-A binding protein is not discussed elsewhere in this dissertation.

MATERIALS AND METHODS

Cloning of Ph-PAB

Approximately 200 μL of *Parhyale* embryos were collected (comprised of representatives from early cleavage stages (1-cell through 32-cell, approximately 40%), gastrulation stages (soccerball through rosette stages, approximately 40%) and segmentation stages through appendage formation (early germ band through appendage elongation S23, approximately 20%). Total RNA was isolated using Trizol reagent (Invitrogen). 5'RACE and 3'RACE cDNA was generated using the SuperScript® Synthesis System for first-strand cDNA kit (Invitrogen) or Firstchoice RLM-RACE kit (Ambion).

Cloning from cDNA was performed using the following degenerate primers:
Parhyale poly-A binding protein (*Ph-PAB*):
forward primer 5'- CAR CAR CCN GCN CAY GCN GA-3'
reverse primer 5'- TTC ATY TCN GTN ACN GCY TTN GT-3'
nested forward primer 5'- GGN GTN GGN AAY GTN TTY ATH AAR AA-3'
Full-length sequence was obtained by 5' and 3'RACE using the Firstchoice RLM-RACE kit (Ambion).

Sequence analysis

All clones were sequenced by the UC Berkeley DNA Sequencing Facility. Sequencher software (Gene Codes) was used to analyze sequence chromatograms and assemble contigs for each gene. A minimum of three overlapping sequences (from multiple amplifications, where possible) was required to generate a consensus sequence. Additional protein sequences and predicted genome proteins were obtained from the National Center for Biotechnology Information (NCBI) and the *Daphnia pulex* Genome Database (wFleaBase). Database searches were performed using the

Basic Local Alignment Search Tool (BLAST) algorithm. All protein alignments were constructed using MacVector software (MacVector, Inc.) and the ClustalW algorithm.

Results

Sequence 5' to 3' (3kb total),
coding region (2kb) in black, untranslated region in blue:

TCGCGGATCCGAACACTGCGTTTGCTGGCTTTGATGAAAACCCTACTGTT
ATAGCGCCAGGGTCCGTAGTGGACGTGGCGTTCTGTTAGTGTCACTATCC
ACTATTTATACAAAAACTTGAAAAAGTAGAAAAAAATATAAAACTCCAAA
AACATAAAAAAMATATAAAAAATTAGTTTTTAGCTGTTGAATTCTCTTAAA
CGAGAGAACGTTGACTGTAGGCCGCAACAATGAATGCGAGTCAAGCTGGA
TCCAACAGCTACCCGCTGGCTTCYCTCTATGTAGGAGATCTGCATGAGGA
CTGCACTGAAGCTATGCTTTTTGAGAAGTTCTCAACTGCTGGCCCAGTGC
TCTCGATTCGTGTGTGCCGCGACATGATCACTCGTCGCTCCCTTGGCTAT
GCATACGTCAACTTCCAACAGCCCTTCGATGCTGAGCGTGCACTCGACAC
CATGAACTTCGATGTGATGAAGGGAAGGCCAATCCGCATCATGTGGTCAC
AGCGCGATCCTTCACTGCGCAAGTCGGGCGTTGGCAACGTTTTCATCAAG
AACTTGGATAAGTCCATTGACAACAAAGCCATGTACGATACTTTCTCAGC
CTTTGGCAAAATTCTCAGCTGCAAGGTCGCACAAGATGAAGGTGGAAACT
CGAAAGGTTATGGATTTGTCCACTTCGAAACYGARGAAGCTGCWCGGACC
GCCATCACAAAGGTGAATGGCATGTTGCTGAACAGCAAGAAGGTCTACGT
GGGCAAATTCATTCCACGGGCTGAGCGAGAGAAAGAACTTGGCGAGAAGG
CCAAGRTGTTCACCAACGTCTACGTGAAGAACTTTGGAGATGAGYTCAAT
GATGACAAGCTATGCGAAACCTTTTCCCGATTCGGGAAGATCACCAGCCA
CAAAGTGATTGTTGGTGAAGATGGCAAGTCCAAAGGCTTCGGTTTCGTCG
CCTTTGAAGATCCTGATGCAGCTGAGGCTGCTGTTCGTGAGATGAACAAC
ATTGAGCTGAACAACAAGCCGCTGTATGTTGGCCGGGCTCAAAAGAAGAG
TGAACGCCAGGCTGAGCTCAAGAAGAAGTTCGACCAAATGAAAATGGATC
GCATCAACCGTACACACGGYGTGAACCTGTACATCAAAAACTTGGATGAT
TGCATTGATGATGAACGTCTGCGAAAGGAATTCTCTCCTTATGGTACTAT
CACCAGTGCTAAAGTAATGATGGAAGACGGACGCTCCAAGGGCTTTGGCT
TCGTTTGCTTCAACCTCCCTGAGGAGGCAACTCGTGCCGTTACAGAGATG
AATGGCCGCATCCTCGTGGCCAAGCCATTGTATGTTGCTCTTGCGCAGCG
TCGTGAAGATCGTAAAGCTCAACTGGCCTCGCAGTACATGCAGCGTGTTG
CTGGCATGCGTTTGCAGCACGTGAACCAAGTGTATCCTACACCTCCTTCT
AGCTACTTTGTGCCTACTGCTCTGCAGACCGCTGGCTATCGCTTCAACAA
TATCATGCCCAACCTGCGCCCTGCCGCCCCGCGCTGGCAACAACCTGGTG
CTCAGGTCCGTCCCGGCCAGGCTCAGTTCTCCGTGCCTGCTGCTGCCACC
TACCGAGCCGGCACTGCCGCCCCTCGCCCAGCTCAACACAACCCCCGAGG
TGTGTCGCCTAATGTTCCTCGCAGCGCTGTGCCGCAACAACAGGTTATGG
GATTGGTTCAGCCCGGCGCTGCTGGTGCGCCTCGCGCCATGGCTGCGGCC
AGTGTTGGTGTGCCTCAGATGGCTGCTGCTAACGCTCCTCGCGTCAATGT
GCATGCTAACCCAGCTGCTGCGGCTGCTGCTGCCTACAGCAACAGCATTG
TCAATGCCTTCAAGTACACTCCCAACATGCGCAACCCGTCTGCTAGCAAC

CAGCAGGACATGAACATGTCCAACGCCAACAGCAATGCTGCCAGTGGCCA
ACAAGCTGTGCACGTGCAGGGACAGGAGCCTCTCACCCTAAACATGTTGG
CTGCCGCTGTTCCTCAGGATCAGAAGCAGATGTTGGGAGAACGCCTCTAC
CCGCTCGTCCAGGACTTCCACCCAGTCCTTTGCGGCAAGATTACGGGCAT
GTTGCTCGAGATGGACAACAGCGATTTGCTGCACATGCTTGAGGATCGCG
CTTCCCTCAAGGCCAAGATGGATGAAGCTCTGGCTGTGCTTCAAGCTCAC
CAGGCCAAGCAAGAAGTTGCTGCCAGCATCAAGAAGGAAGAGCAAACTCA
GATCTAAATCTGGCGAGTTGCTTTTATCATCATTTTTCATTGTTTTATTG
CATTTCATTTAGGAGTTTTAAATTATTTTTACCCGTGTGGGGCCCTGCTT
TTATCACCTATATGAAATGCATTCTAAACAACAAAAACAGGAAAAAAAAA
AACCTATAGTGAGTCGTATTAATTCGGATCCGCGAATCTGAATT::TCGA
MAAGCTTCTCGA:CCTAGGCTAGCTCTAGACCACACGTGTGGGGGCCCGA
GCTCGCGGCCGCTGTATTCTATAGTSTMACCTAAATGGCCGCACAATTCA
CTGGCCGTCGTKTTACAACRTCGTGACTSSGAAAACCCTGGCGTTACCCA
ACTTAATCGCCTTGCAGCACATCCCCCTTTCGCCAGCTGGCGTAATAGCG
AAGAGGCCCGCACCGATCGCCCTTCCCAACAGTTGCGCAGCCTGAATGGC
GAATGGAAATTGTAAGCGTTAATATTTTGTTAAAATTCGCGTTAAATTTT
TGTTAAATCAGCTCATTTTTTAACCAATAGGCCGAAATCGGCAAAATCCC
TTATAAATCAAAAGAATAGACCGAGATAGGGTTGAGTGTTGTTCCAGTTT
GGAACAAGAGTCCACTATTAAAGAACGTGGACTCCAACGTCAAAGGGCGA
AAAACCGTCTATCNNNNNATGGCCCACTACGTGAACCATCNCCCTAATCA
AGTTTTTTGGGGTCGAGGTGNCGTANNCACTAAATCGGAACCCTAAAGGG
ANCCCCCNATTTANANCTTGANGGGGAAAGCCGGCNAACGTGNNNA

Figure D.1. Alignment of Ph-PAB coding region with PAB amino acid sequences from various species.
Abbreviations used and accession numbers: Dr, *Danio rerio,* AAH53126.1; Dm, *Drosophila melanogaster,* AAF57746.1; Ce, *Caerabnorditis elegans,* AAA65224.1; Ag, *Anopholes gambiae,* AGAP011092-PA; Tc, *Tribolium castenum,* XP_975975.1; Dp, *Daphnia pulex;* Ph, *Parhyale hawaiensis*.

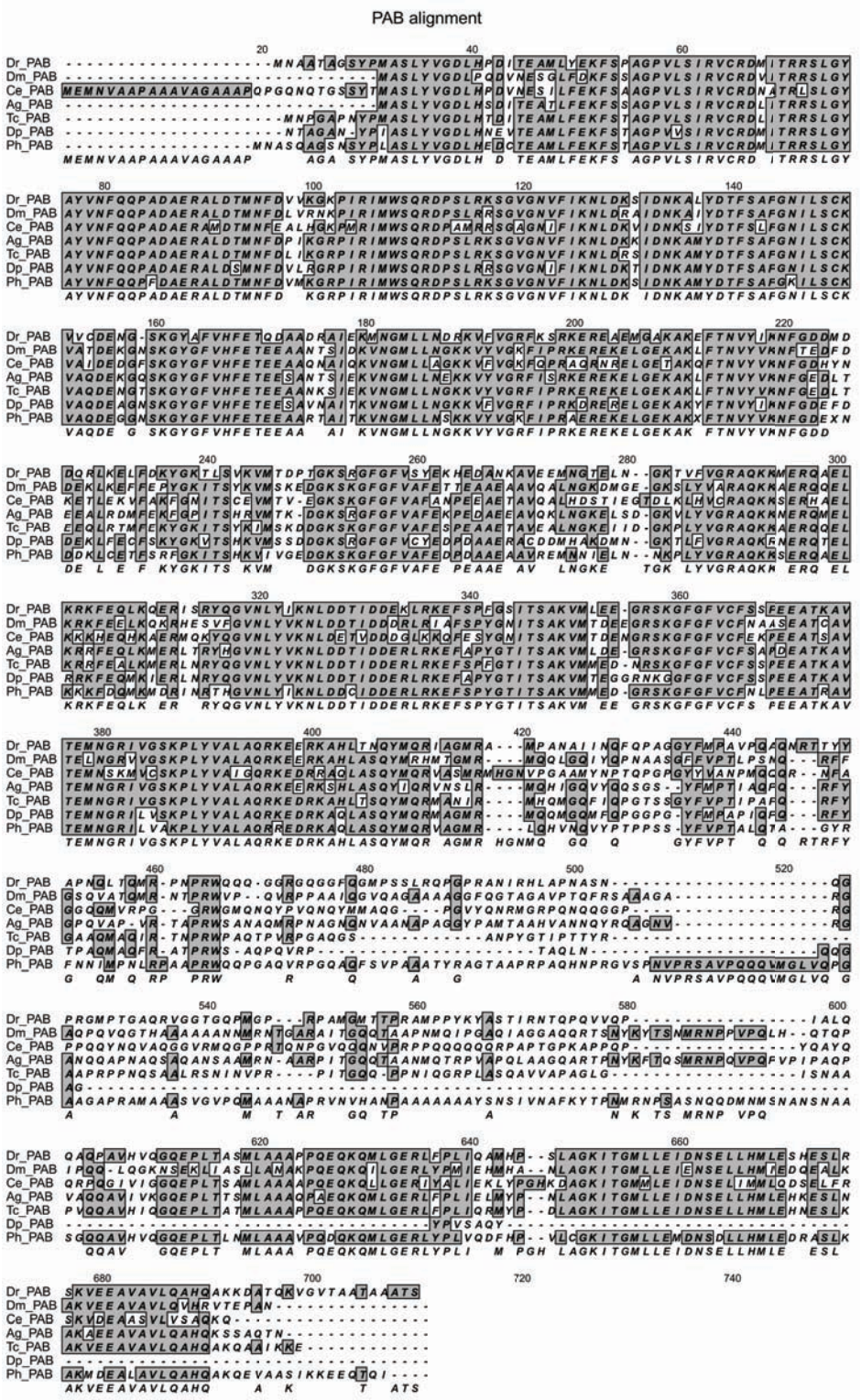
PAB alignment
Dr_PAB
Dm_PAB
Ce_PAB
Ag_PAB
Tc_PAB
Dp_PAB
Ph_PAB

Appendix E: Notes on TEM in *Parhyale* embryos

Due to the presence of a chorion and the yolky nature of the cells during gastrulation stages, normal fixation protocols for transmission electron microscopy (TEM) introduce too many fixation artifacts. With the help of Reena Zalpuri and Dr. Kent McDonald at the EM lab at UC Berkeley, I did some preliminary work with cryo-EM and found that it has the potential to provide information about cell junctions at the soccerball stage of *Parhyale* development. This appendix has the protocol I developed for normal fixing and infiltration techniques done with Zalpuri and describes the protocol for cryo-em done in conjunction with McDonald. Results from the experiments are shown side by side in Fig. E.1.

MATERIALS AND METHODS

Fixation and Infiltration (Reena Zalpuri/Crystal Chaw):

Fixation:

1) 2% Glutaraldehyde + 4% Paraformaldehyde in Artificial Seawater (ASW), microwave process:
    a. Microwave Power Level 1, 1 min microwave/ 1 minute hold/ 1 minute microwave
2) Dissect with tungsten needles in 2% Glutaraldehyde + 4% Paraformaldehyde in ASW
3) Rinse embryos once with 3% Glutaraldehyde
4) Leave embryos in 3% Glutaraldehyde overnight at 4ºC

Osmium fix/UA stain:

5) Rinse embryos in ASW 2x10 minutes
6) 1% Osmium fix: 2x 1/1/1 microwave process at PL 1. Leave in 1% Osmium on rocker for 30 minutes- keep embryos in the dark
7) Rinse in ASW 1x10 minutes, 3x10 minutes in dH20.
8) Leave in 1% Uranyl Acetate (UA) at 4ºC overnight

Dehydration:

9) Rinse with dH2O 2x10 minutes
10) Dehydration series:

% EtOH	Time (minutes)	Temperature ºC (location)
11) 35	10	4º (fridge)

12)	50	10	0º (ice)
13)	70-75	10	-20º (freezer)
14)	80	10	-20 º (freezer)
15)	90	10	-80º (dry ice)
16)	100	10	-80º (dry ice)
17)	100	10	-80º (dry ice)

18) Warm embryos- 5 minutes at room temp

19) Wash with 100% Acetone 1x10 minutes

Infiltration:

20) Infiltrate with resin (Epon+DDSA+Aradalite, no accelerant): 10% stepwise increase in resin with Acetone, 1/1/1 microwave processing PL2, 2x washes at each step.

21) 3 changes of 100% resin, 1/1/1 microwave processing, PL2

22) Left in 100% resin for three days.

23) Exchange resin for resin +accelerator. Make sure embryos are in new resin. Rock for 1.5 hours.

24) Embed samples into molds with resin + accelerator, leave in 60º oven, 2 days.

25) Cut samples into sections and image.

High pressure freezing (HPF) and Fixation (Kent McDonald/Crystal Chaw)

Freezing and fixation were done according to previous protocols for *Drosophila* embryos with a few exceptions (McDonald, 1999). A solution of 50% BSA and ASW was used as the cryoprotectant. Soccerball stage embryos were placed into the solution using a mouth pipette and forceps. They were fixed by freeze substitution in 0.01% OsO4 + 0.2% in uranyl acetate in acetone. Samples were infiltrated with Epon-Araldite (Embed-812), cut into 100 nm sections and imaged on a FEI Tecnai 12 Transmission Electron Microscope.

Results

Fixation with HPF is a superior method. Embryos fixed without HPF show a high number of electron-dense yolk elements that may be crystalline in nature. The extracellular layer is completely absent as evidenced by a lack of the chroion and vitelliene membrane. Cell boundaries are present, but are often fragmented or unclear. Images fixed with HPF show possible tight junctions near the apical surface of the cells (Fig. E.1). Future work could focus on replicating these results, trying different fixation techniques, and studying different stages. In addition, immunolabeling combined with TEM would be particularly useful in discerning junctional changes between the cells of the rosette and neighboring cells during internalization.

Figure E.1. Comparison of TEM images with and without high pressure freezing (HPF).
Top: Different magnifications of the same area in a 100 nm section of a single embryo after high pressure freezing and fixation. Red box indicates a putative tight junction. Bottom. Images from different areas of a 100 nm section from a single embryo without high pressure freezing. Asteriks indicate torn areas of the embryo that are probably fixation artifacts. Xs indicate electron-dense elements that appear to be part of the yolk. Blue arrowheads indicate cell boundaries at putative sites of cell-cell contact.

HPF
No HPF
A
outside the embryo
chorion
vitelliene (?)
0.5 µm
B
0.2 µm
C
0.2 µm
D
outside the embryo
2.0 µm
E
0.2 µm
fixation artifacts
unknown yolk element
putative tight junction
cell boundaries

Appendix F: Non-Essential Supplemental Material

The figures in this dissertation draw from a number of timelapse videos that are included as non-essential supplemental materials. This appendix lists the videos and gives a short description of each.

Supplemental Movie 1: 20x brightfield time-lapse video of Parhyale gastrulation with cells false colored. A cell of the rosette (purple) and a cell of the epithelial sheet (red) tracked through 129 frames of a timelapse video. Color was limited to the cytoplasm surrounding the nucleus. Frames are at 3-minute intervals. Time is shown in the upper right in red (hours:minutes:seconds).

Supplemental Movie 2: Rosette photoablation. Time-lapse video of fluorescently labeled control and photoablated embryos. A representative ablated and control embryo are shown with Volocity tracks super imposed in the upper left (see Fig. 3.3 for key to colors of tracks). Rosette (green) is labeled with FITC, ectoderm (red nuclei) is labeled with dsRed-NLS. Photoablated embryos have dim rosettes due to photobleaching from the ablation procedure. Scale bar is 100 μm. Time is shown in upper right in red (hours: minutes: seconds).

Supplemental Movie 3a: Leading edge photoablation can result in a normal phenotype. Time-lapse video of fluorescently labeled control (n=2) and photoablated (n=2) embryos. Photo ablated embryos are to the upper right with dimmer leading edge cells immediately surrounding the rosette. The rosette (red) is labeled with TRITC, and the ectoderm (green) is labeled with FITC. 5-minute intervals. Scale bar is 70 μm, time is shown in upper right in red (hours: minutes: seconds).

Supplemental Movie 3b: Leading edge photoablation can result in an abnormal phenotype. Time-lapse video of control (n=3) and photoablated (n=2) embryos. Photoablated embryos are to the right with dim ectoderm cells adjacent to the rosette. The rosette (red) is labeled with TRITC and the ectoderm (green) is labeled with FITC. 5-minute intervals. Scale bar is 70 μm, time is shown in upper right in red (hours: minutes: seconds).

Supplemental Movie 4a: Control embryos from the same brood as the Cytochalasin D treated embryos in supplemental movie 4b. The rosette (green) is labeled with FITC and the ectoderm (red) is labeled with TRITC. 5- minute intervals, time is shown in upper right in red (hours: minutes: seconds).

Supplemental Movie 4b: Cytochalasin D treatment arrests gastrulation. Cytochalasin D treated embryos from the same brood as the control embryos in 4a. The rosette (green) is labeled with FITC and the ectoderm (red) is labeled with TRITC. 5-minute intervals, time is shown in upper right in red (hours: minutes: seconds).

Supplemental Movie 5: Photoablation of a portion of the epithelial sheet adjacent to the rosette does not affect rosette internalization or migration of the remaining epithelial sheet cells. Descendants of El, Er, and Ep are labeled with dsRed-NLS (red nuclei). Descendants from El or Er are also labeled with FITC (green). The rosette is labeled with TRITC (red). Photoablated embryos (n=2) are at either end of the second row. The ablated cells are visible as dimly lit cells in the green portion of the epithelial sheet just adjacent to the rosette. 5-minute intervals. Scale bar is 70 μm, time is shown in upper right in red (hours: minutes: seconds).

Supplemental Movie 6: Treatment with Olomoucine results in an abnormal germ cap. See chapter 4 for treatment conditions. 5-minute intervals. Scale bar is 100μm, time is shown in upper right in red (hours: minutes: seconds).